Southern California Earthquake Center

Full 3D Tomography (F3DT)

Theory and Application to Southern California

Thomas H. Jordan

Director, Southern California Earhquake Center

University of Southern California

Based on research with

En-Jui Lee, Po Chen, and the CME Collaboration

2014 VISES Summer School

29 September 2014

Probabilistic Seismic Hazard Model

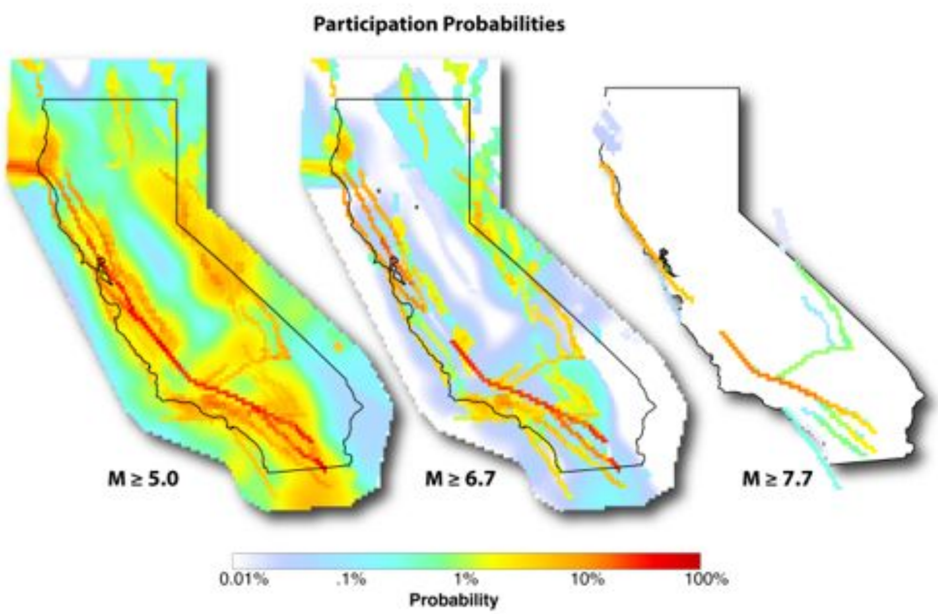

SCEC-USGS-CGS Working Group on California Earthquake Probabilities (2008)

Uniform California Earthquake Rupture Forecast (UCERF2)

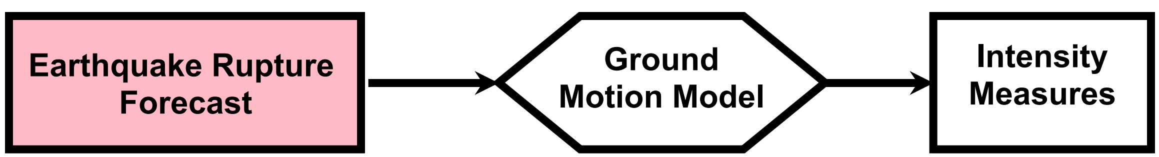

$P(S)$ $P(Y_n \mid S)$ $P(Y_n)$

Probabilistic Seismic Hazard Model

Hazard Curve:

- **Shaking intensity: Peak Ground Acceleration (PGA)**
- **Interval: 50 years**
- **Site: Downtown LA**

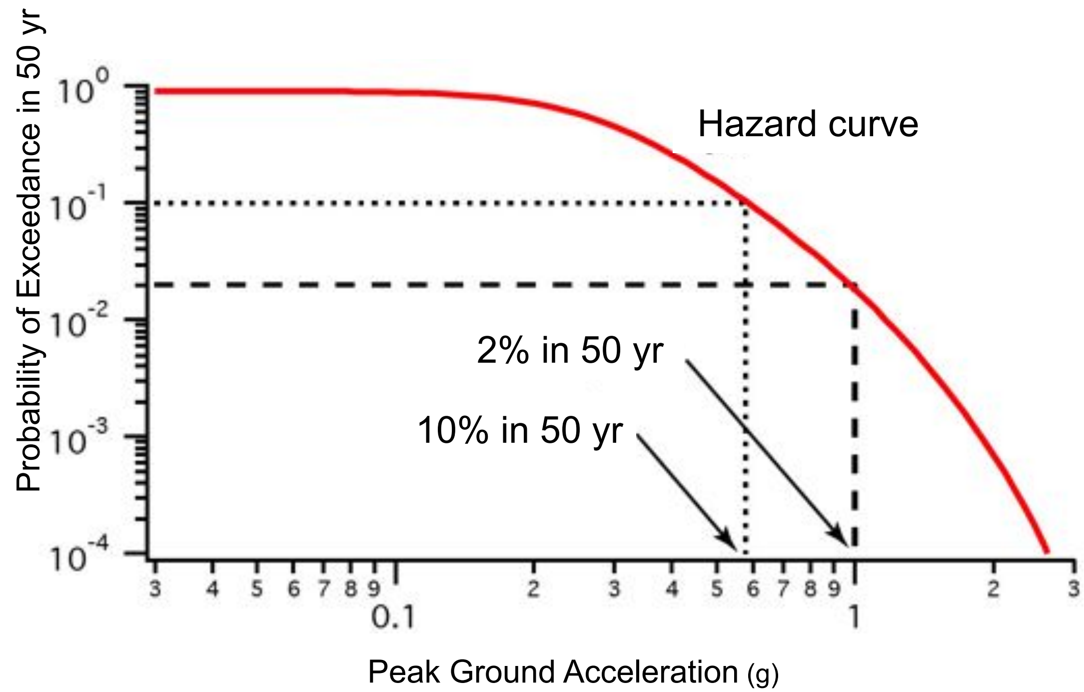

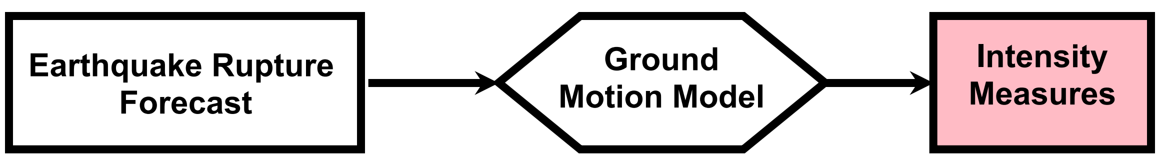

$P(S_k)$ $P(Y_n \mid S_k)$ $P(Y_n)$

Probabilistic Seismic Hazard Model

National Seismic Hazard Map

PGA (%g) with 2% Probability of Exceedance in 50 years

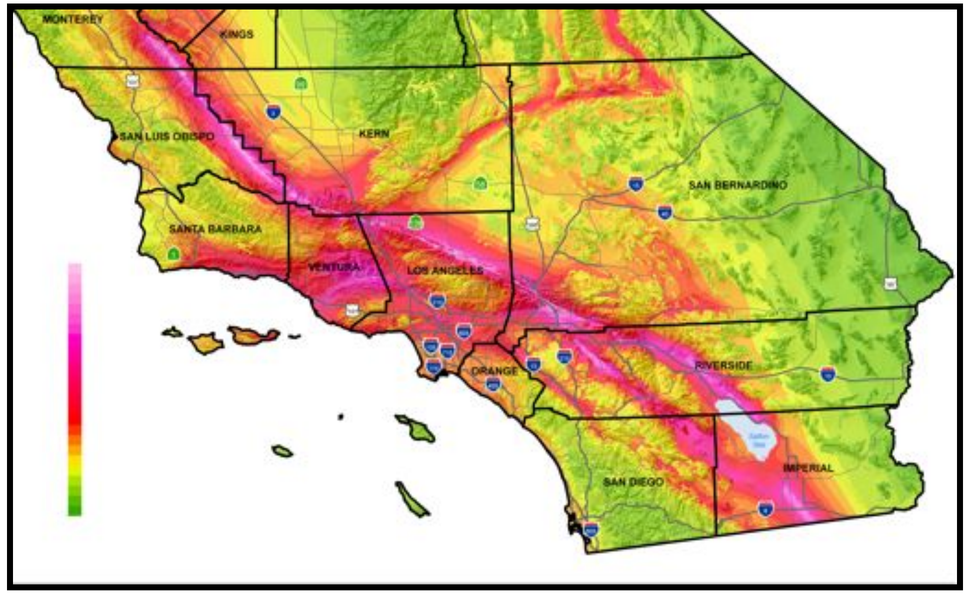

Earthquake Rupture Forecast → **Ground Motion Model** → **Intensity Measures**

$P(S_k)$ $P(Y_n \mid S_k)$ $P(Y_n)$

Probabilistic Seismic Hazard Model

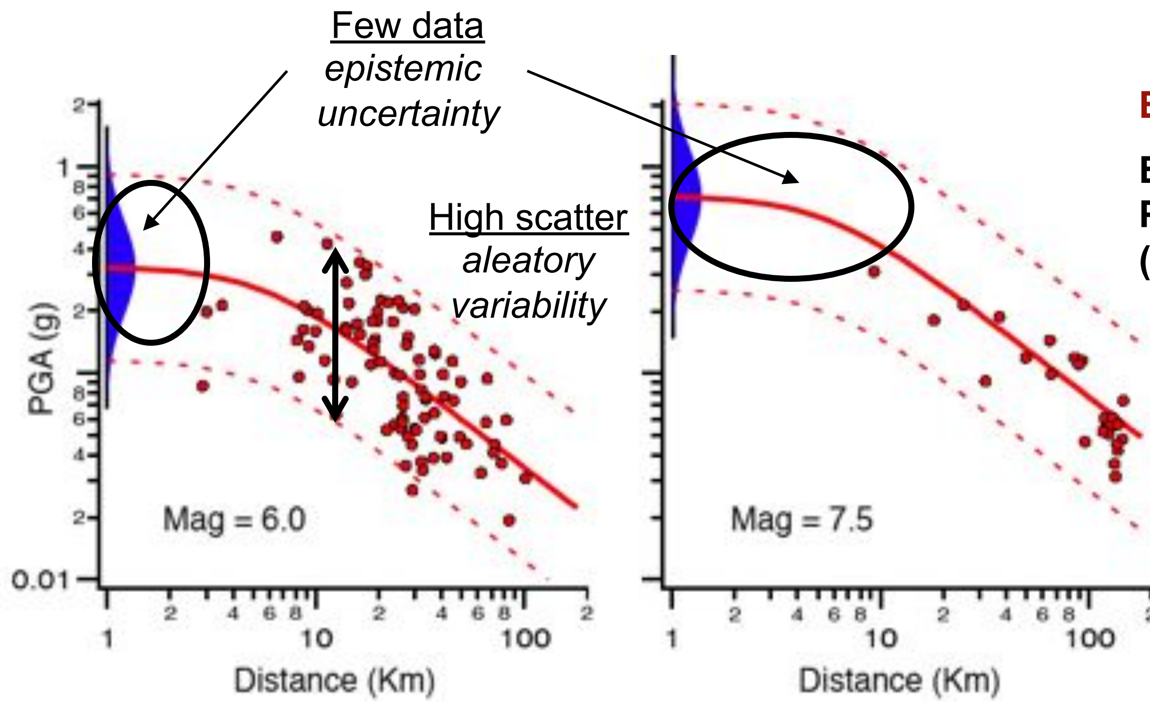

Boore et al. (1997)

Empirical Ground Motion Prediction Equations (GMPEs)

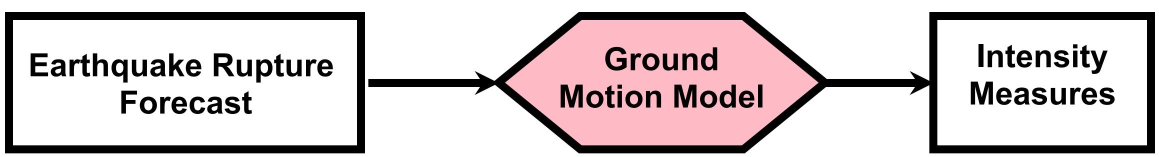

$P(S_k)$ $P(Y_n \mid S_k)$ $P(Y_n)$

Probabilistic Seismic Hazard Model

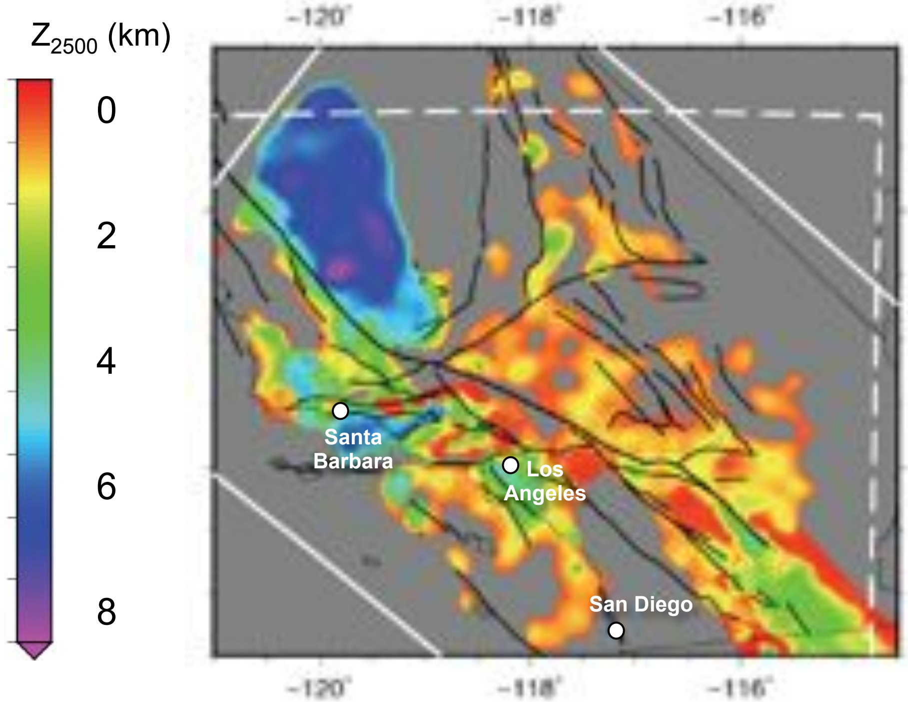

Much of the aleatory variability in the GMPEs comes from 3D heterogeneity in crustal structure

Earthquake Rupture Forecast → **Ground Motion Model** → **Intensity Measures**

$P(S_k)$ $P(Y_n \mid S_k)$ $P(Y_n)$

ShakeOut Scenario

M7.8 Earthquake on Southern San Andreas Fault

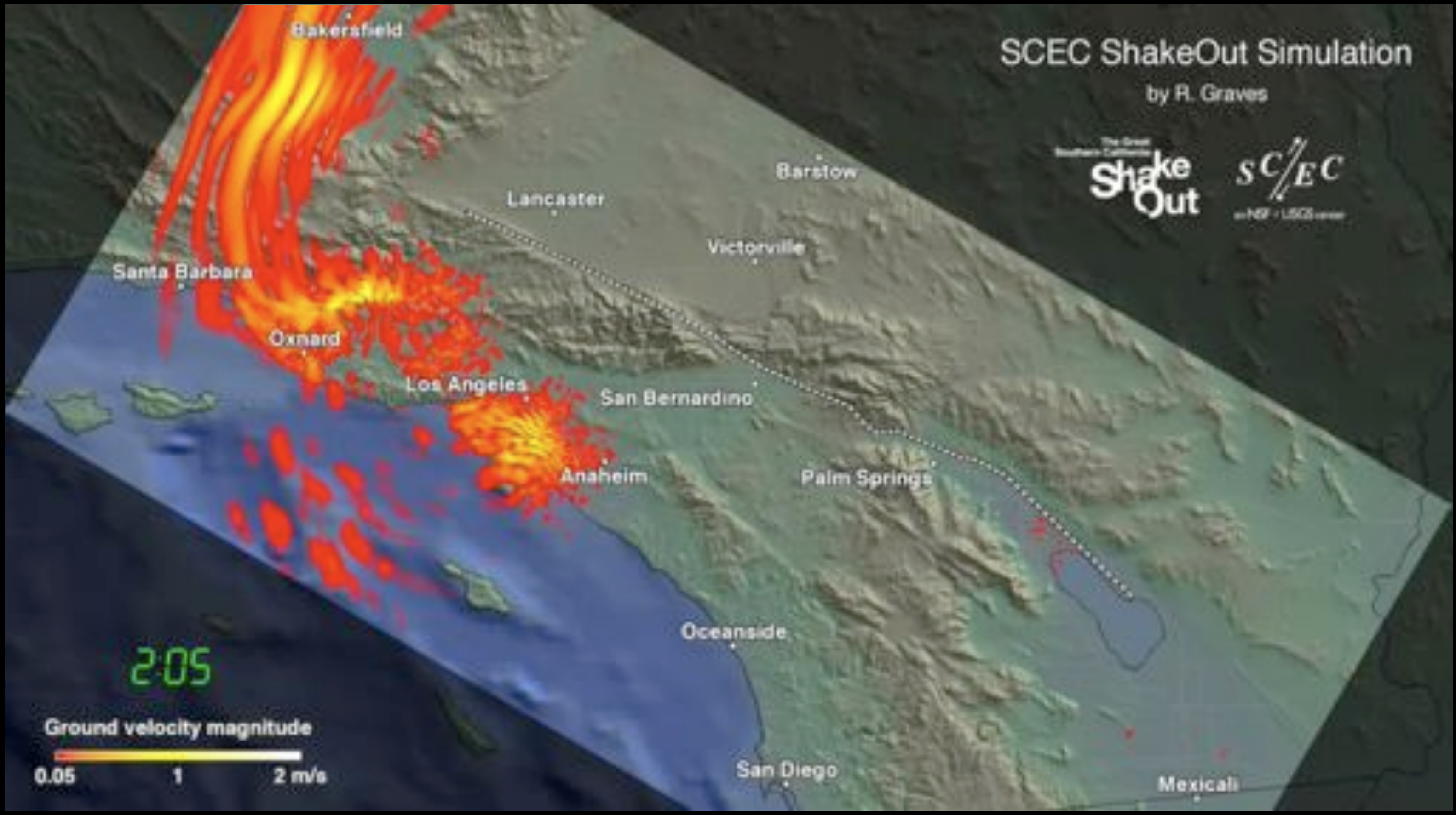

Importance of Reducing Aleatory Variability

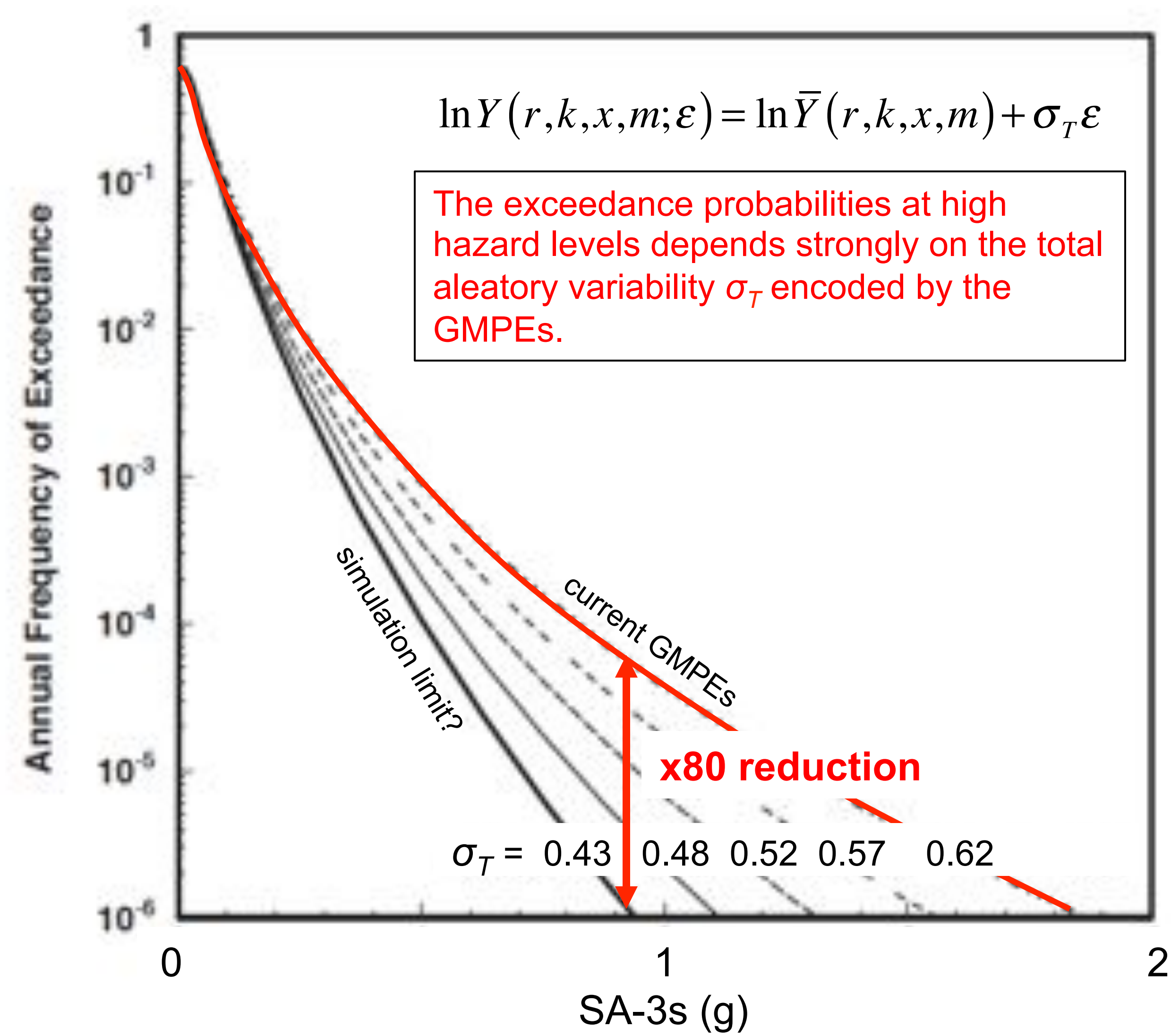

Reducing Aleatory Variability

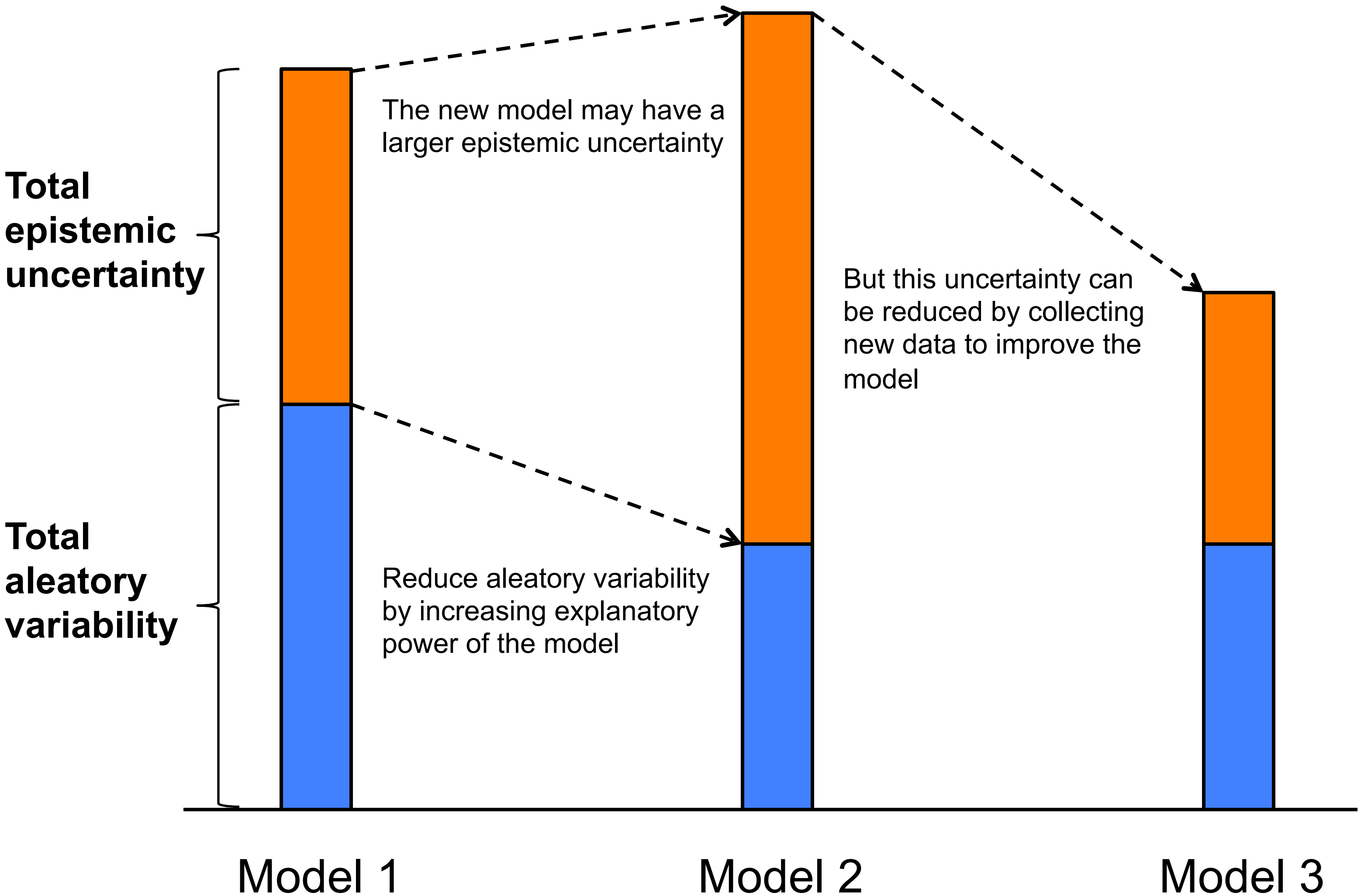

CyberShake Hazard Model for the LA Region

- **3D crustal model:**
  - **CVM-S4.26**
- **Sites:**
  - **283 sites in the greater Los Angeles region**
- **Ruptures:**
  - **All UCERF2 ruptures within 200 km of site (~14,900)**
- **Rupture variations:**
  - **~415,000 per site using Graves-Pitarka pseudo-dynamic rupture model**
- **Seismograms:**
  - **~235 million per model**

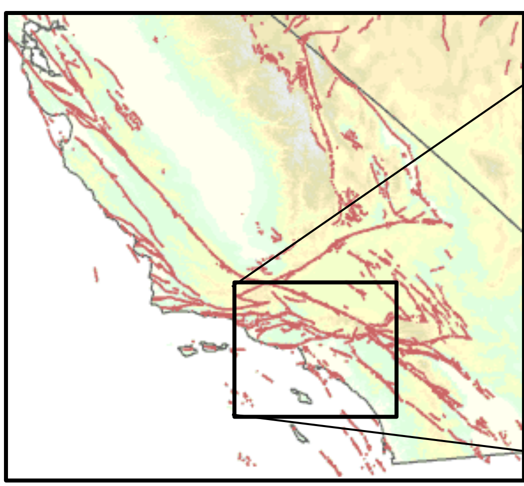

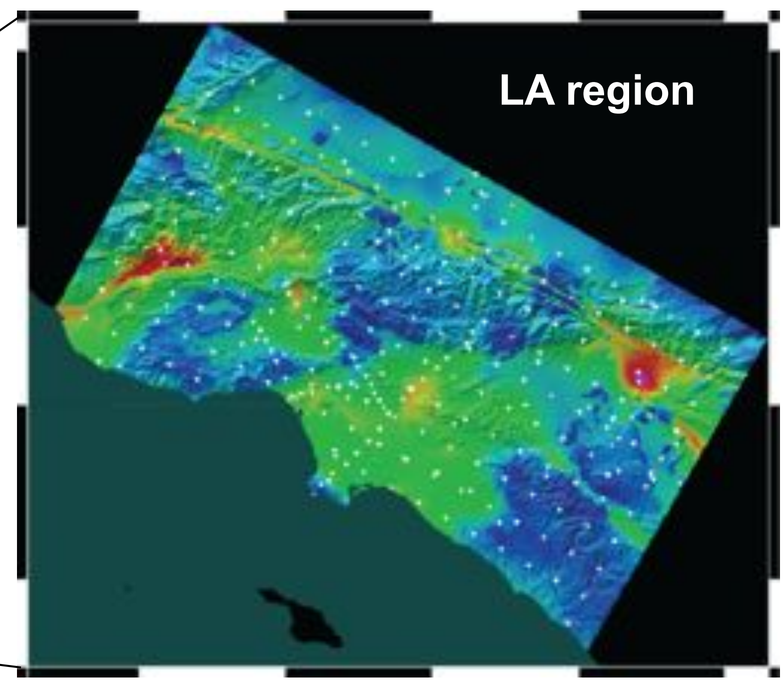

CyberShake Workflow

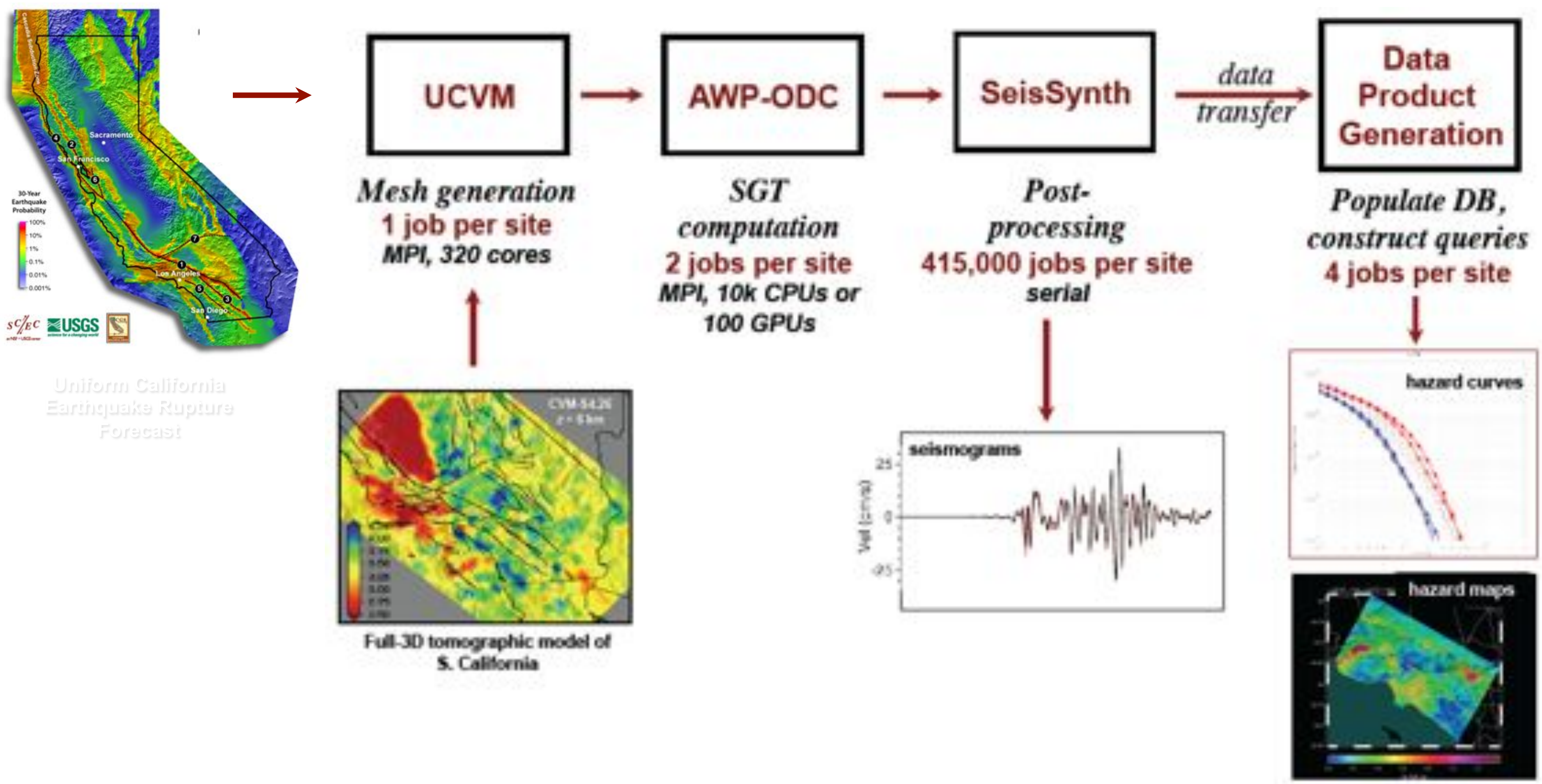

Comparison of 1D and 3D CyberShake Models for the Los Angeles Region

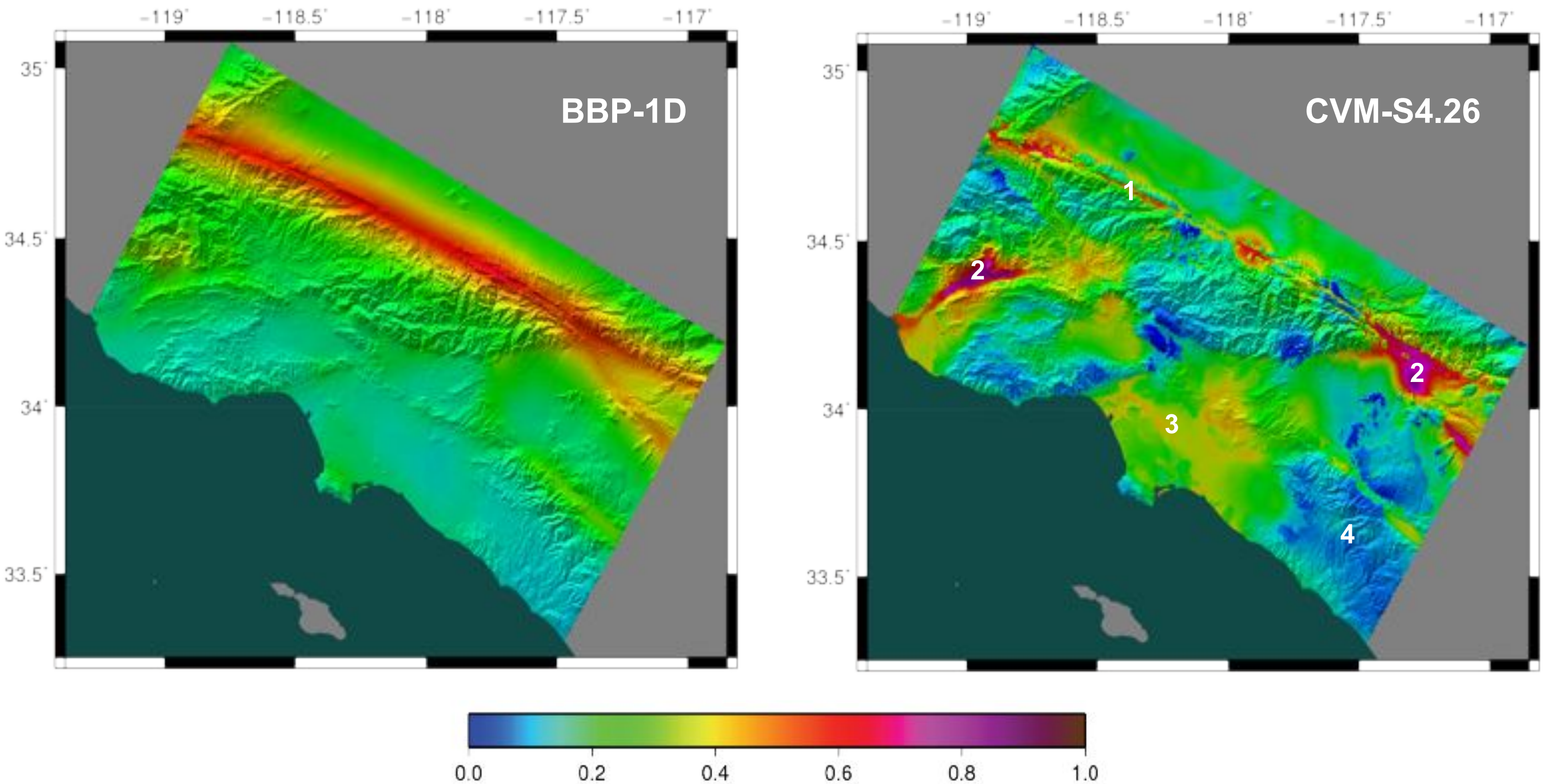

CyberShake Hazard Map, 3sec SA, 2% in 50 yrs

1. lower near-fault intensities due to 3D scattering
2. much higher intensities in near-fault basins
3. higher intensities in the Los Angeles basins
4. lower intensities in hard-rock areas

Averaging-Based Factorization

- **Representation of excitation functionals**

Expected shaking intensities constructed by averaging over slip variations (s), hypocenters (x), sources (k), and sites (r)

$$G(r,k,x,s) \;=\; A + B(r) + C(r,k) + D(r,k,x) + E(r,k,x,s)$$

G = ln (Y); A = level; B = site effect; C = path effect; D = directivity effect; E = slip complexity effect

- **Representation of excitation variance**

$$\mathrm{Var}[G] \;=\; \bar{\sigma}_G^2 \equiv \left\langle [G(r,k,x,s) - A]^2 \right\rangle_{S,X,K,R}$$

$$= \;\sigma_B^2 + \left\langle \sigma_C^2(r) \right\rangle_R + \left\langle \sigma_D^2(r,k) \right\rangle_{K,R} + \left\langle \sigma_E^2(r,k,x) \right\rangle_{X,K,R}$$

$$\equiv \;\sigma_B^2 + \bar{\sigma}_C^2 + \bar{\sigma}_D^2 + \bar{\sigma}_E^2$$

ABF Variance Analysis of the CyberShake Model

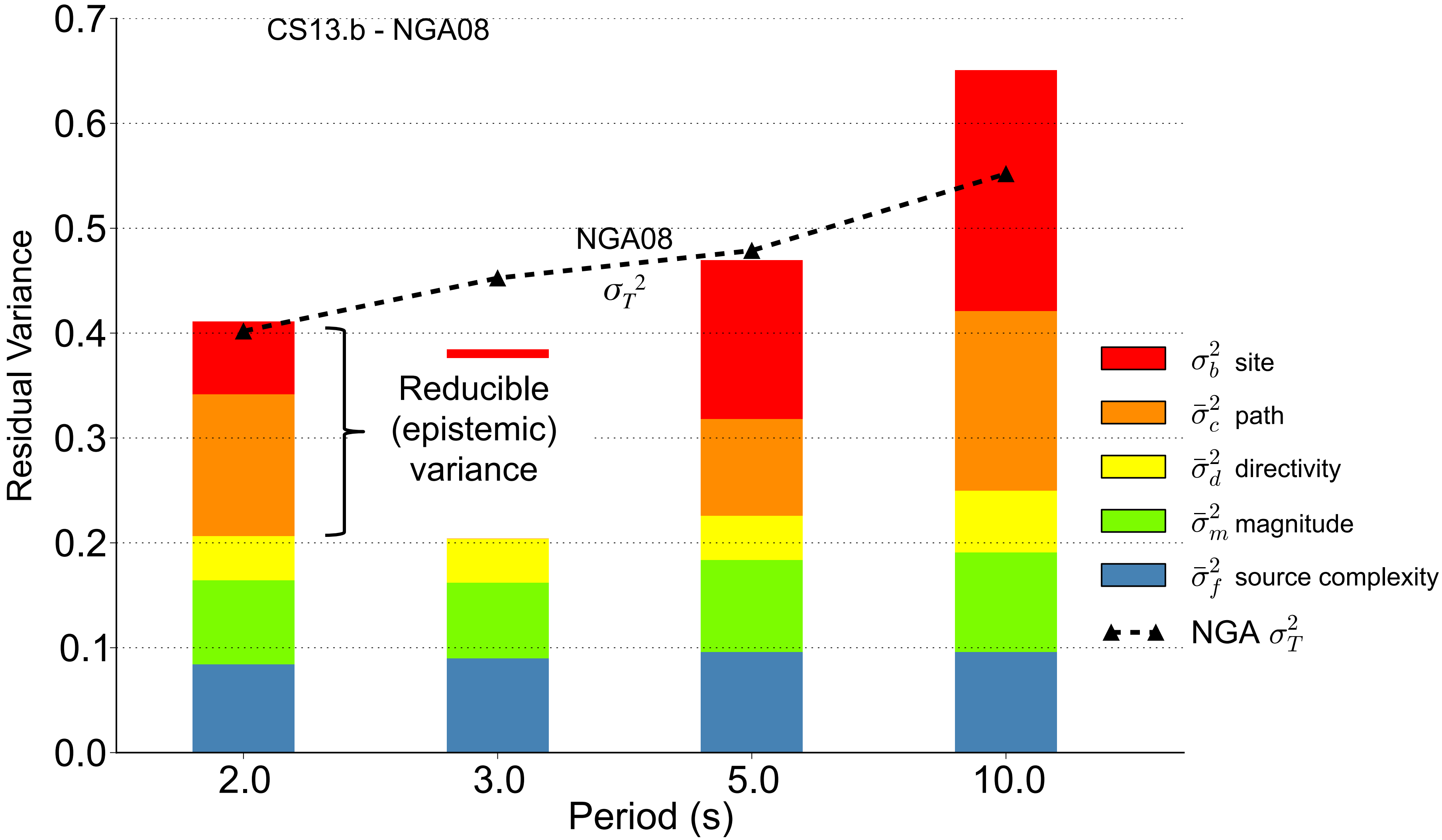

Importance of Reducing Aleatory Variability

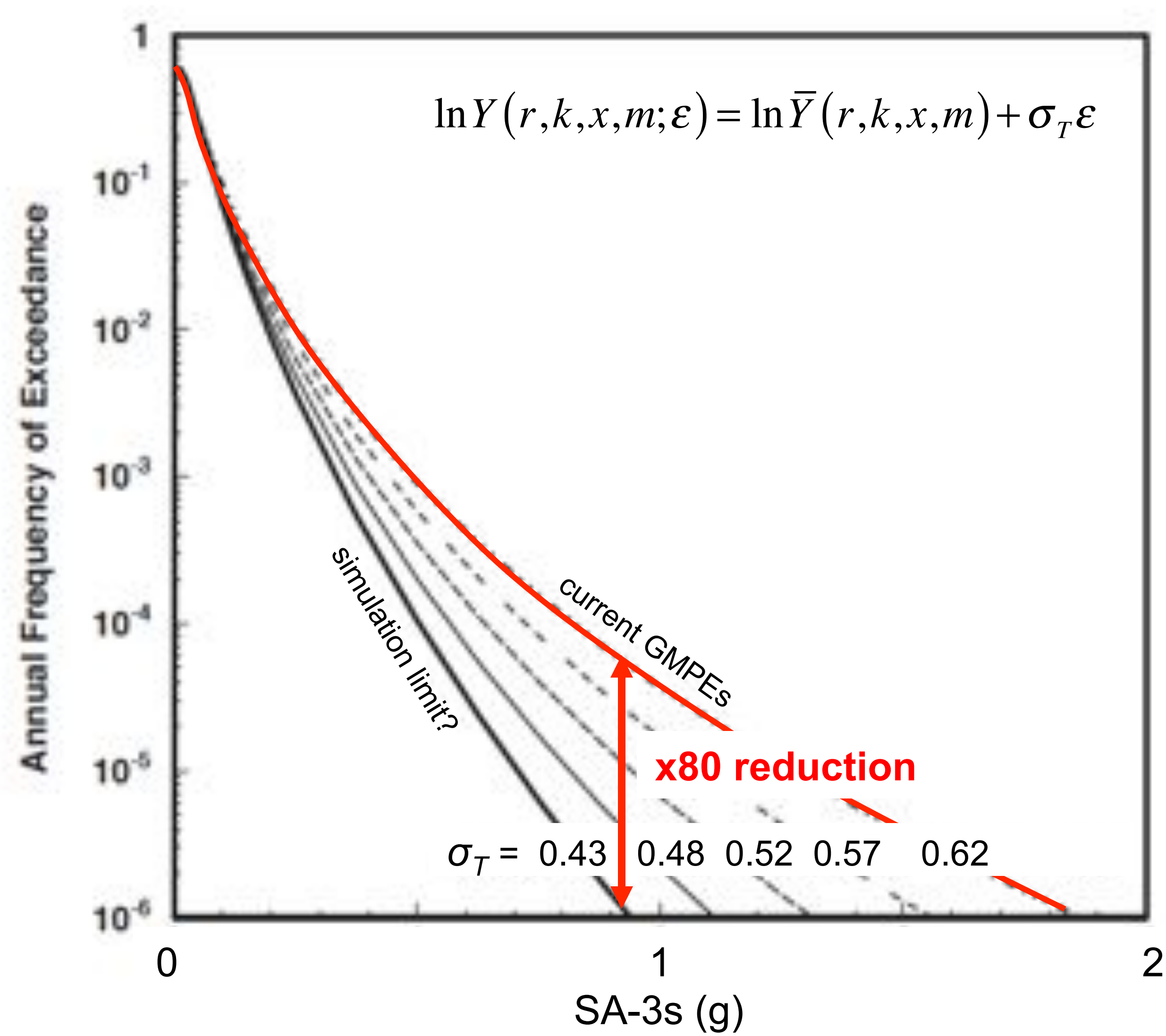

CyberShake Platform: Physics-Based PSHA

Essential ingredients

1. **Extended earthquake rupture forecast**
   - **probabilities of all fault ruptures (e.g., UCERF2)**
   - **conditional hypocenter distributions for rupture sets**
   - **conditional slip distributions from pseudo-dynamic models**

2. **Three-dimensional models of geologic structure**
   - **large-scale crustal heterogeneity**
   - **sedimentary basin structure**
   - **near-surface properties ("geotechnical layer")**

   from SCEC CVMs

3. **Ability to compute large suites (> 10^8) of seismograms**
   - **efficient anelastic wave propagation (AWP) codes**
   - **reciprocity-based calculation of ground motions**

SCEC Community Velocity Models (CVMs)

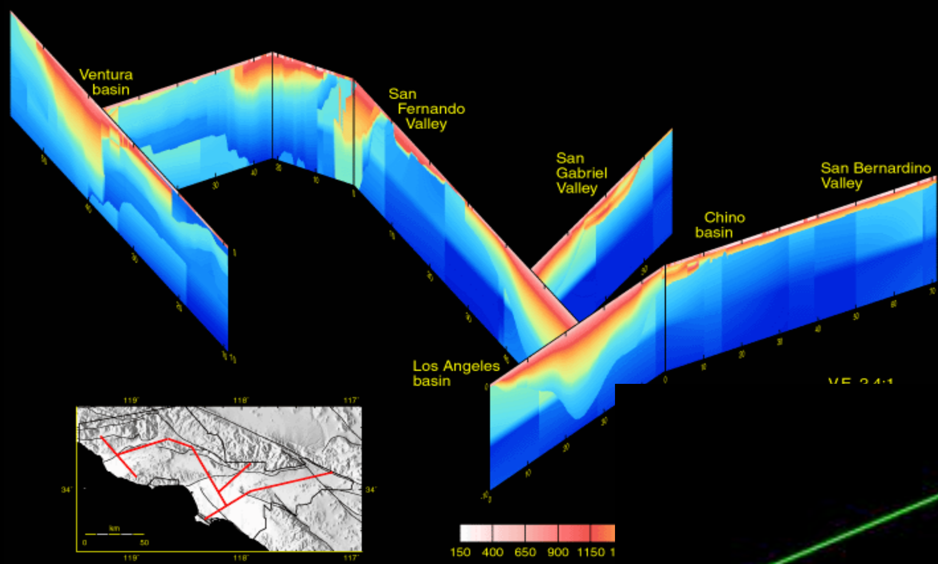

CVM-S series

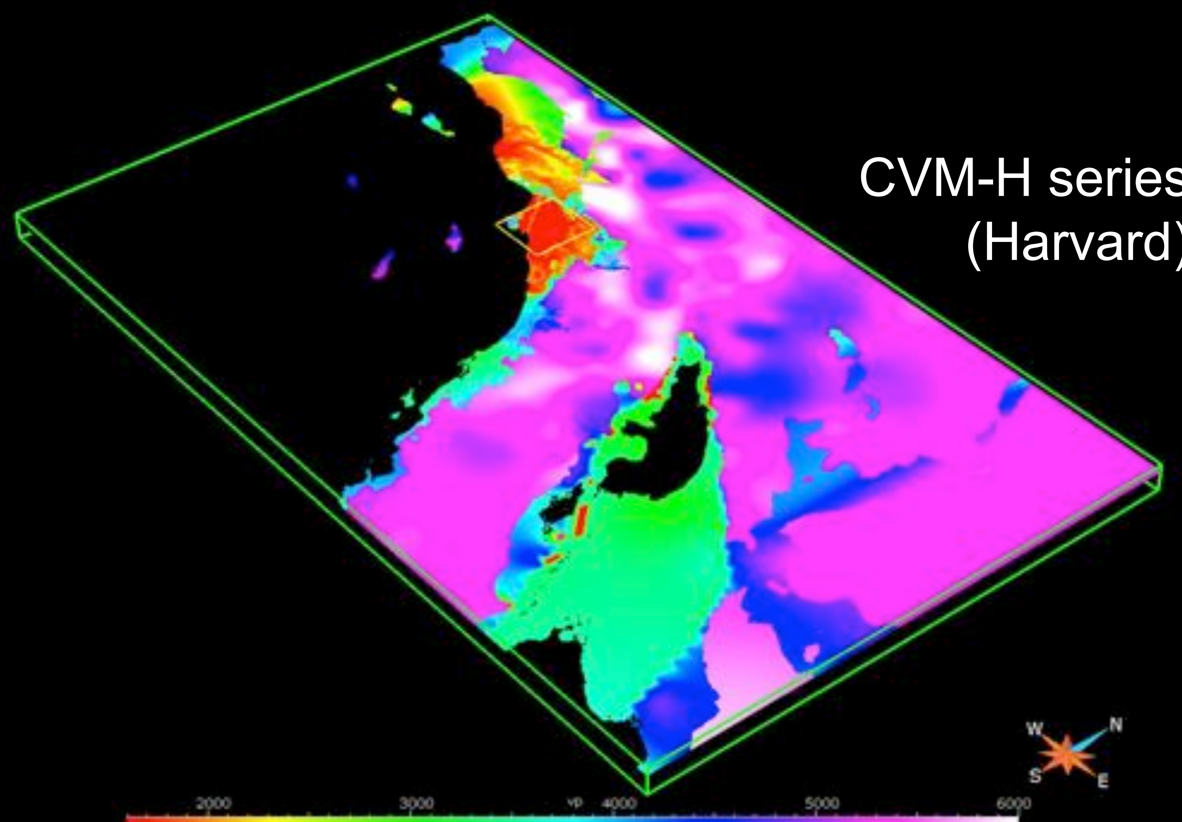

CVM-H series
(Harvard)

Data sources

- **Surface geology**
- **Well logs**
- **Refraction surveys**
- **Reflection surveys**
- **Seismic tomography**
- **Geologic models**

Lecture Outline

- ✓ Simulation-based seismic hazard analysis
  - – How F3DT can reduce “irreducible” uncertainties
- Tomographic inverse problem
  - – Adjoint wavefield method
  - – Scattering integral method
- Application of F3DT to Southern California
  - – Validation of CVM-S4.26 by waveform prediction
  - – Structural features of CVM-S4.26
- Outstanding issues
  - – USR interface problem
  - – Anisotropy
  - – Push to higher frequencies

References

- Zhao, L., T. H. Jordan, K. Olsen, and P. Chen, Fréchet kernels for imaging regional Earth structure based on three-dimensional reference models, *Bull. Seismol. Soc. Am., 95*, 2066-2080.
- Tromp, J., C. Tape, and Q. Liu (2005), Seismic tomography, adjoint methods, time reversal and banana-doughnut kernels, *Geophys. J. Int., 160*(1), 195–216, doi:10.1111/j.1365-246X.2004.02453.x.
- Chen, P., T. H. Jordan, and L. Zhao (2007a), Full three-dimensional waveform tomography: a comparison between the scattering-integral and adjoint-wavefield methods, *Geophys. J. Int., 170*, 175-181, doi: 10.1111/j.1365-246x.2007.03429.x.
- Chen, P., L. Zhao, and T. H. Jordan (2007b), Full 3D tomography for crustal structure of the Los Angeles region, *Bull. Seismol. Soc. Am., 97*, 1094-1120, doi: 10.1785/0120060222.
- Tape, C., Q. Liu, A. Maggi, and J. Tromp (2010), Seismic tomography of the southern California crust based on spectral-element and adjoint methods, *Geophys. J. Int., 180*(1), 433–462, doi:10.1111/j.1365-246X.2009.04429.x.
- **Lee E.-J., P. Chen, T. H. Jordan, P. B. Maechling, M. A.M. Denolle and G. C. Beroza (2014a), Full-3D Tomography for Crustal structure in Southern California based on the scattering-integral and the adjoint-wavefield methods, *J. Geophys. Res., 119*, 6421-6451, doi:10.1002/2014JB011346**
- Lee, E.-J., P. Chen, and T. H. Jordan (2014b), Testing waveform predictions of 3D velocity models against two recent Los Angeles earthquakes, *Seismol. Res. Lett.*, 85(6)

Structural Models

We consider a three-dimensional (3D), isotropic, elastic structure

$\mathbf{m}(\mathbf{x}) = \mathbf{m}(x_1, x_2, z) = [v_P(\mathbf{x}), v_S(\mathbf{x}), \rho(\mathbf{x})]$ for $0 \le z \le z_{\max} \approx 50\ \mathrm{km}$

The 1D lateral average of $\mathbf{m}$ is an integral over $(x_1, x_2) \in R$

$$\bar{\mathbf{m}}(z) = \frac{1}{A_R}\int_R \mathbf{m}(x_1, x_2, z)\, dA$$

The 1D average along a path $\sigma(x_1, x_2) = 0$ with element of length ds is

$$\mathbf{m}_\sigma(z) = \frac{1}{L_\sigma}\int_\sigma \mathbf{m}(x_1, x_2, z)\, ds$$

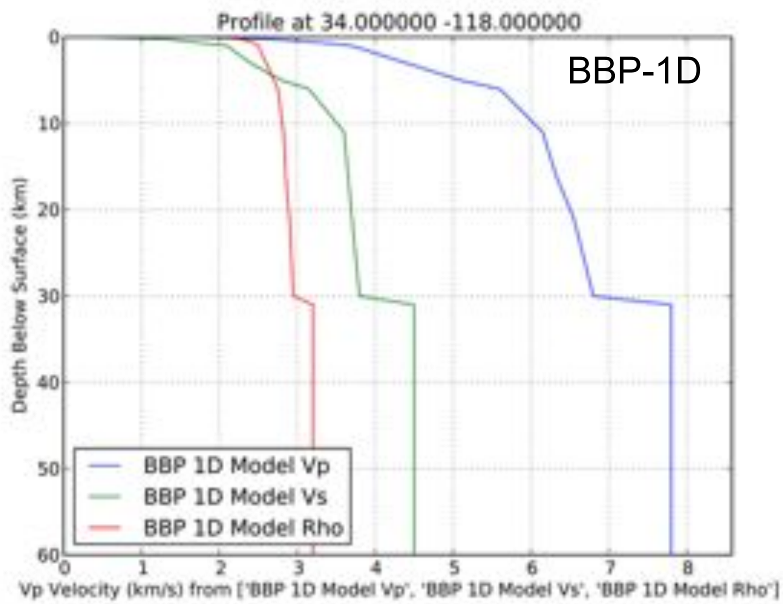

BBP-1D Regional Model

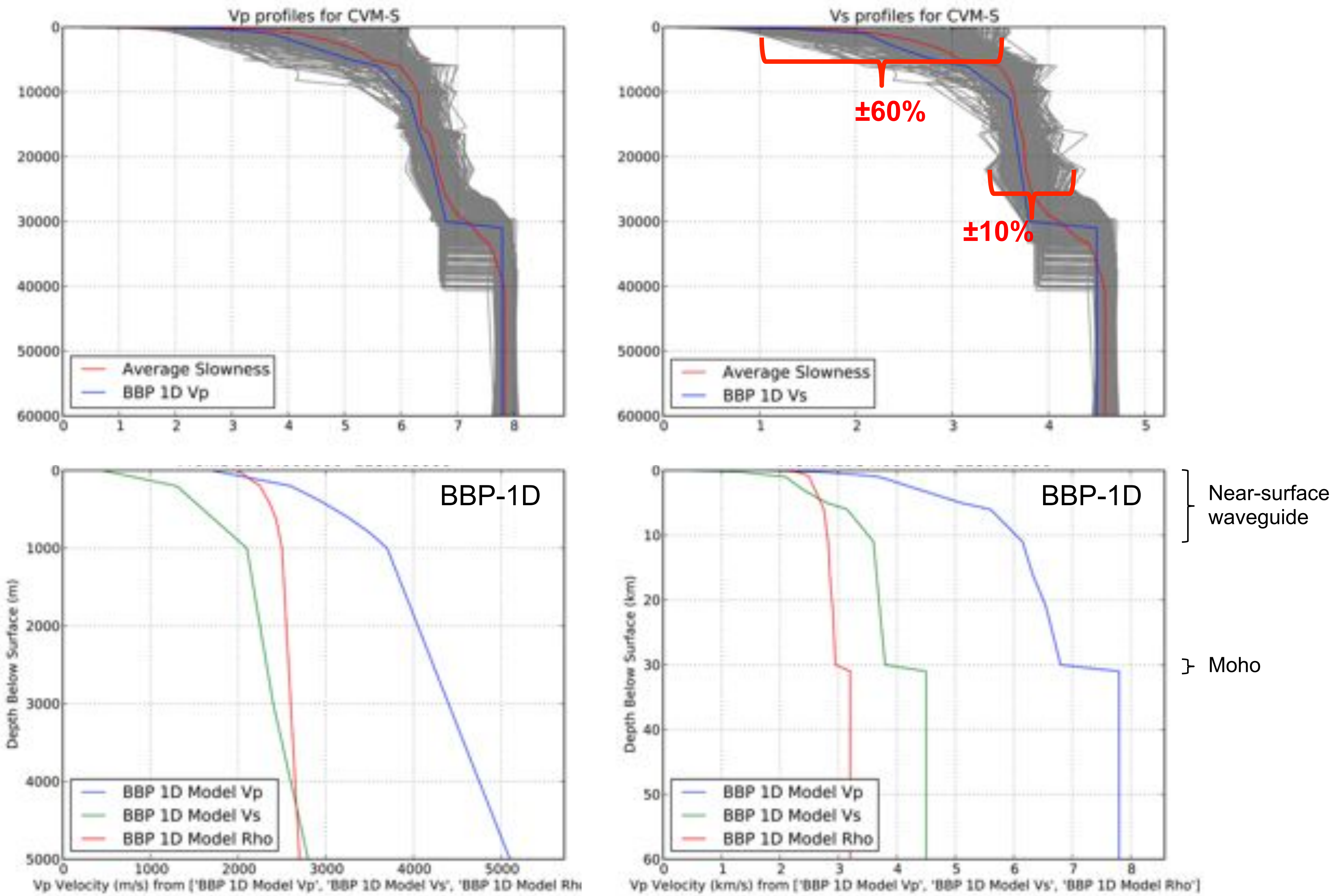

CVM Components

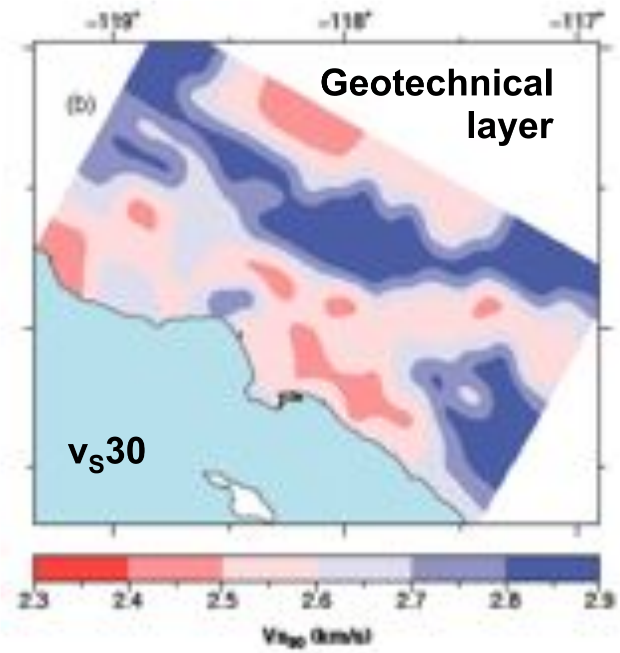

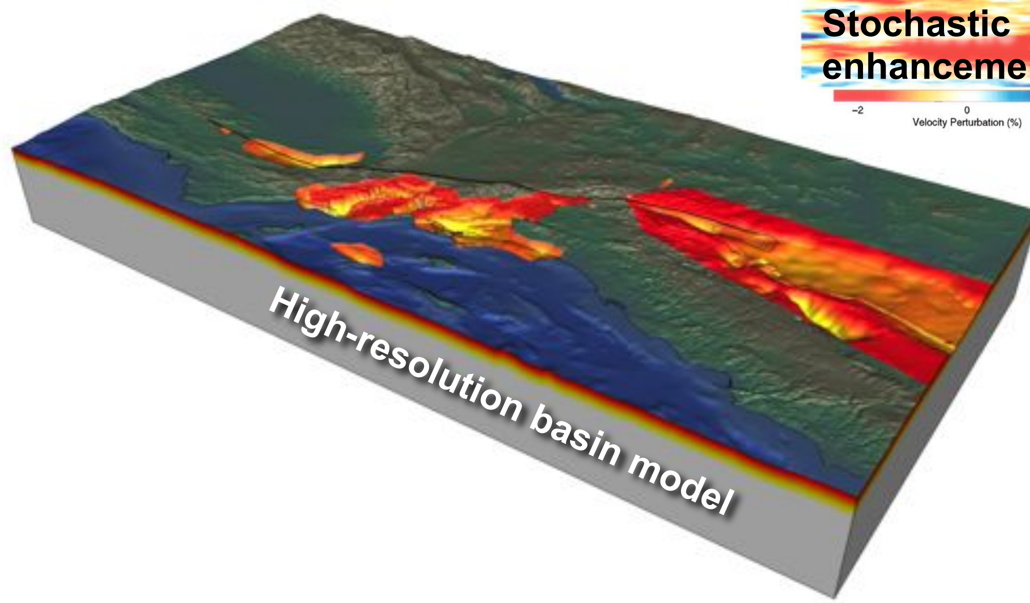

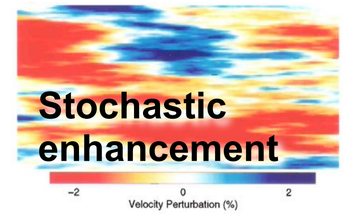

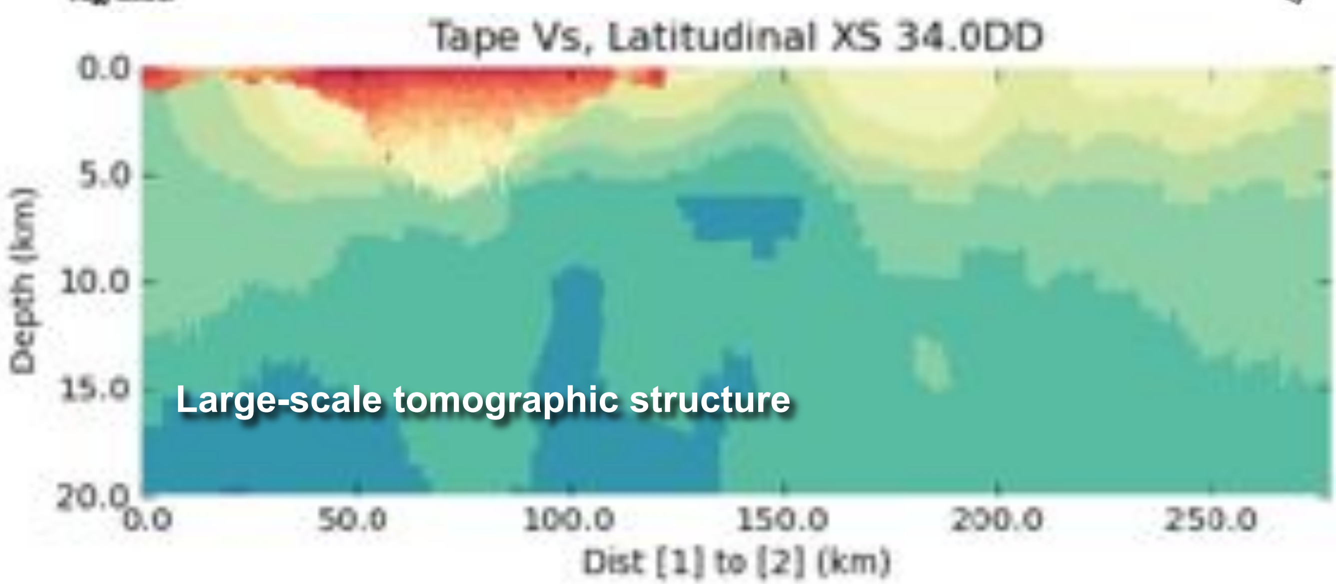

Components of 3D Seismic Velocity Structure

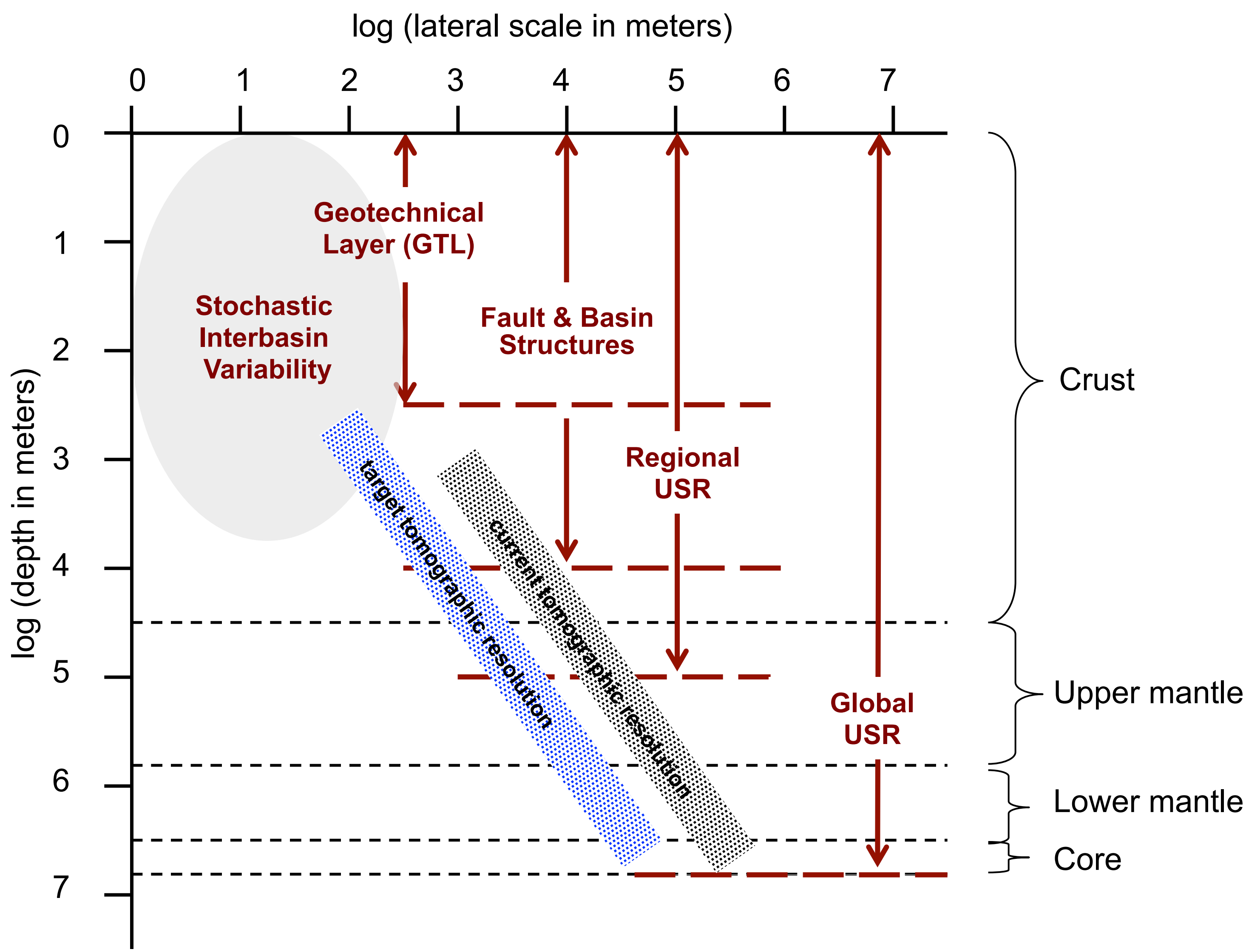

Dimensionalities of the Forward and Inverse Problems

	DESCRIPTION	DIMENSION OF REFERENCE MODEL	DIMENSION OF FRÉCHET KERNEL	DIMENSION OF INVERTED MODEL	EXAMPLES
INFINITE FREQUENCY	geometrical optics & linear inversion	1	3	3	Aki et al. (1977); Dziewonski et al. (1977)
	geometrical optics & 3-D ray tracing	3	3	3	Bijwaard & Spakman (2000)
INFINITE & FINITE FREQUENCY	geometrical optics for body waves & path average for surface waves	1	3/1	3	Su et al. (1994); Ritsema & van Heijst (2000)
FINITE FREQUENCY	path average	1	1	2	Nolet et al. (1986)
	surface-wave phase/group velocity inversion	1	1	3	Ekström et al. (1997); Wu & Levshin (1994)
	partitioned waveform inversion				Nolet (1990); Zielhaus & Nolet (1994)
	asymptotic mode coupling & 2-D inverison	1	2	2	Zhao & Jordan (1998); Katzman, Zhao & Jordan (1998)
	asymptotic mode coupling & 3-D inversion	1	2	3	Li & Tanimoto (1993); Li & Romanowicz (1996)
	mode-splitting function inversion				Widmer, Masters & Gilbert (1992)
	fully 3-D & linear inversion	1	3	3	Zhao , Jordan & Chapman (2001); Chen, Zhao & Jordan (2003)
F3DT	fully 3-D & non-linear inversion	3	3	3	Zhao , Jordan & Olsen (2003)

F3DT Formulation

Iterative model improvement

$$\mathbf{m}_{k+1} = \mathbf{m}_k + \Delta\mathbf{m}_k, \quad k = 0, 1, \ldots, K$$

At each iteration, we calculate a set of synthetic seismograms $\mathbf{u}_k = \mathbf{u}(\mathbf{m}_k)$ and measure a set of data functionals

$$\mathbf{d}_k = \mathbf{d}(\mathbf{u}_{\text{obs}}, \mathbf{u}_k)$$ functionals of the seismograms

$$= \mathbf{d}(\mathbf{m}_\oplus, \mathbf{m}_k) + \mathbf{n}$$ functionals of the Earth model

$$\mathbf{d}(\mathbf{u}_k, \mathbf{u}_k) = 0, \ \langle \mathbf{n} \rangle = 0$$ zero-bias assumption

$\mathbf{m}_\oplus$ is the "target model" (best approximation to data-generating model within considered model space)

Typically,

$$\dim[\mathbf{d}] \gg \dim[\mathbf{u}]$$

$$\dim[\mathbf{d}] \ll \dim[\mathbf{m}]$$

Data set for CVM-S4.26

Seismograms	
Earthquake seismograms	38,069
ANGF-h	10,853
ANGF-l	12,581
Total	61,503
Waveforms	
Earthquake waveforms	43,496
ANGF-h waveforms	10,853
ANGF-l waveforms	12,581
Total	66,930
GSDF Phase Delays	
Earthquake measurements	401,838
ANGF-h measurements	61,939
ANGF-l measurements	50,090
Total	513,867

F3DT Formulation

Construct model perturbation $\Delta\mathbf{m}_k$ by minimizing the quadratic objective function

$$\chi^2(\mathbf{m}_\oplus, \mathbf{m}_k) = \mathbf{d}^{\mathrm{T}}(\mathbf{m}_\oplus, \mathbf{m}_k)\, \mathbf{C}_d^{-1}\, \mathbf{d}(\mathbf{m}_\oplus, \mathbf{m}_k) \;+\; (\mathbf{m}_\oplus - \mathbf{m}_k)^{\mathrm{T}}\, \mathbf{C}_m^{-1}\, (\mathbf{m}_\oplus - \mathbf{m}_k)$$

Expand about $\mathbf{m}_k$ using the Jacobian

$$\mathbf{A}_k \equiv \partial \mathbf{d}(\mathbf{m}_\oplus, \mathbf{m}_k)/\partial \mathbf{m}_k$$ Fréchet derivative

$$\chi^2(\mathbf{m}_\oplus, \mathbf{m}_k) \approx \chi_k^2 + \mathbf{a}_k(\mathbf{m}_\oplus - \mathbf{m}_k) \;+\; \frac{1}{2}(\mathbf{m}_\oplus - \mathbf{m}_k)^{\mathrm{T}}\mathbf{H}_k\,(\mathbf{m}_\oplus - \mathbf{m}_k)$$

Constant term:

$$\chi_k^2 = \chi^2(\mathbf{m}_k, \mathbf{m}_k) = 0 \quad \text{if} \quad \mathbf{d}(\mathbf{u}_k, \mathbf{u}_k) = 0$$

Linear term:

$$\mathbf{a}_k \equiv \nabla_{\mathbf{m}_k}\chi^2(\mathbf{m}_\oplus, \mathbf{m}_k) = -\mathbf{A}_k^{\mathrm{T}}\mathbf{C}_d^{-1}\, \mathbf{d}(\mathbf{m}_\oplus, \mathbf{m}_k)$$ data-weighted Fréchet kernel

Quadratic term:

$$\mathbf{H}_k \equiv \nabla_{\mathbf{m}_k}\nabla_{\mathbf{m}_k}\chi^2(\mathbf{m}_\oplus, \mathbf{m}_k) = \mathbf{A}_k^{\mathrm{T}}\mathbf{C}_d^{-1}\,\mathbf{A}_k + \mathbf{C}_m^{-1} + (\nabla_{\mathbf{m}_k}\mathbf{A}_k)^{\mathrm{T}}\mathbf{C}_d^{-1}\,\mathbf{d}(\mathbf{m}_\oplus, \mathbf{m}_k)$$ Hessian

F3DT Formulation

Scattering-integral method (SI-F3DT):

Minimize objective function by zeroing its gradient with respect to the target model

$$\nabla_{\mathbf{m}_\oplus}\chi^2(\mathbf{m}_\oplus,\mathbf{m}_k) = \mathbf{a}_k + \mathbf{H}_k(\mathbf{m}_\oplus - \mathbf{m}_k) = 0$$

Make two approximations:

$$\mathbf{H}_k \approx \mathbf{A}_k^{\mathrm{T}}\mathbf{C}_d^{-1}\mathbf{A}_k + \mathbf{C}_m^{-1}$$

$$\mathbf{d}(\mathbf{m}_\oplus,\mathbf{m}_k) \approx \mathbf{d}_k = \mathbf{d}(\mathbf{u}_{\mathrm{obs}},\mathbf{u}_k)$$

This yields the Gauss-Newton (Gaussian-Bayesian) normal equations

$$(\mathbf{A}_k^{\mathrm{T}}\mathbf{C}_d^{-1}\mathbf{A}_k + \mathbf{C}_m^{-1})\Delta\mathbf{m}_k = \mathbf{A}_k^{\mathrm{T}}\mathbf{C}_d^{-1}\mathbf{d}_k$$

More efficient to solve the equivalent linear system by a parallelized LSQR algorithm

$$\begin{bmatrix}\mathbf{C}_d^{-1/2}\mathbf{A}_k \\ \mathbf{C}_m^{-1/2}\end{bmatrix}\Delta\mathbf{m}_k = \begin{bmatrix}\mathbf{C}_d^{-1/2}\mathbf{d}_k \\ \mathbf{0}\end{bmatrix}$$

F3DT Formulation

Adjoint-wavefield method (AW-F3DT):

Minimize objective function by a conjugate gradient method.

Approximate the gradient with the data value

$$\mathbf{a}_k \approx -\mathbf{A}_k^{\mathrm{T}}\mathbf{C}_d^{-1}\,\mathbf{d}_k$$

Solve for this data-weighted Fréchet kernel by integrating the seismic wavefield against an adjoint wavefield that has $\mathbf{d}_k$ as its source.

Owing to linearity, the adjoint source for a particular seismic source can be summed over seismograms of a particular component, so only a single adjoint-wavefield calculation is required for each source and component, no matter how many receivers are measured.

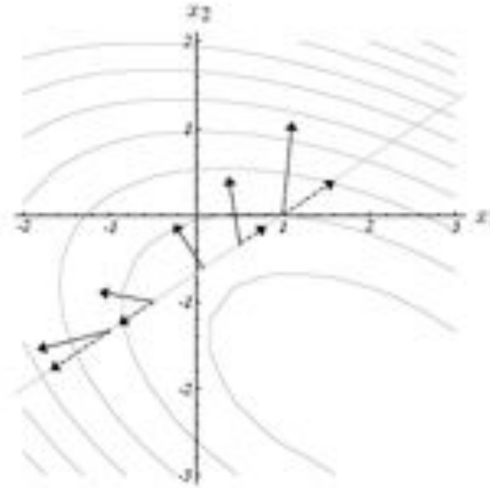

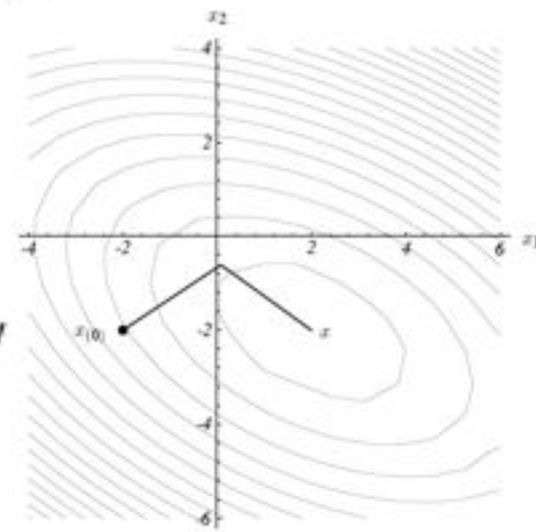

F3DT Formulation

Table 1. Comparison of computational costs for a single optimization step of the scattering-integral (SI) and adjoint-wavefield (AW) methods.

Cost	SI method	AW–CG[a]	AW–GN[b]
Storage requirement	$3N_r N_V N_T$	N_V	N_V
Number of simulations	$3N_r + N_s$	$6N_s$	$4N_{CG}N_s + 2N_s$
Number of time integrations	$2N_r N_V N_u$	$2 N_V N_s$	$N_V (2N_{CG}N_s + N_s)$
I/O cost	$N_u N_T N_V$	$2N_s N_V$	$(2N_{CG}N_s + N_s)N_V$
Requires solving a linear system?	Yes	No	Yes
Optimization algorithm	Gauss–Newton	Conjugate-Gradient	Gauss–Newton
Number of iterations needed to match one Gauss–Newton step	1	6–7	1

Table 2. Computational parameters for the Los Angeles Basin tomography using the SI method.

Number of stations N_r	48
Number of earthquakes N_s	67
Number of seismograms N_u	2000
Number of FD simulations $3N_r + N_s$	211
Simulation grid spacing, time interval	200 m, 0.01 s
Simulation grid points N_V, time steps N_T	36 140 440, 6000
Number of CPUs	128
Total CPU time per iteration	62 000 CPU-hours
Total disk space $3N_r N_V N_T$	24 TB

From Chen et al. (2007a)

SI vs. AW-CG methods:

- **SI requires much more storage; quadratic convergence**
- **AW requires much more computation; linear convergence**
- **SI provides Fréchet kernels and source partial derivatives, as well as RGTs for CyberShake**

Seismological Data Functionals

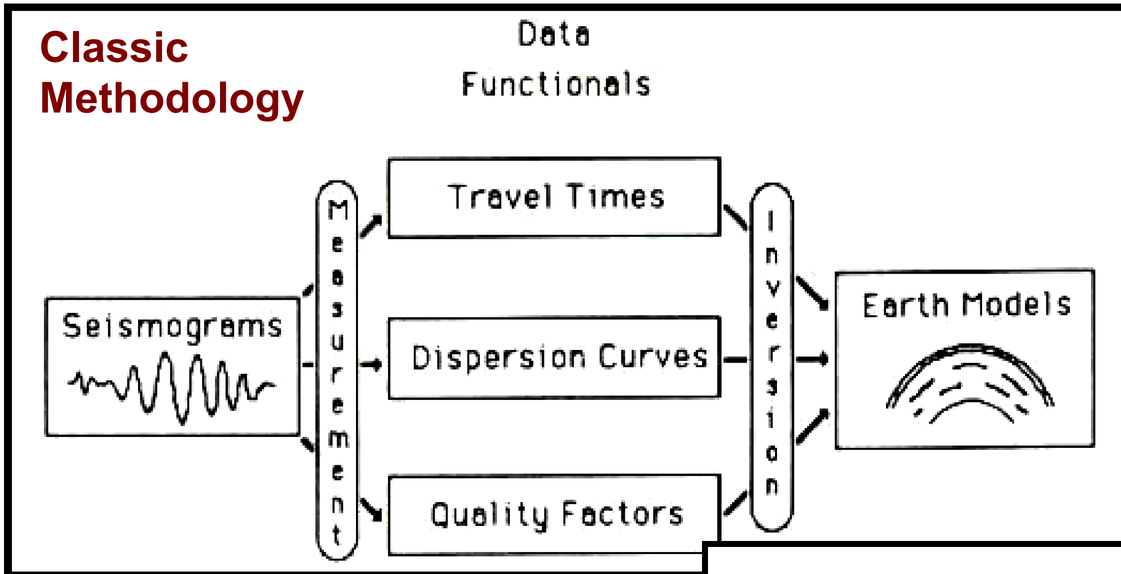

Data assimilation principle:

- **Revise earth model to reduce data discrepancies**
- **Invert *differential* data functionals for Earth structure to improve synthetic seismograms**

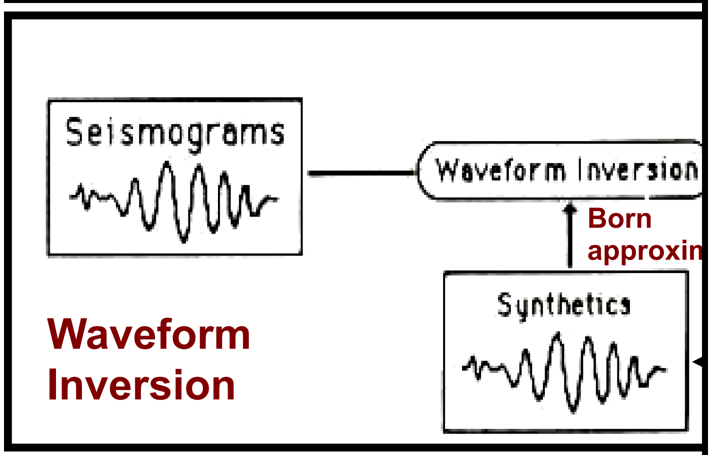

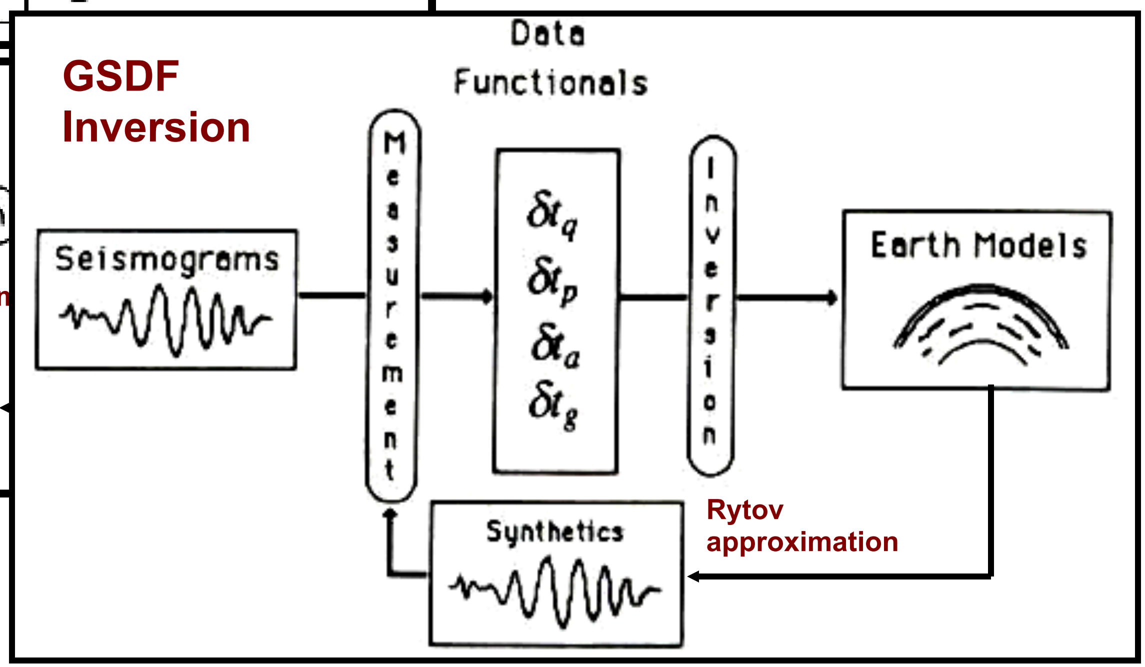

Differential Data Functionals

Observed seismogram from unknown (target) model $\mathbf{m}$ $\quad u_i^s(\mathbf{x}_r, t)$

Synthetic seismogram from reference model $\tilde{\mathbf{m}}$ $\quad \tilde{u}_i^s(\mathbf{x}_r, t)$

s source index
r receiver index
i component index

$$d_{in}^{sr} = D_n[u_i^s(\mathbf{x}_r, t), \tilde{u}_i^s(\mathbf{x}_r, t)]$$

Differential data functional
(n waveform/frequency index)

$$D_n[\tilde{u}_i^s(\mathbf{x}_r, t), \tilde{u}_i^s(\mathbf{x}_r, t)] = 0$$

No-bias constraint

$$\delta d_{in}^{sr} = \int dt\ J_{in}^{sr}(t)\ \delta u_i^s(\mathbf{x}_r, t)$$

Seismogram perturbation kernel

Differential Data Functionals

$$\delta\mathbf{m} = \mathbf{m} - \tilde{\mathbf{m}} = \begin{bmatrix} \delta\rho(\mathbf{x}) \\ \delta c_{jklm}(\mathbf{x}) \end{bmatrix}$$

Model perturbation

$$\delta u_i^s(\mathbf{x}_r, t) = -\int dV(\mathbf{x}) \int d\tau \sum_j [G_{ij}(\mathbf{x}_r, t-\tau; \mathbf{x})\, \partial_\tau^2 u_j^s(\mathbf{x}, \tau)\, \delta\rho(\mathbf{x}) + \sum_{jklm} \partial_k G_{ij}(\mathbf{x}_r, t-\tau; \mathbf{x})\ \partial_l u_m^s(\mathbf{x}, \tau)\, \delta c_{jklm}(\mathbf{x})]$$

Born approximation

$$G_{ij}(\mathbf{x}_r, t-\tau; \mathbf{x}) = \boxed{G_{ji}(\mathbf{x}, t-\tau; \mathbf{x}_r)}$$

"receiver Green tensor" (RGT)

Green tensor reciprocity

$$K^{\rho}_{d_{in}^{sr}}(\mathbf{x}) = -\int dt \int d\tau J_{in}^{sr}(t) \sum_j G_{ji}(\mathbf{x}, t-\tau; \mathbf{x}_r)\partial_\tau^2 u_j^s(\mathbf{x}, \tau)$$

$$K^{c_{jklm}}_{d_{in}^{sr}}(\mathbf{x}) = -\int dt \int d\tau J_{in}^{sr}(t)\, \partial_k G_{ji}(\mathbf{x}, t-\tau; \mathbf{x}_r)\, \partial_l u_m^s(\mathbf{x}, \tau)$$

Model perturbation kernels (exact)

$$\delta\mathbf{d} = \mathbf{A}\,\delta\mathbf{m} = \int dV(\mathbf{x})\mathbf{K}_d(\tilde{\mathbf{m}}, \mathbf{x}) \cdot \delta\mathbf{m}(\mathbf{x}) \approx \mathbf{d}(\mathbf{m}) - \mathbf{d}(\tilde{\mathbf{m}}).$$

Model perturbation equation (first-order)

Seismic Reciprocity: Key to CyberShake

- **To account for source variability requires very large sets of simulations**
  - **13,000 ruptures in SoCal; 600,000 rupture variations to sample rupture variability**
- **Ground motions can be calculated at much smaller number of surface sites to produce hazard map**
  - **225 in LA region, interpolated using empirical attenuation relations**
- **Elastodynamic representation theorem**

$$u_n(x,t) = \int_{-\infty}^{\infty} d\tau \int_{\Sigma} d\sigma(\xi) \frac{\partial}{\partial \xi_j} G_{ni}(x,t;\xi,\tau)\, \Gamma_{ij}(\xi,t-\tau)$$

- **Reciprocity**

$$G_{ni}(x,t;\xi,\tau) = G_{ni}(\xi,-\tau;x,-t)$$

- **Strain Green tensor (SGT)**

$$H_{ijn}(x,t;\xi,\tau) = \frac{1}{2}\left[\frac{\partial}{\partial x_i} G_{jn}(x,t;\xi,\tau) + \frac{\partial}{\partial x_j} G_{in}(x,t;\xi,\tau)\right]$$

- **Site-oriented simulation**

$$u_n(x,t) = \int_{-\infty}^{\infty} d\tau \int_{\Sigma} d\sigma(\xi) H_{ijn}(\xi,\tau;x,t)\, \Gamma_{ij}(\xi,t-\tau)$$

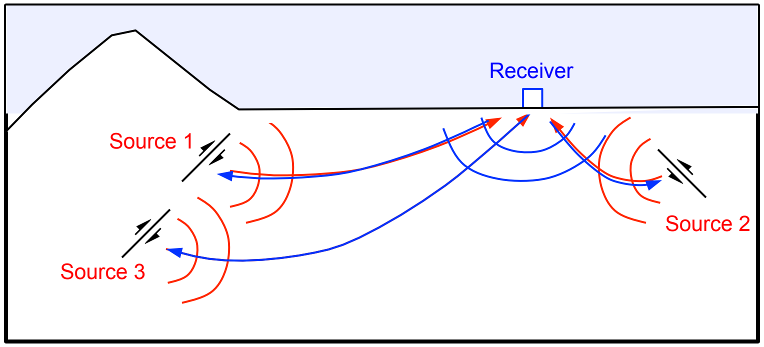

***M* sources to *N* receivers requires *M* simulations**

***M* sources to *N* receivers requires 3*N* simulations**

- ***Use of reciprocity reduces CPU time by a factor of ~1,000***

Differential Data Functionals

Example: differential waveform inversion

$$d_{in}^{sr} = u_i^s(\mathbf{x}_r, t_n) - \tilde{u}_i^s(\mathbf{x}_r, t_n)$$

$$\delta d_{in}^{sr} = \int dt \; J_{in}^{sr}(t) \; \delta u_i^s(\mathbf{x}_r, t)$$

$$J_{in}^{sr}(t) \quad \delta(t - t_n)$$

But this use of the Born approximation requires that the time shift be small compared to a wavelength:

$$\omega_0 \Delta T_{in}^{sr} << 1$$

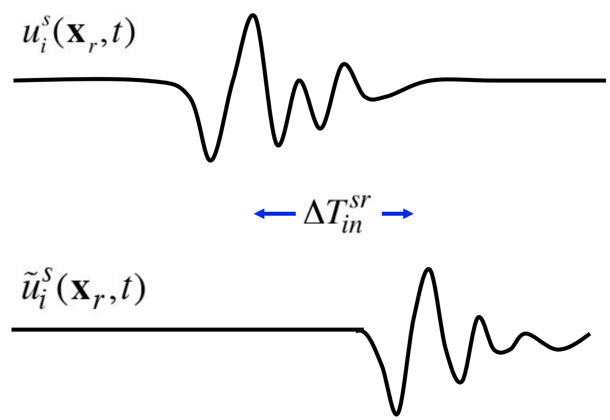

Differential Data Functionals

Better functionals:

Differential travel time

$$d_{in}^{sr} = \Delta T_{in}^{sr}$$

$$J_{in}^{sr}(t) = -\frac{\partial_t u_i^s(\mathbf{x}_r,t)[H(t-t_n)-H(t-t_n')]}{\int_{t_n}^{t_n'} |\partial_t u_i^s(\mathbf{x}_r,t)|^2\, dt}$$

Differential relative amplitude

$$d_{in}^{sr} = \Delta(\ln U_{in}^{sr}) \approx \Delta U_{in}^{sr} / \tilde{U}_{in}^{sr}$$

$$J_{in}^{sr}(t) = \frac{u_i^s(\mathbf{x}_r,t)[H(t-t_n)-H(t-t_n')]}{\int_{t_n}^{t_n'} [u_i^s(\mathbf{x}_r,t)]^2\, dt}$$

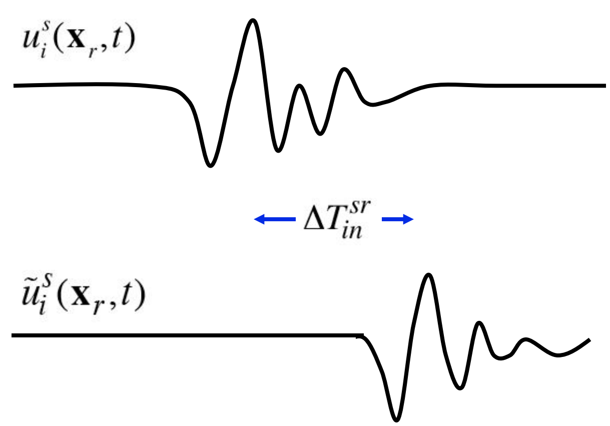

Differential Data Functionals

Generalized seismological data functionals:

Observed phase delay time Δt_{p}

$$d_{in}^{sr} = \Delta T_{in}^{sr}(\omega)$$

Observed amplitude reduction time Δt_{q}

$$d_{in}^{sr} = -\frac{1}{\omega} \Delta \ln U_{in}^{sr}(\omega)$$

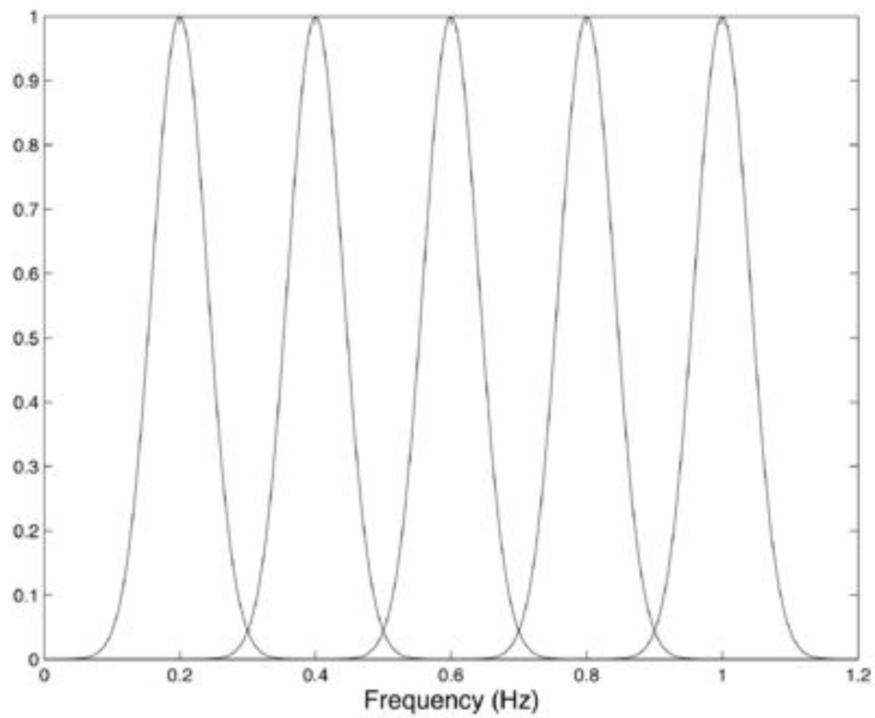

Differential waveform operator:

$$w_n[u_i^s(x_r,\omega)] = D_{in}^{sr}(\omega)\, w_n[\bar{u}_i^s(x_r,\omega)]$$

$$D_{in}^{sr}(\omega) = \mathrm{e}^{i\omega\Delta T_{in}^{sr}(\omega)}\, \mathrm{e}^{-\Delta \ln U_{in}^{sr}(\omega)} = \mathrm{e}^{i\omega[\Delta t_{\mathrm{p}}(\omega) + i\Delta t_{\mathrm{q}}(\omega)]}$$

GSDF Processing

Windowed, filtered cross-correlagram is a Gaussian wavelet:

$$C_{w\bar{w}}(t) \sim e^{-\omega_0 \Delta t_q} e^{-\sigma(t-\Delta t_g)^2} \cos[(\omega - \sigma^2 \Delta t_a)(t - \Delta t_p)]$$

Data

Synthetic

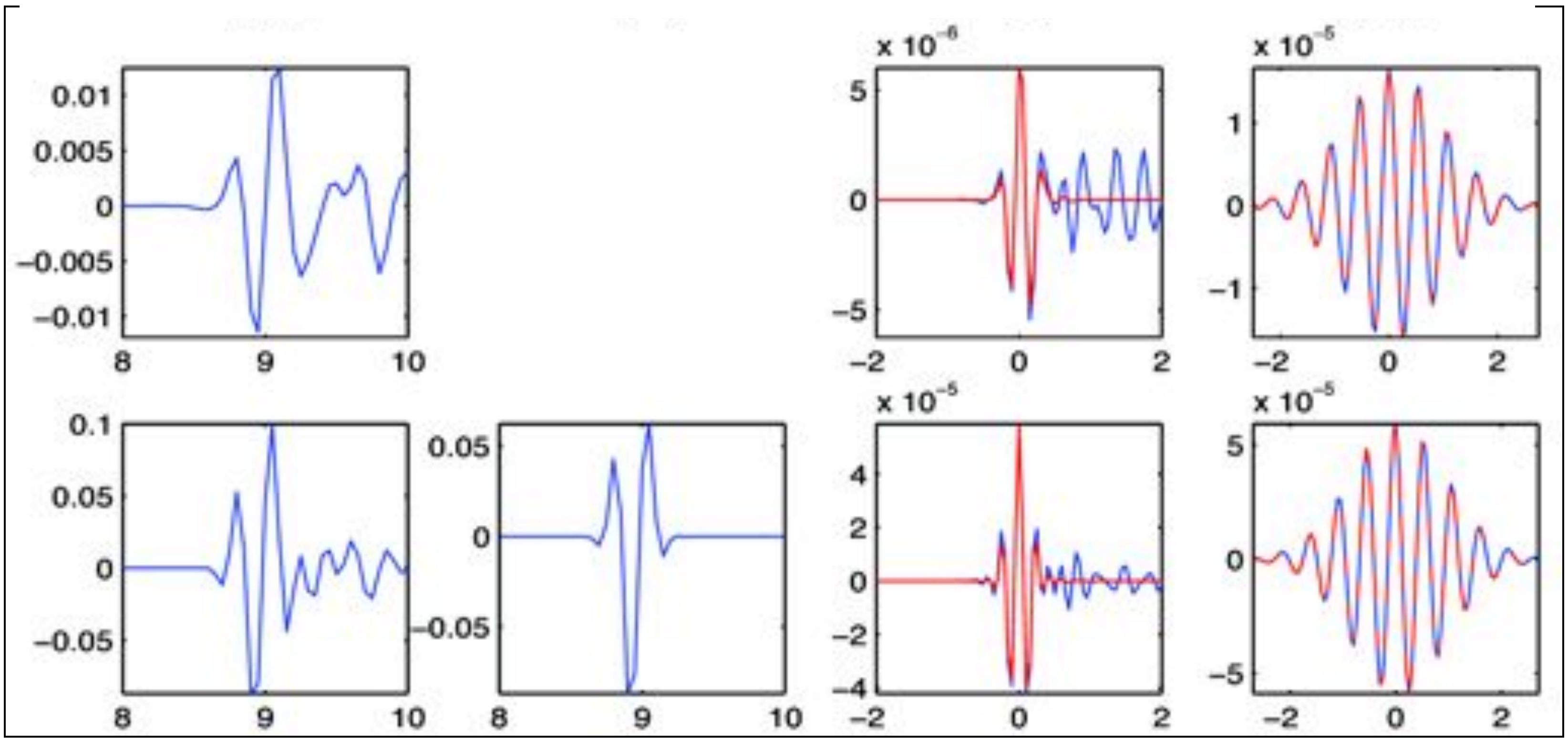

Seismogram | Isolation filter | Windowed cross-correlagram | Filtered cross-correlagram

GSDF Waveform Fitting

Unperturbed

Fit at 1 frequency

Fit at 3 frequencies

Fit at 5 frequencies

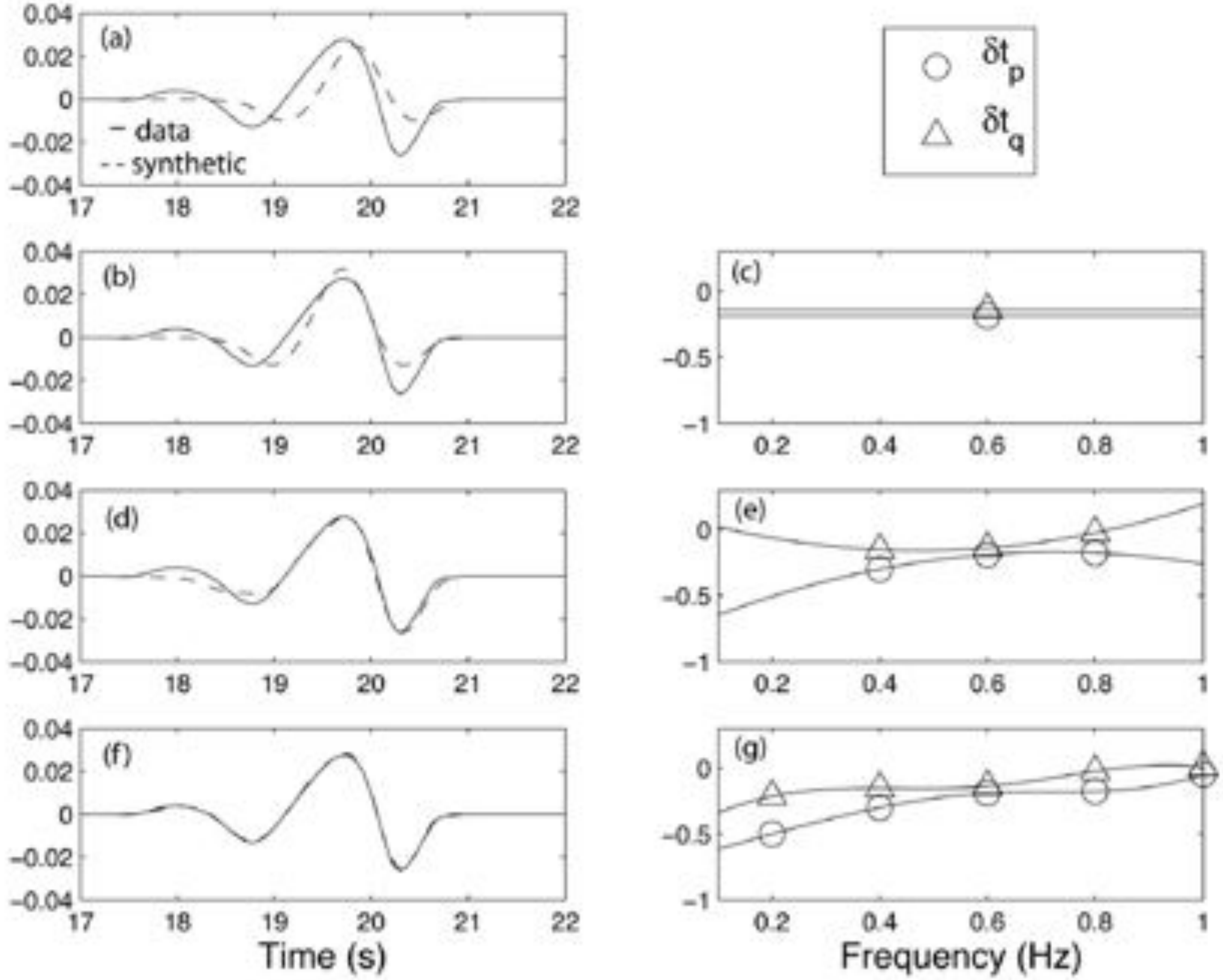

GSDF Measurements

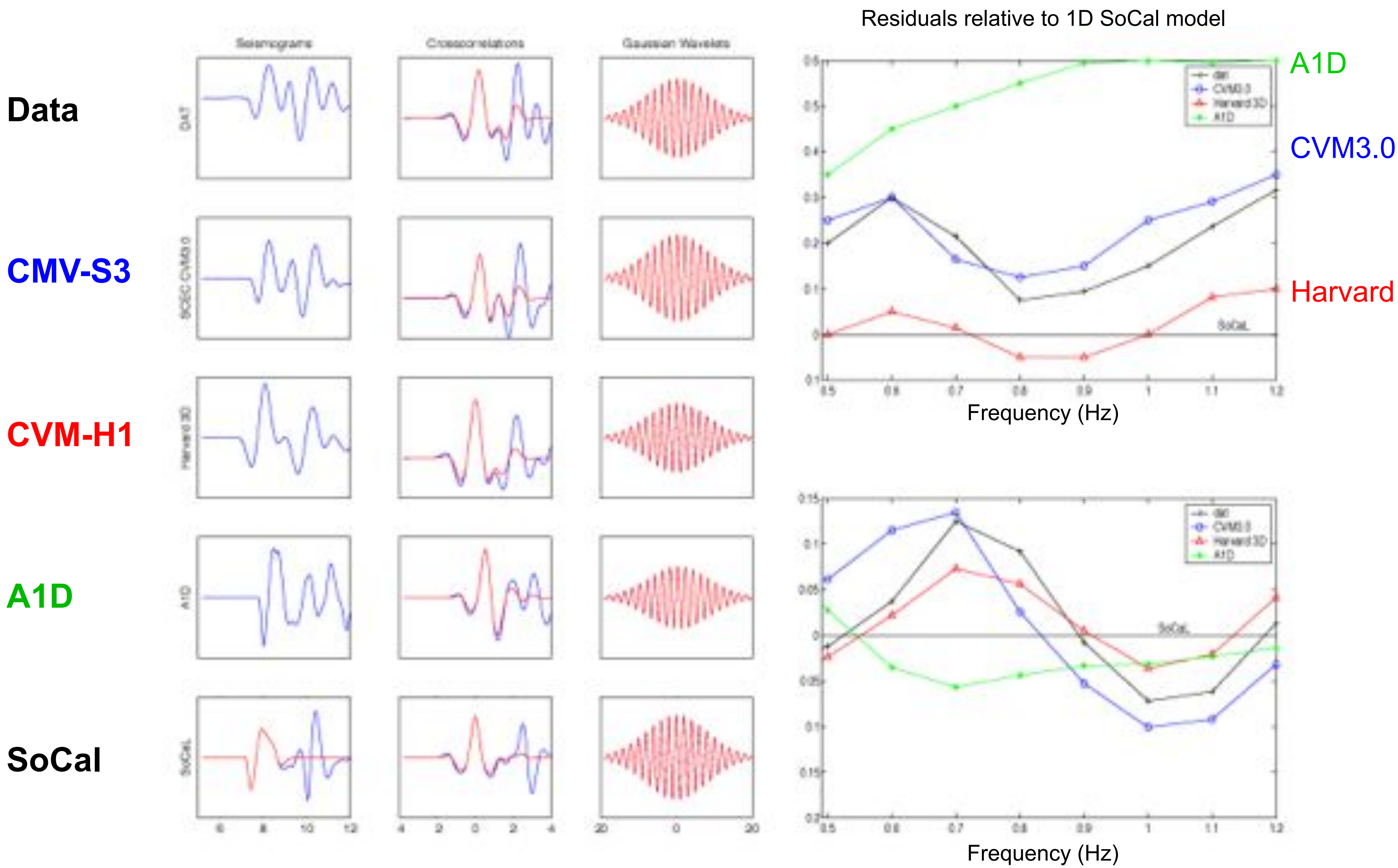

GSDF residuals, LA region

- **Harvard Model (Süss & Shaw, 2003)**
  - full 3D model
  - v_s scaled from v_p
  - topography & attenuation included
- **SCEC CMV3.0 (Kohler et al., 2003)**
  - full 3D model
  - v_s scaled from v_p
  - no topography or attenuation
- **A1D**
  - 1D path averages of CMV 3.0
- **SoCal (Dreger & Helmberger, 1993)**
  - 1D reference model for Southern California

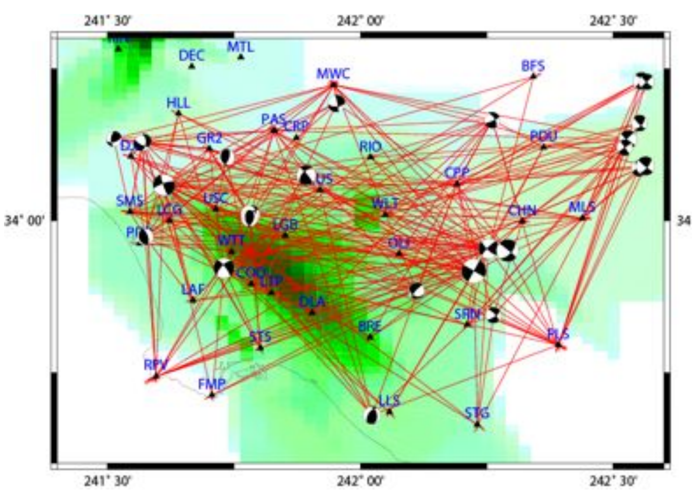

From Chen et al. (2007)

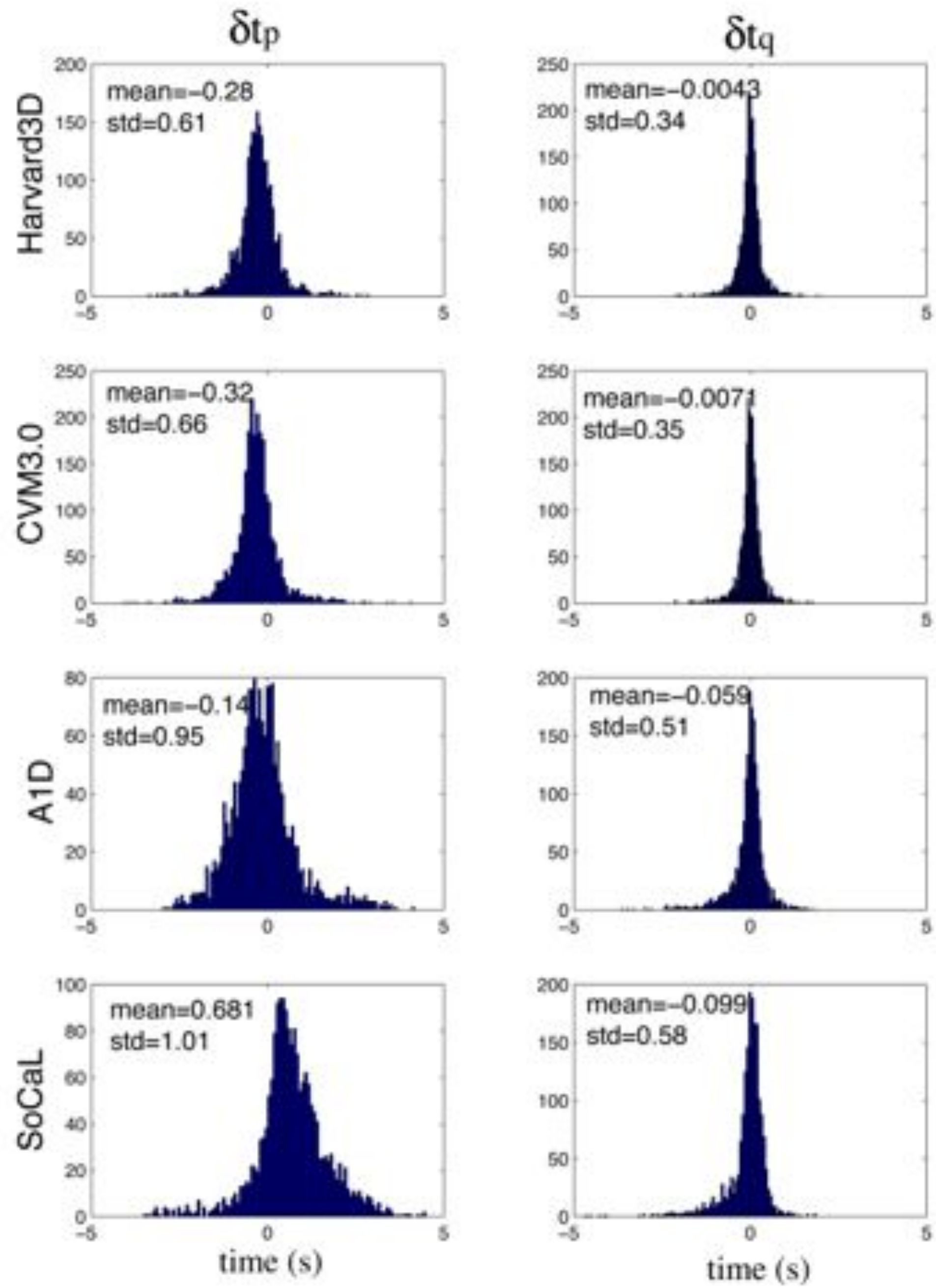

4940 GSDF measurements

GSDF residuals, LA region

- **Harvard Model (Süss & Shaw, 2003)**
  - full 3D model
  - v_s scaled from v_p
  - topography & attenuation included
- **SCEC CMV3.0 (Kohler et al., 2003)**
  - full 3D model
  - v_s scaled from v_p
  - no topography or attenuation
- **A1D**
  - 1D path averages of CMV 3.0
- **SoCal (Dreger & Helmberger, 1993)**
  - 1D reference model for Southern California

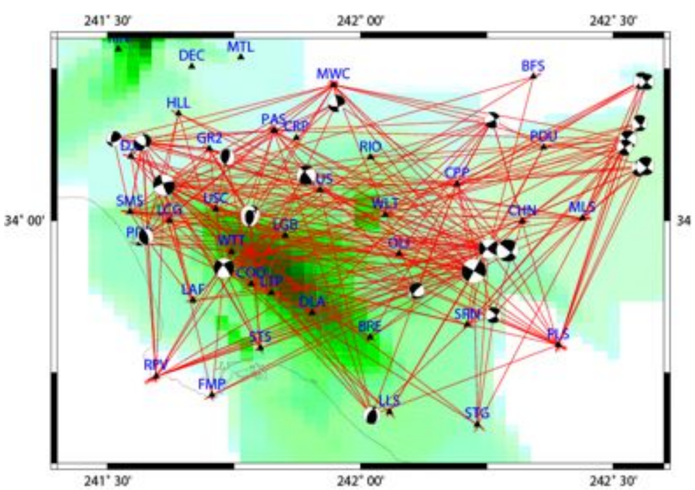

From Chen et al. (2007)

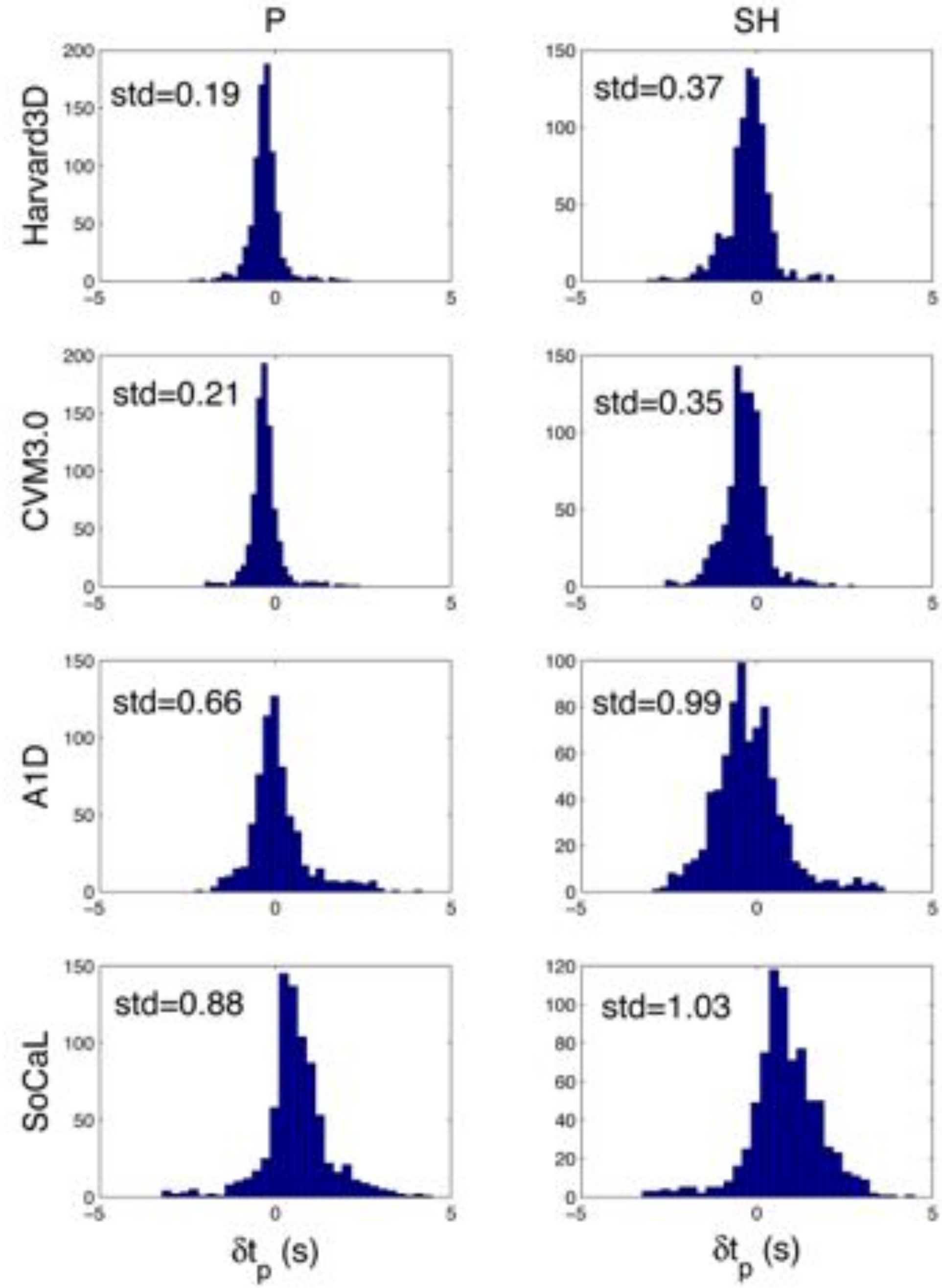

Full 3D Waveform Tomography in Southern California

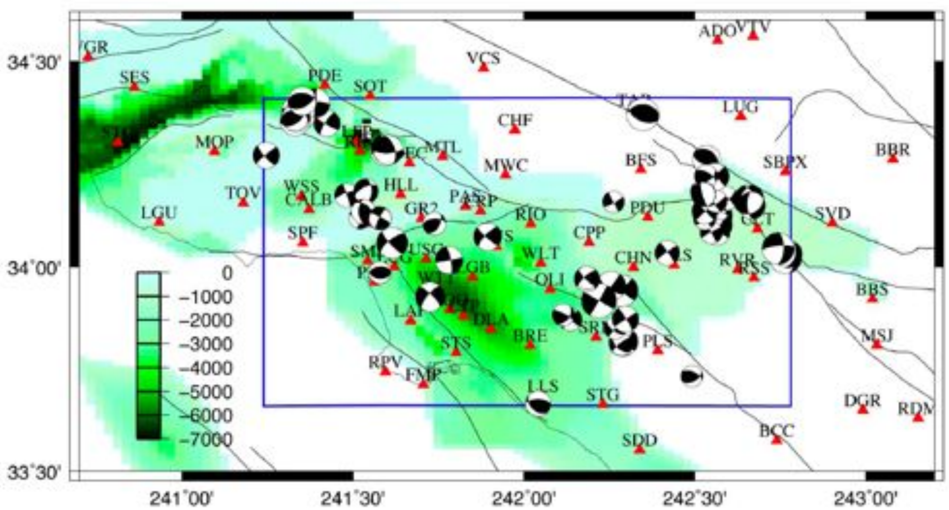

LA Region
Chen et al. (2007)

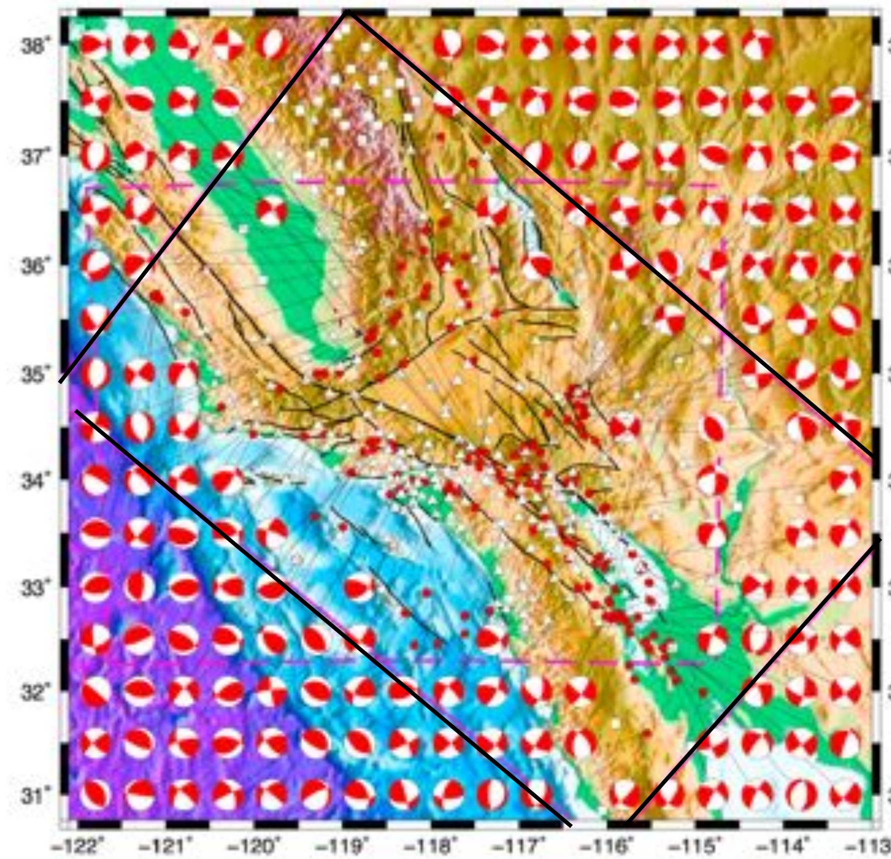

TeraShake Simulation Box
Lee et al. (2014)

GSDF Kernels

P waves

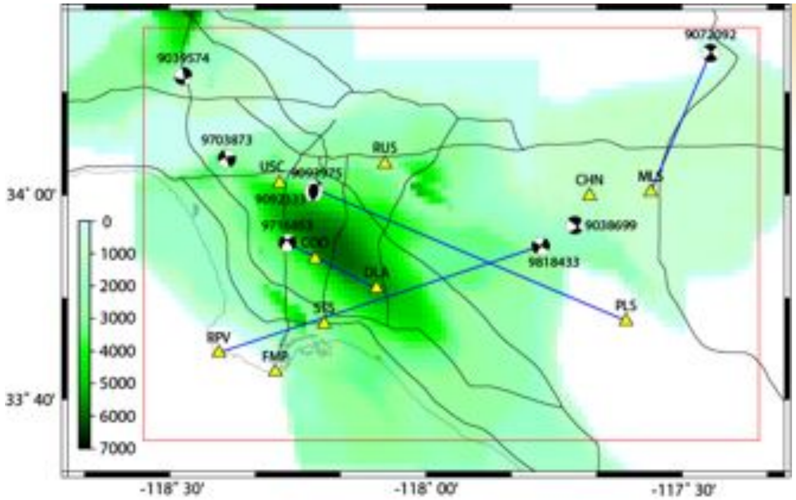

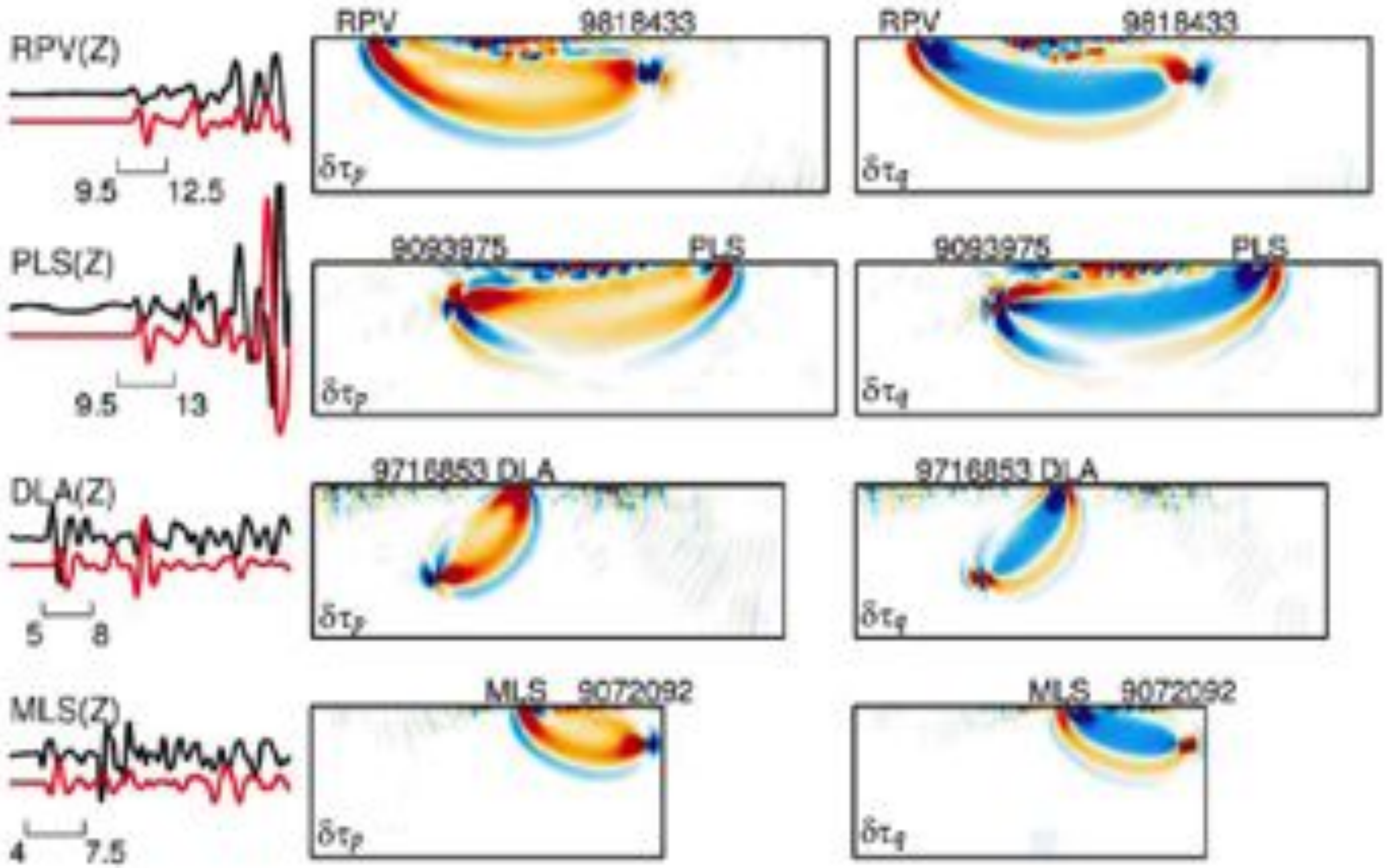

GSDF Kernels

S waves

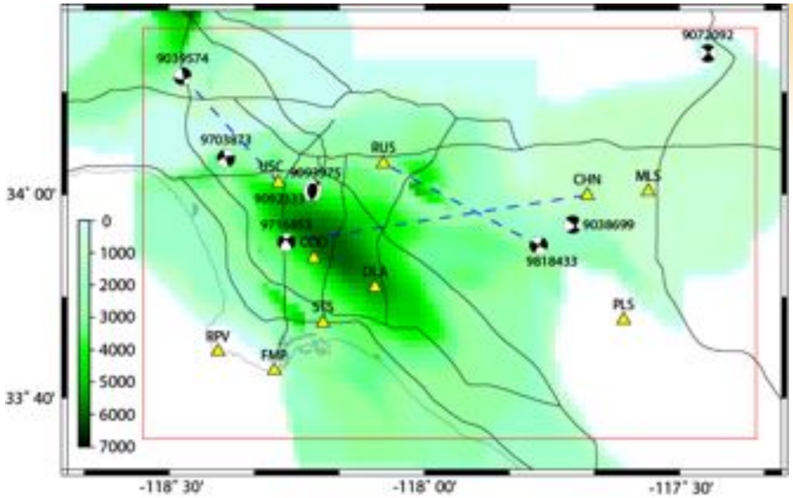

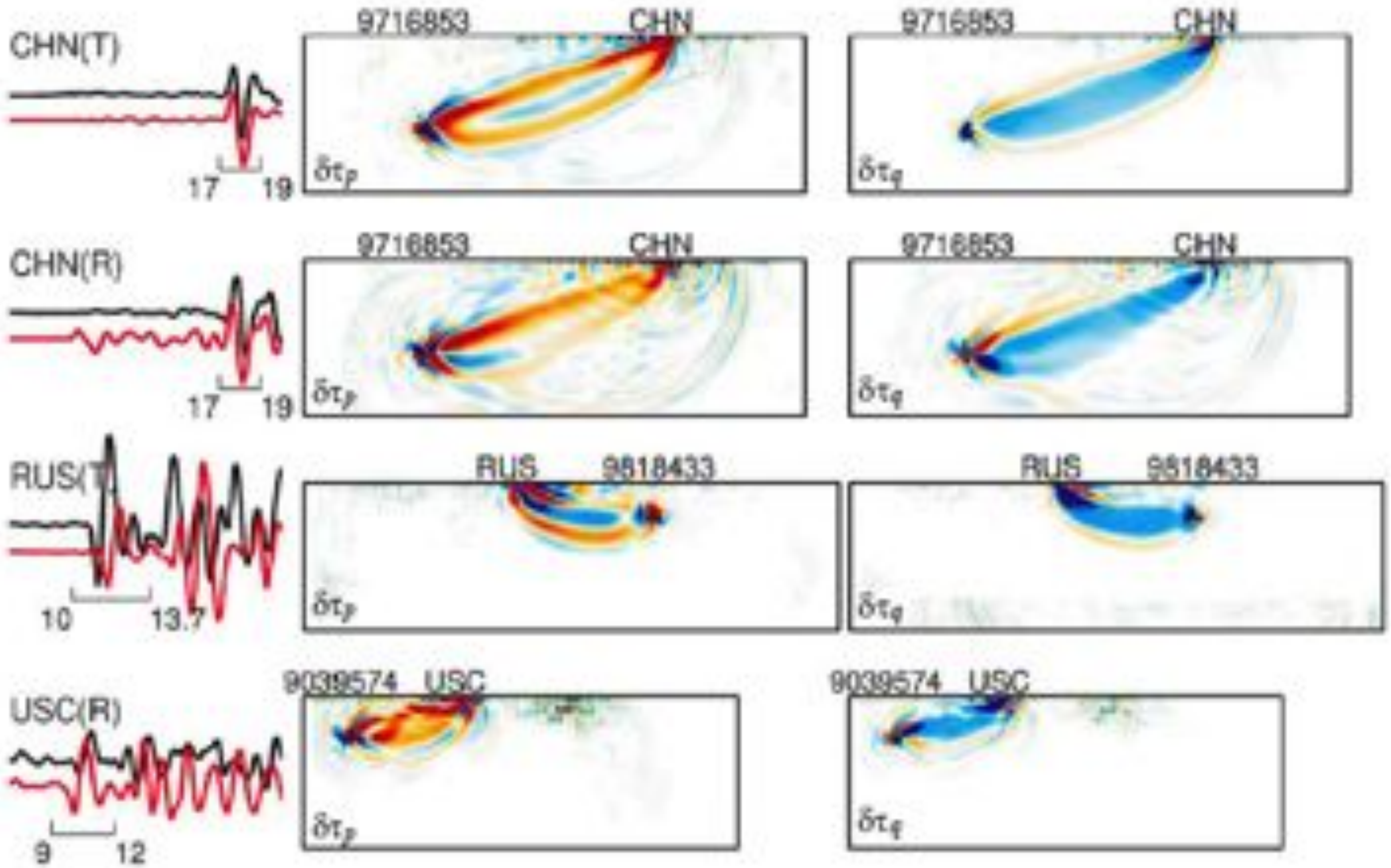

GSDF Kernels

Other phases

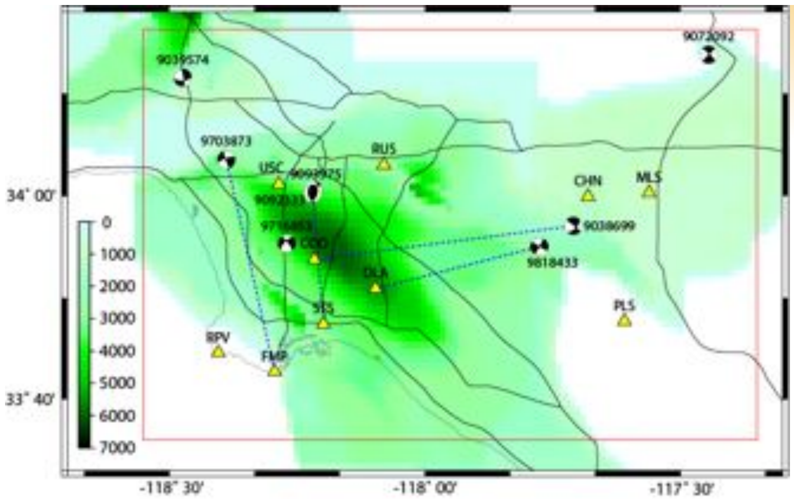

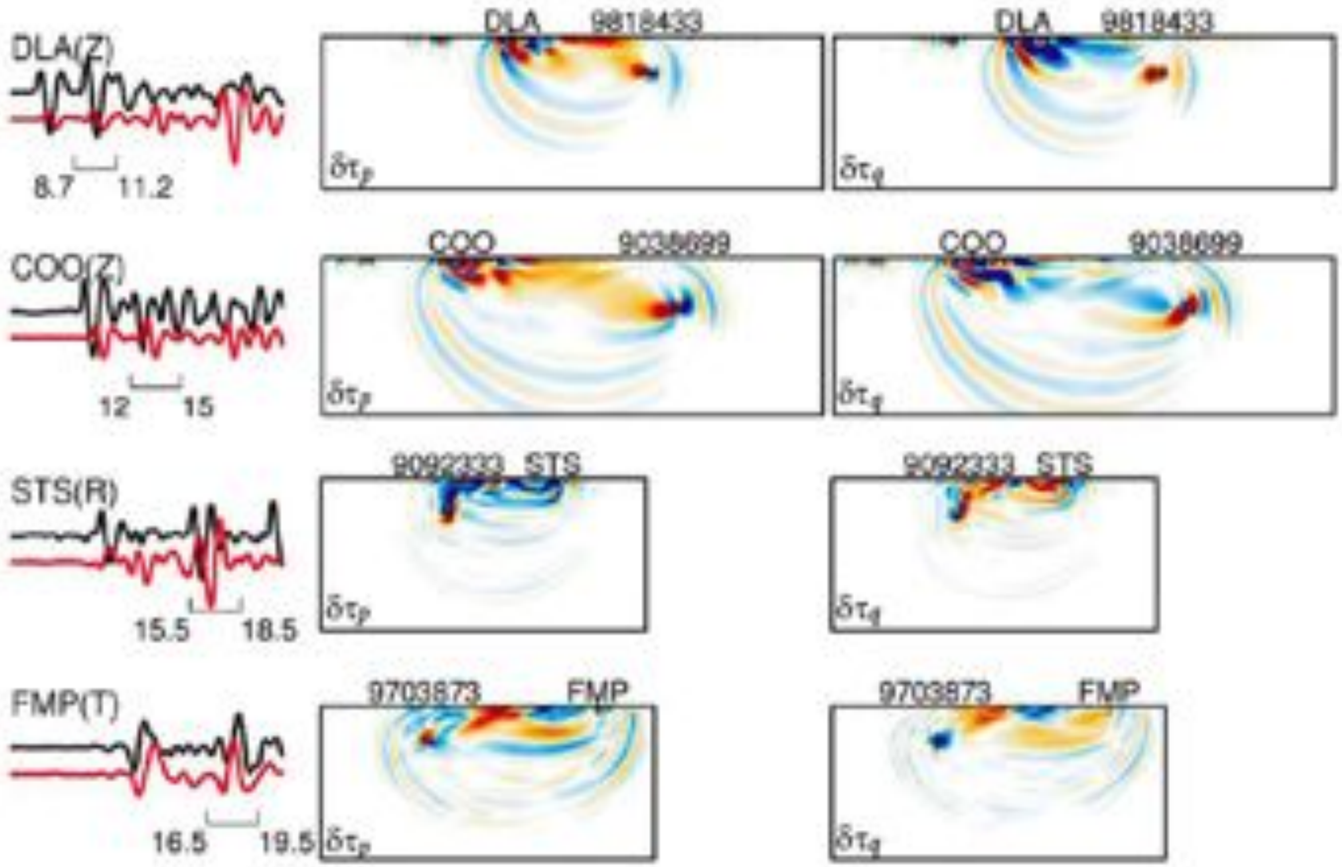

GSDF Kernels

Frequency Dependence

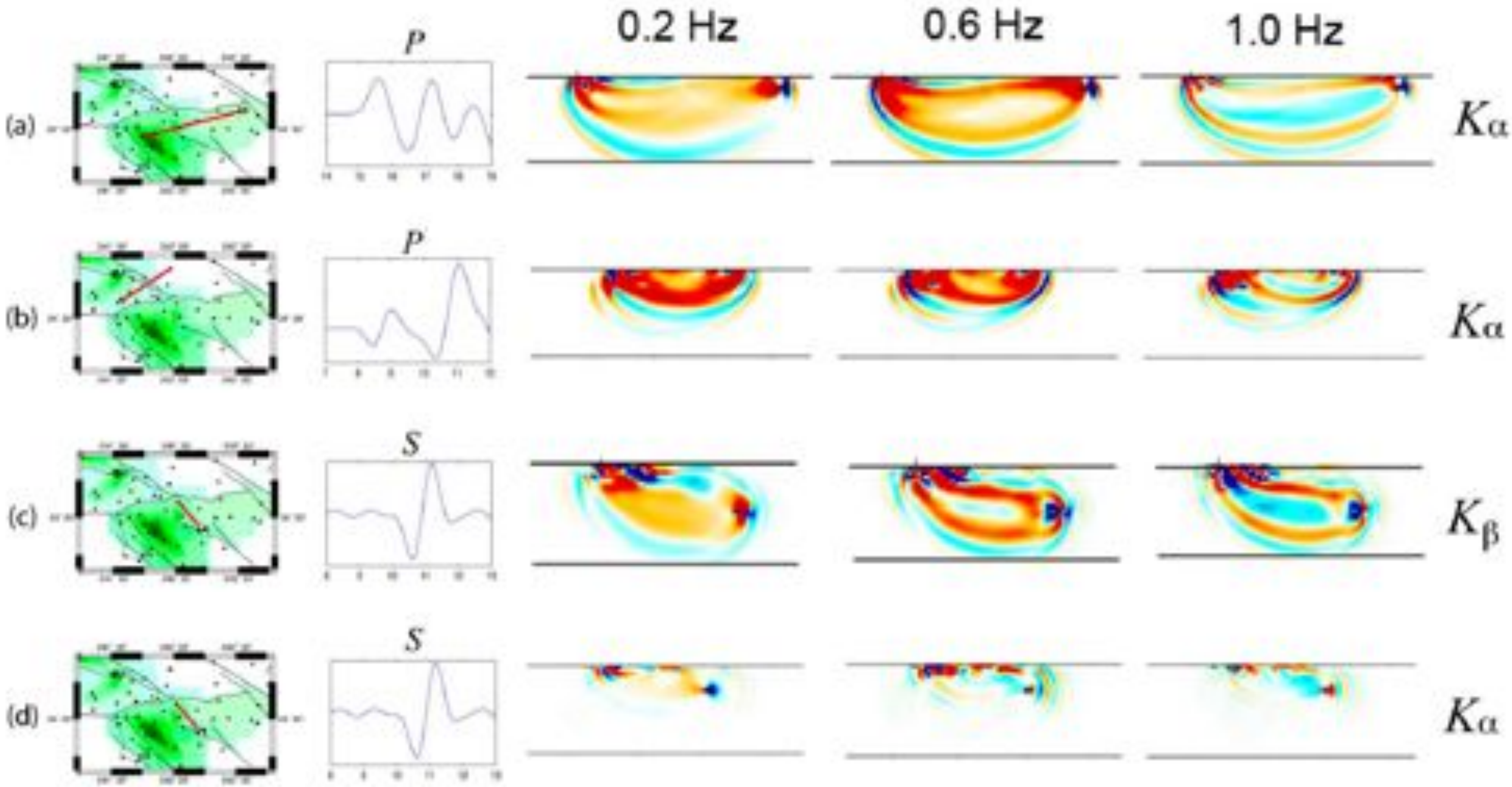

Paths **Waveforms** **Fréchet kernels**

Full-3D Waveform Tomography

SI-F3DT method (Chen, Zhao & Jordan, 2007)

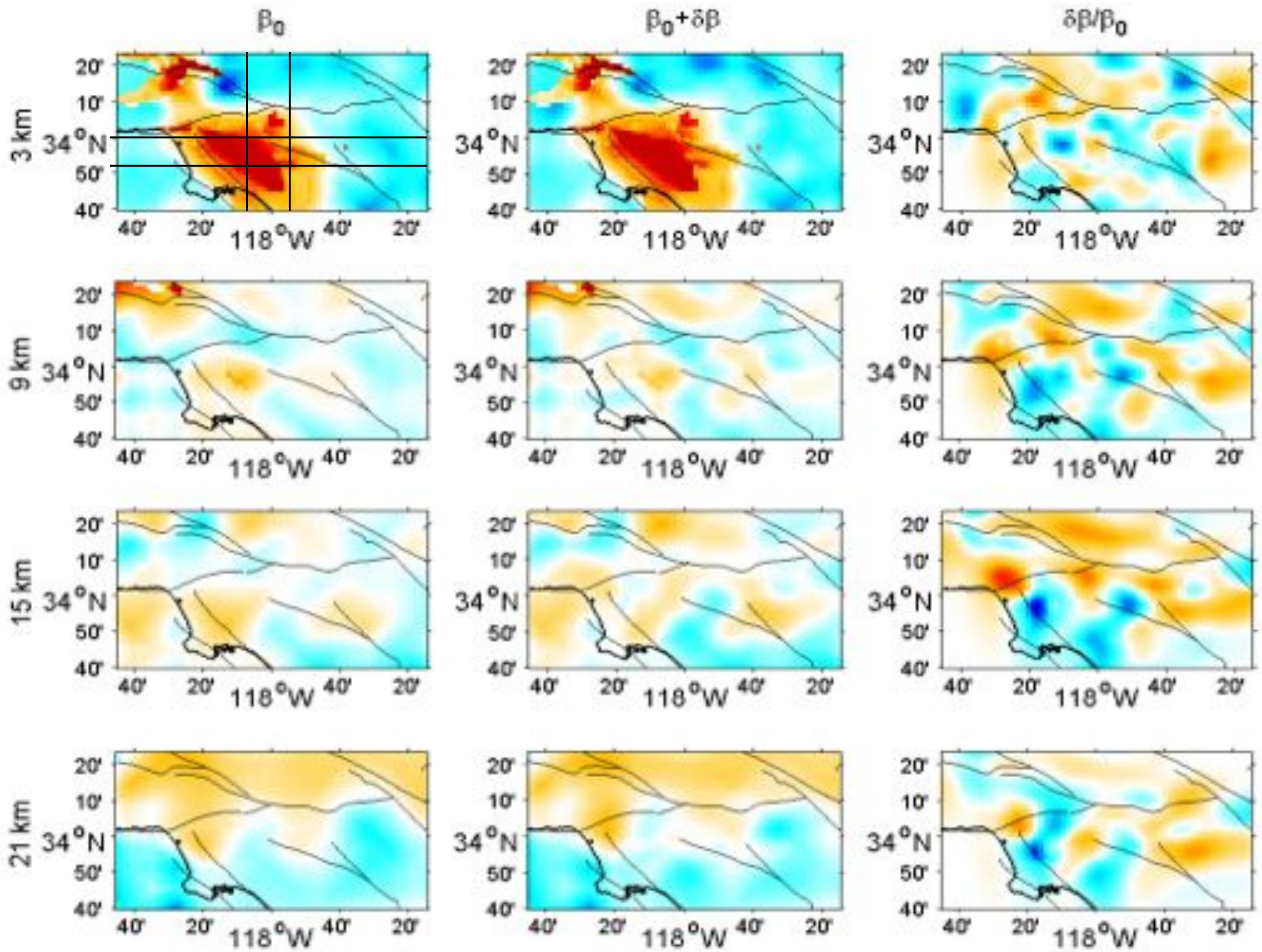

Starting Model **Improved Model** **Model Perturbation**

Full-3D Waveform Tomography

AW-F3DT method (Tape, Liu, Maggi & Tromp, 2010)

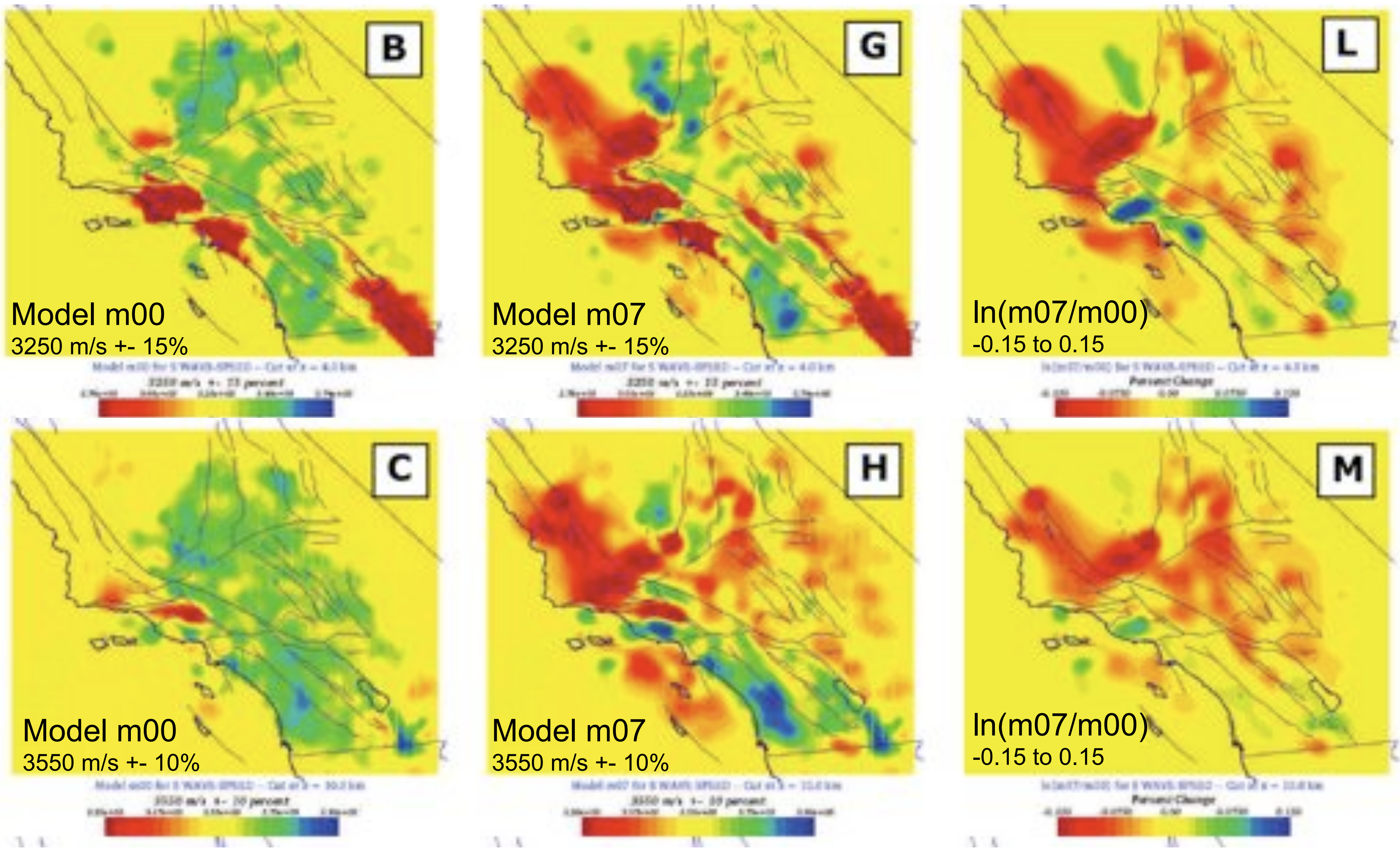

Full-3D Waveform Tomography

Both AW and SI methods (Lee, Chen, Jordan, Maechling, Denolle & Beroza, 2010)

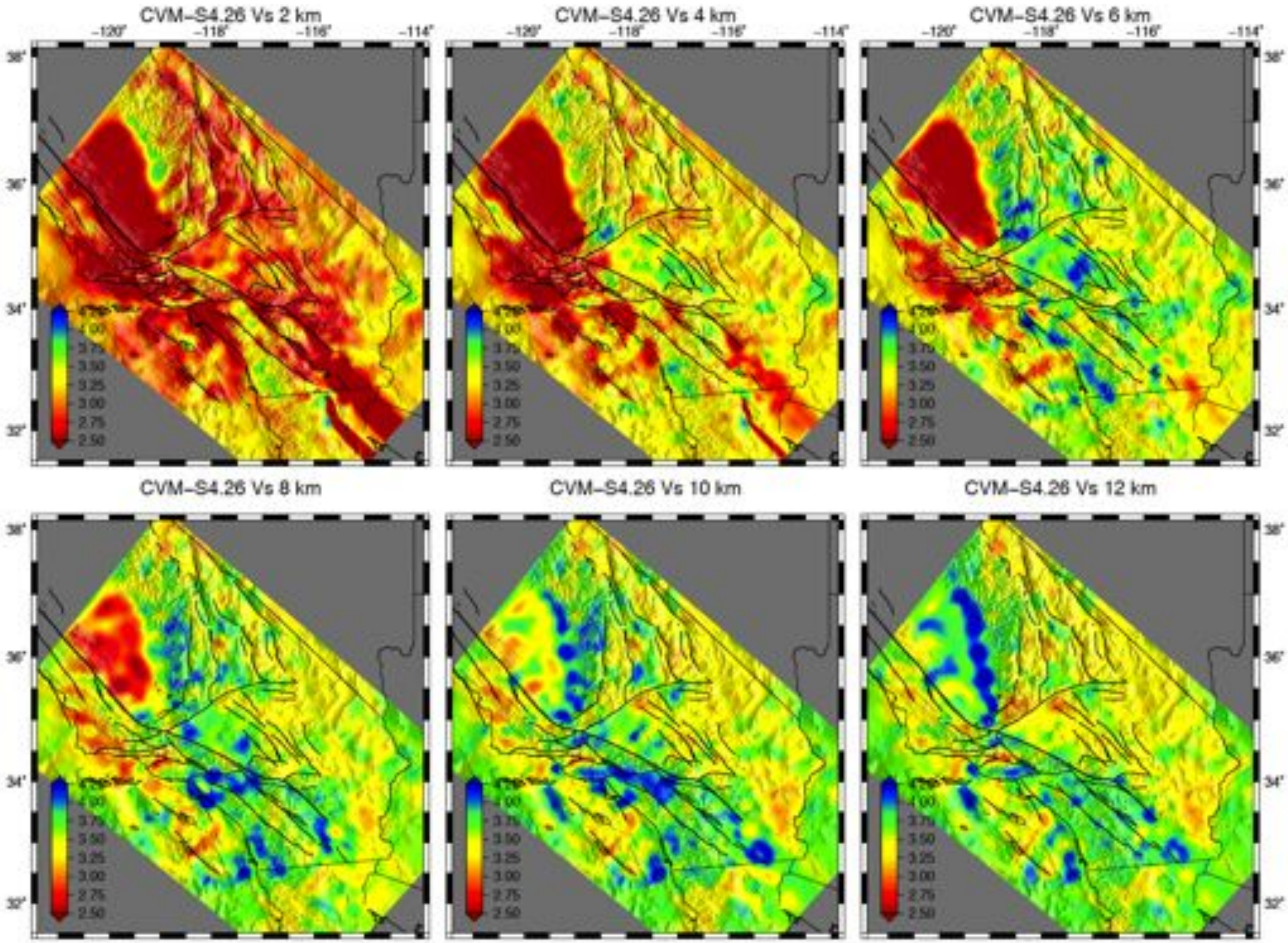

CVM-S4.26

Full-3D tomography model of Southern California crustal structure

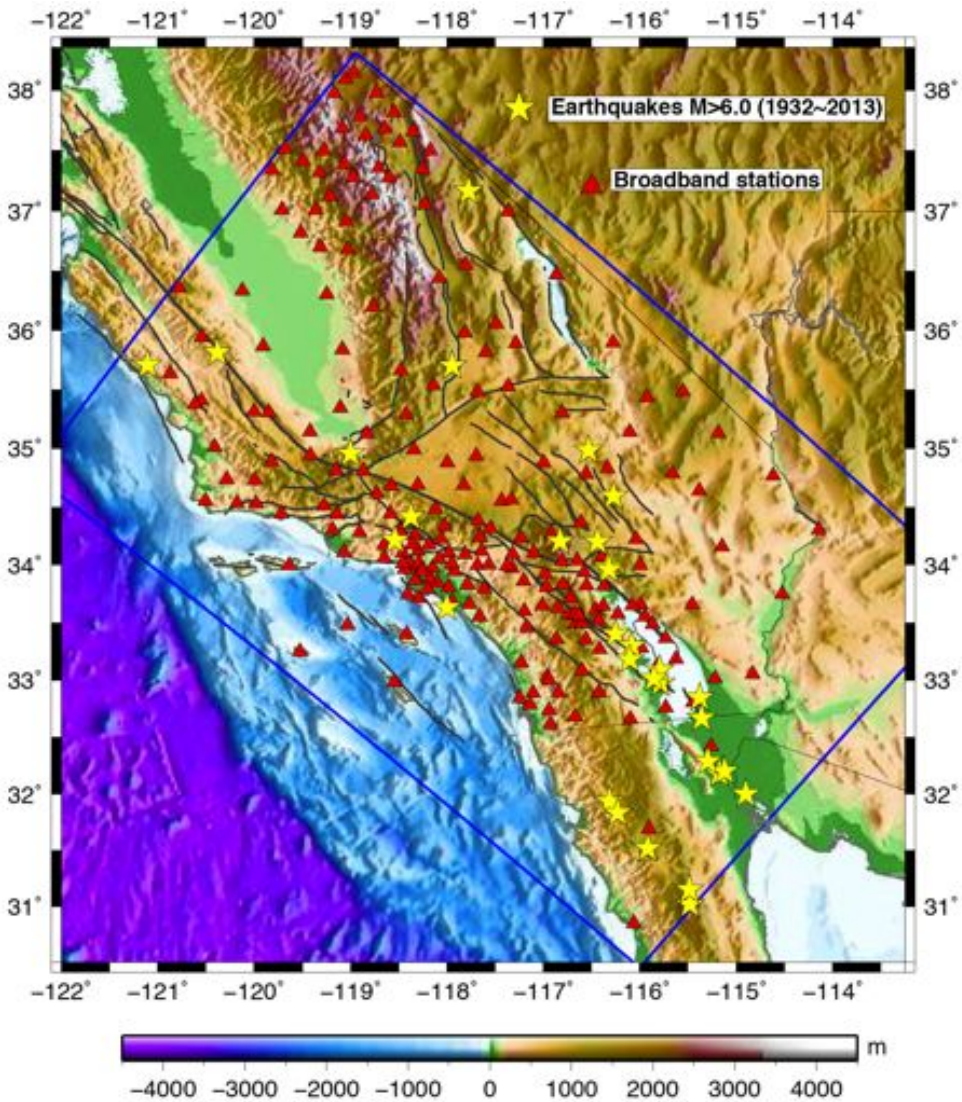

- **CVM-S4 starting model**
- **26th iterate of a F3DT inversion procedure (Lee et al., 2014)**
- **Data sets comprise ~ 514,000 differential waveform measurements at *f* ≤ 0.2 Hz**
  - **38,000 earthquake seismograms**
  - **12,600 ambient-noise Green functions**
- **Nonlinear iterative process involved two methods:**
  - **adjoint-wavefield (AW-F3DT)**
  - **scattering-integral (SI-F3DT)**

CVM-S4.26

Full-3D tomography model of Southern California crustal structure

"Tomographic navigation"

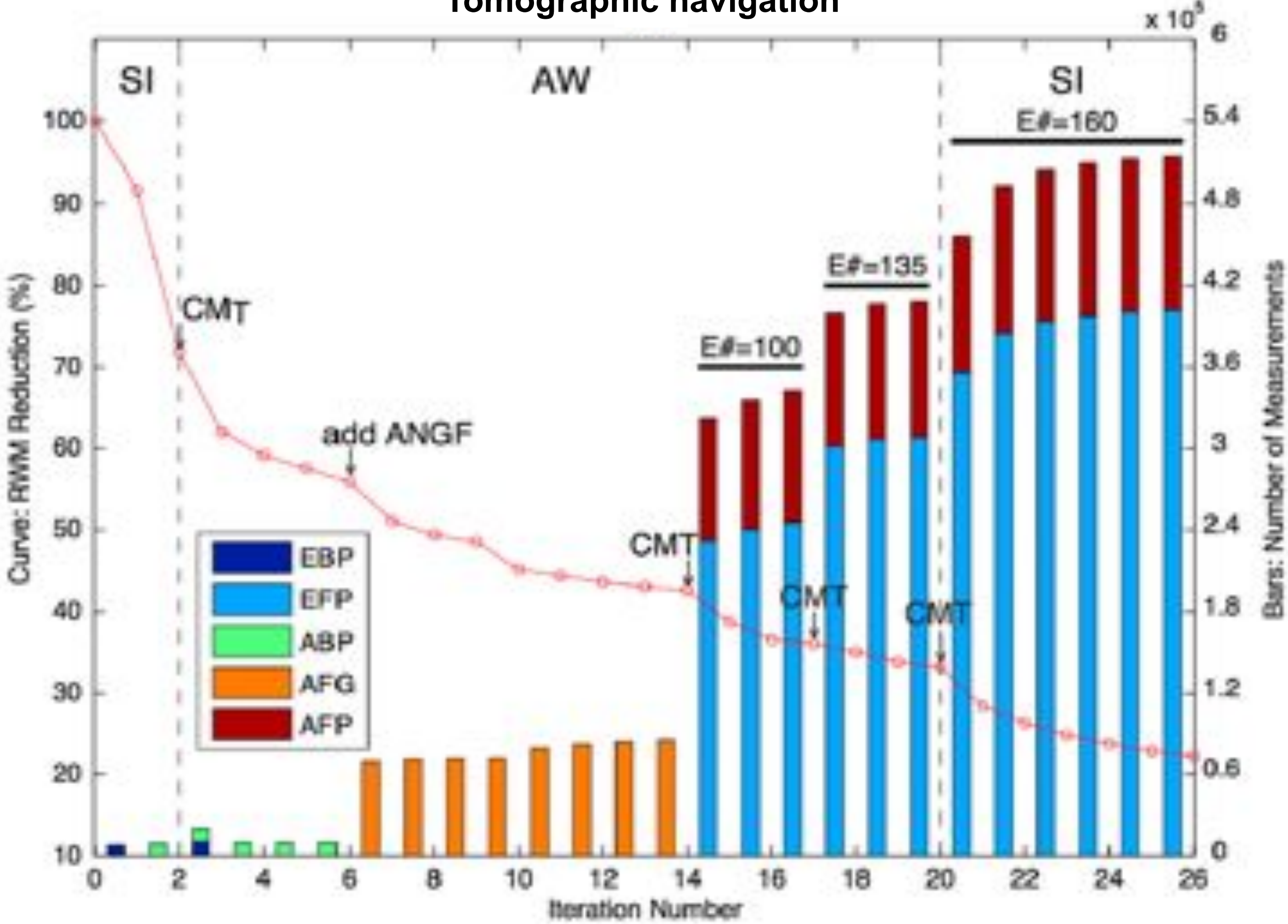

Reference data set

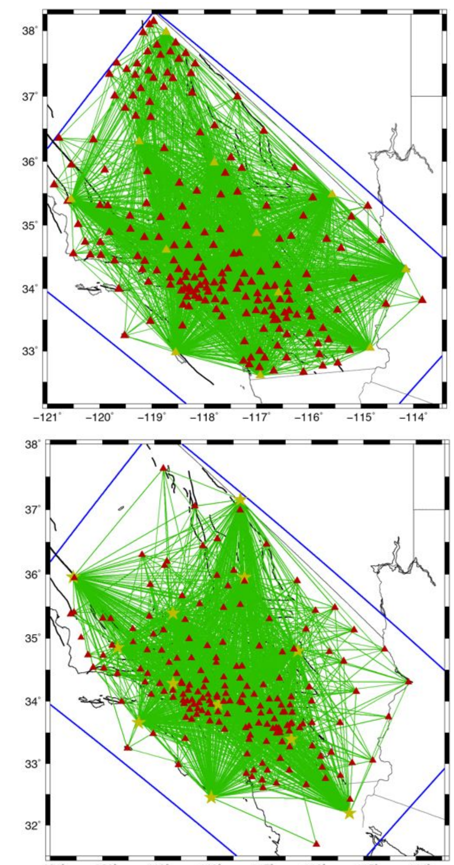

CMT Inversion

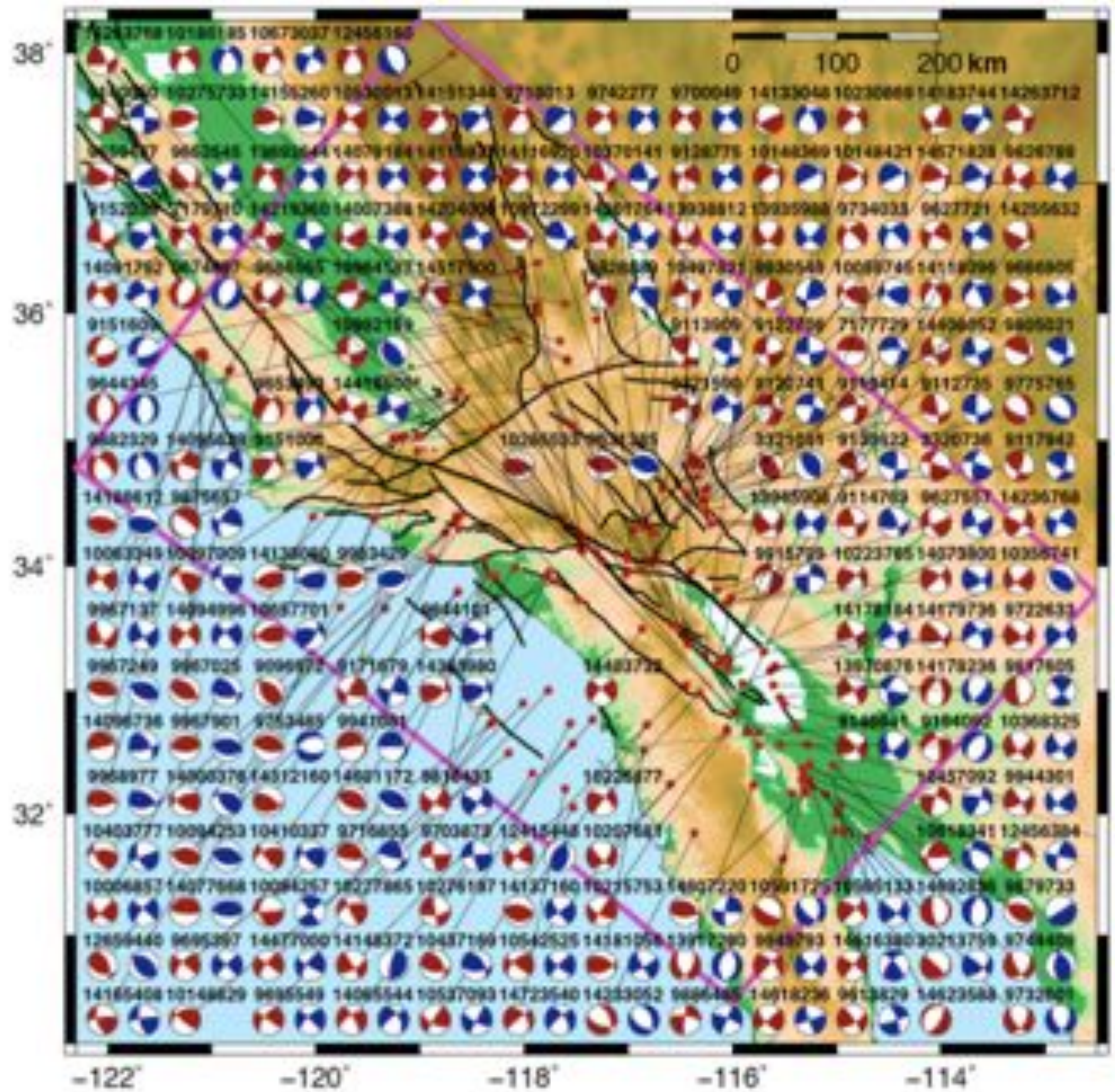

Lee, Chen, Jordan & Wang (2011), Rapid full-wave centroid moment tensor (CMT) inversion in a three-dimensional earth structure model for earthquakes in Southern California , *GJI, 186,* 311-330.

CVM-S4.26

Full-3D tomography model of Southern California crustal structure

"Tomographic navigation"

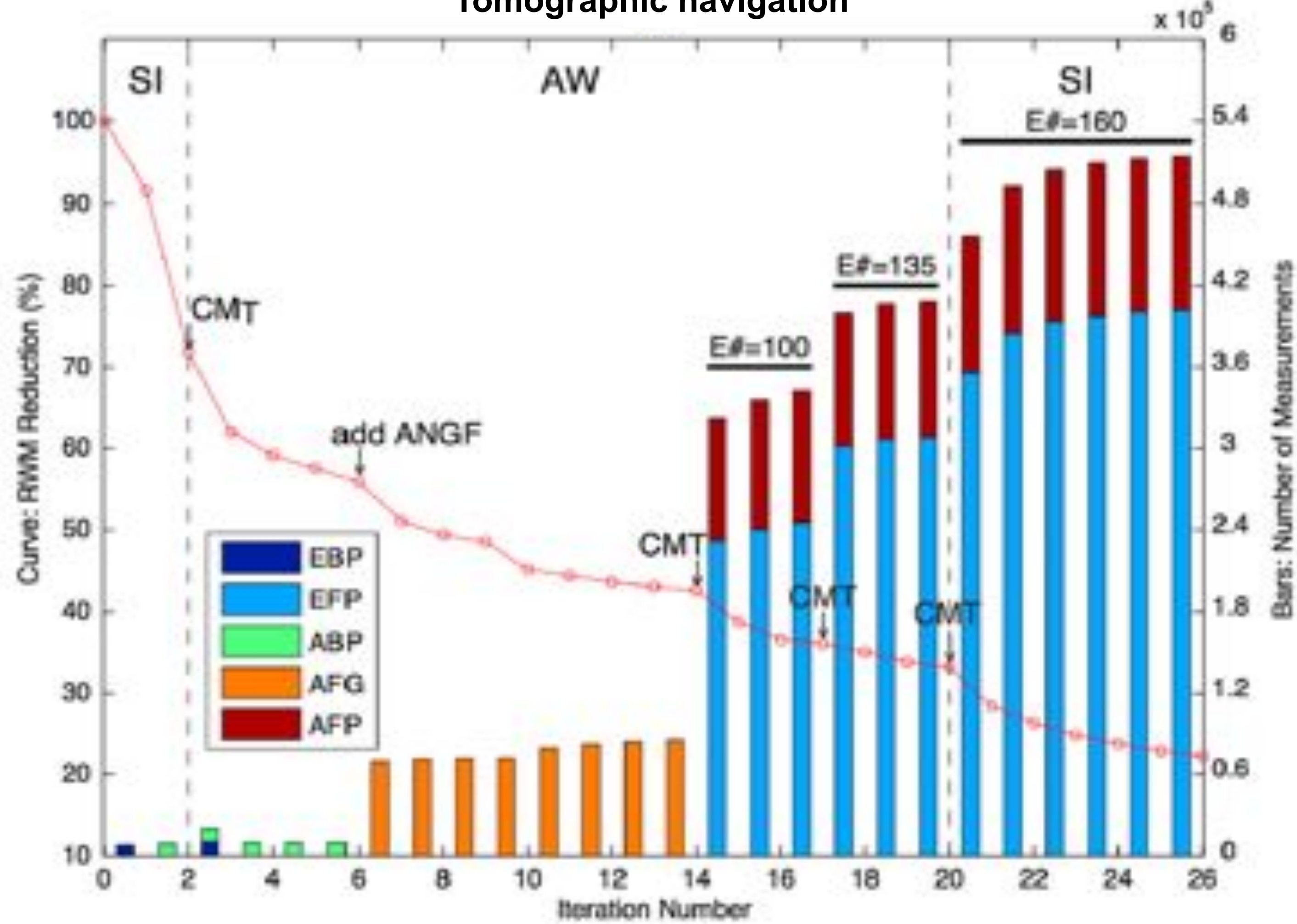

Reference data set

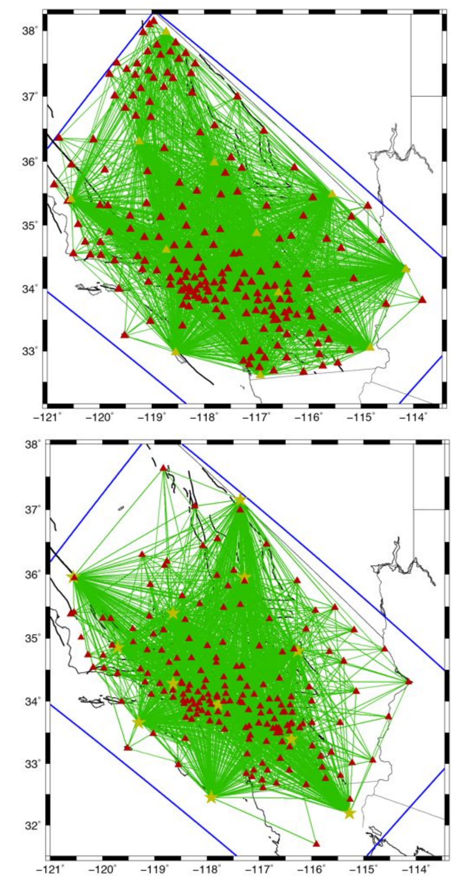

Example of Data Sensitivity

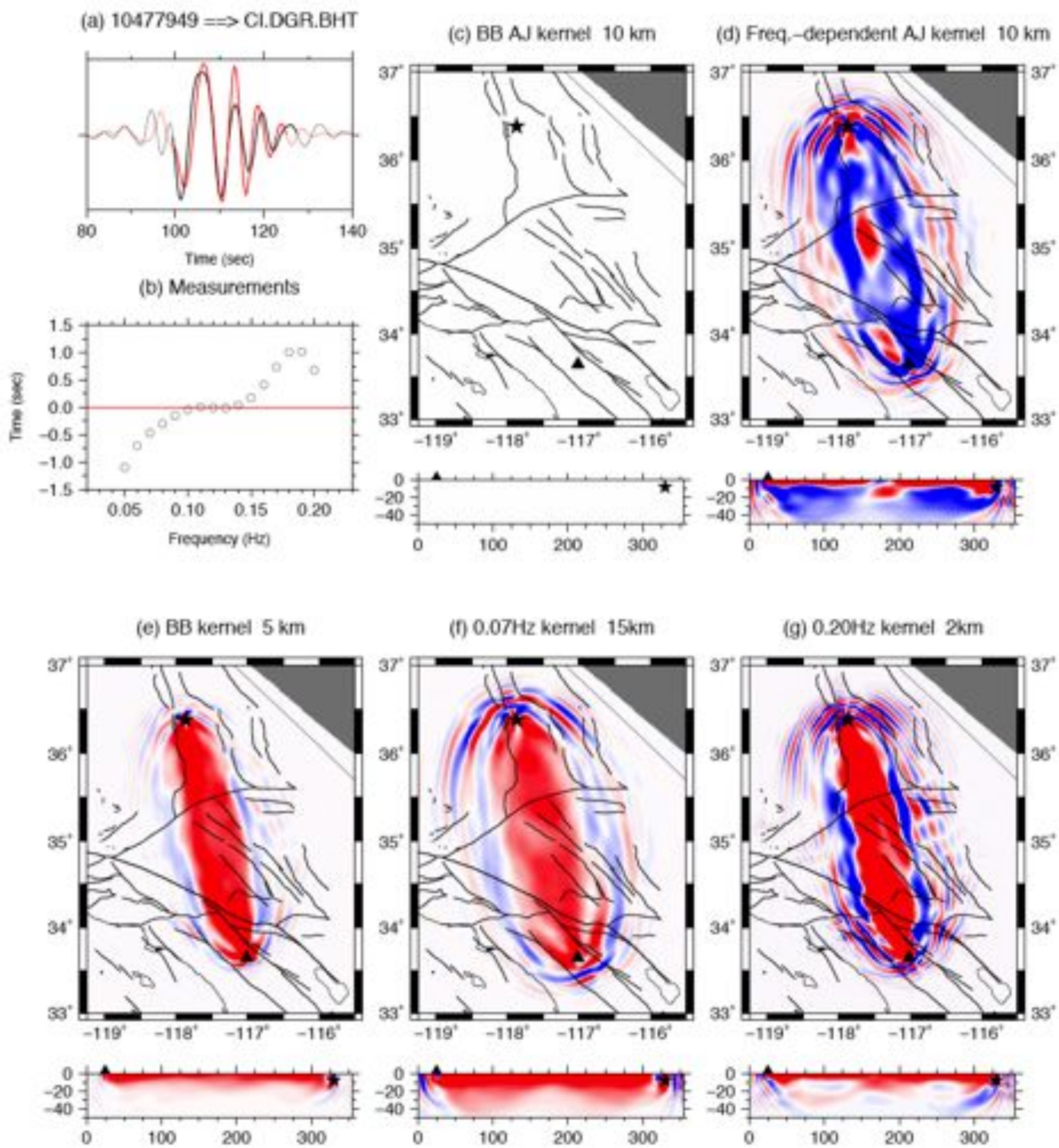

CVM-S4.26

Full-3D tomography model of Southern California crustal structure

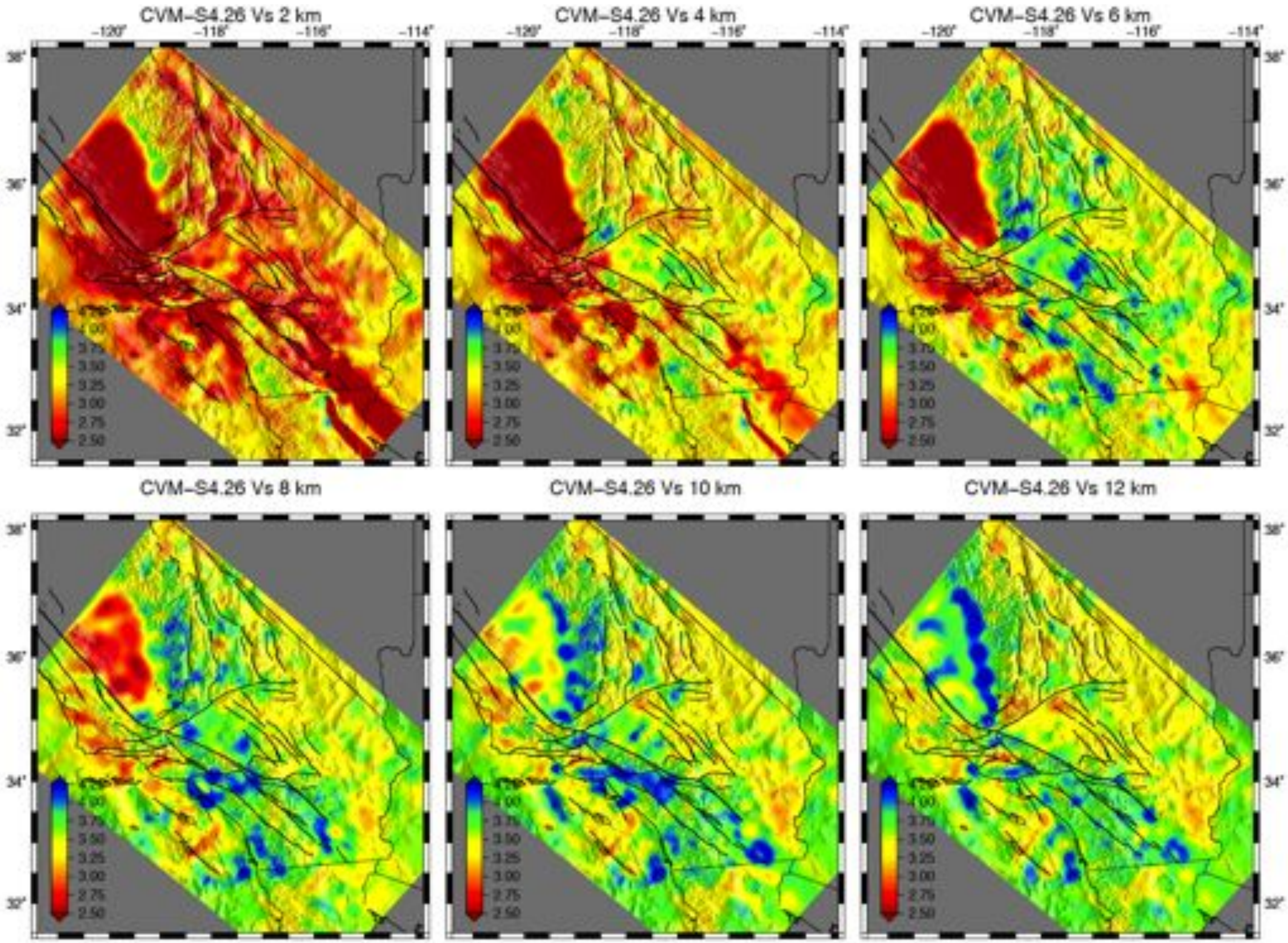

CVM-S4.26

Full-3D tomography model of Southern California crustal structure

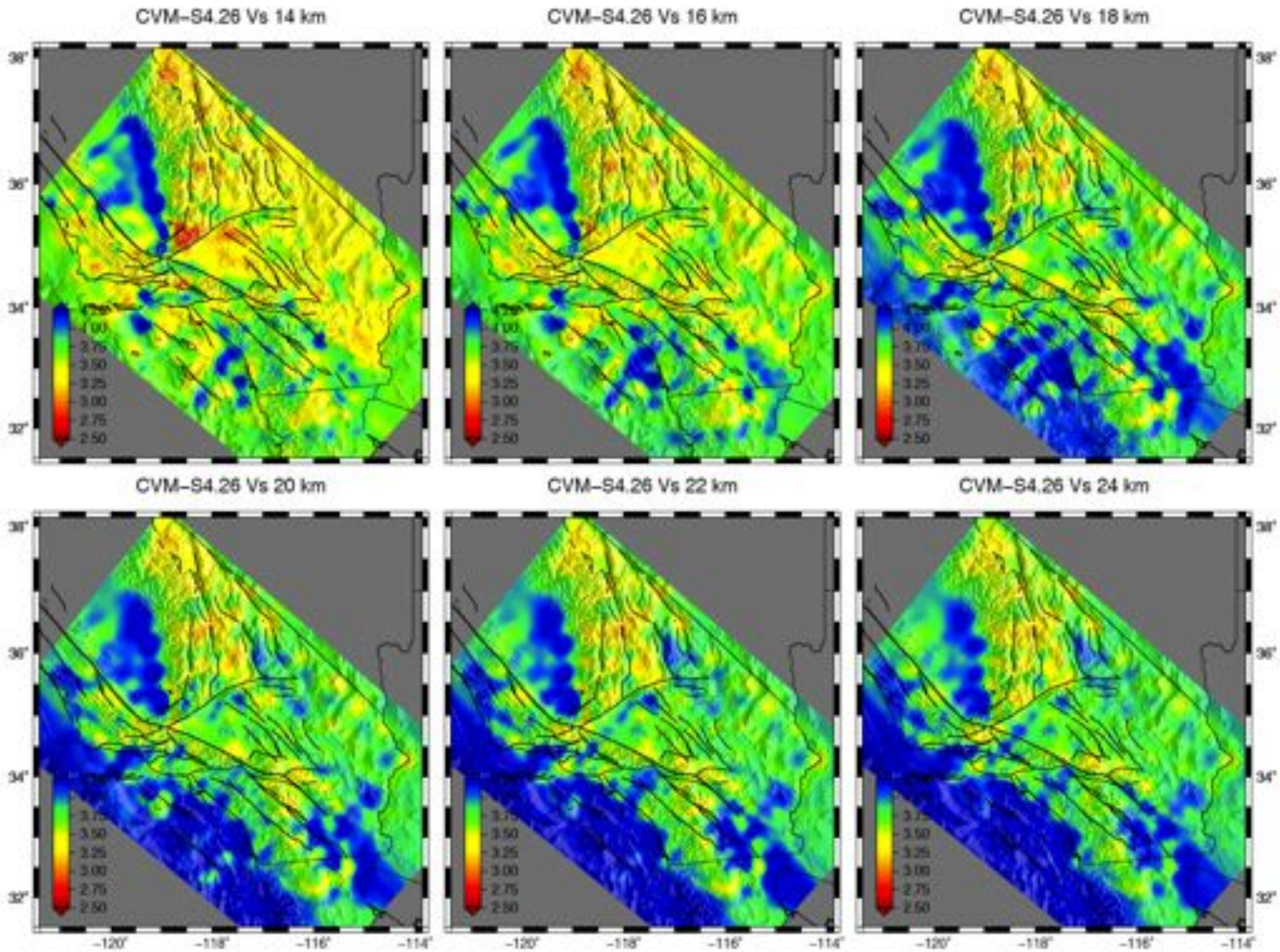

Regional Vertical Profiles for CVM-S4.26

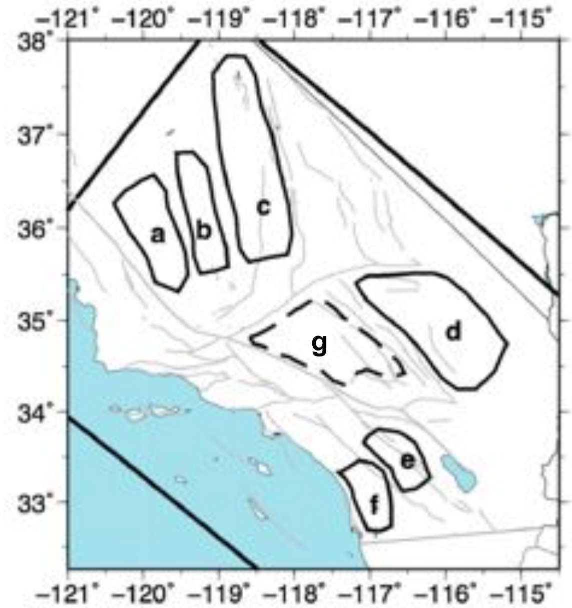

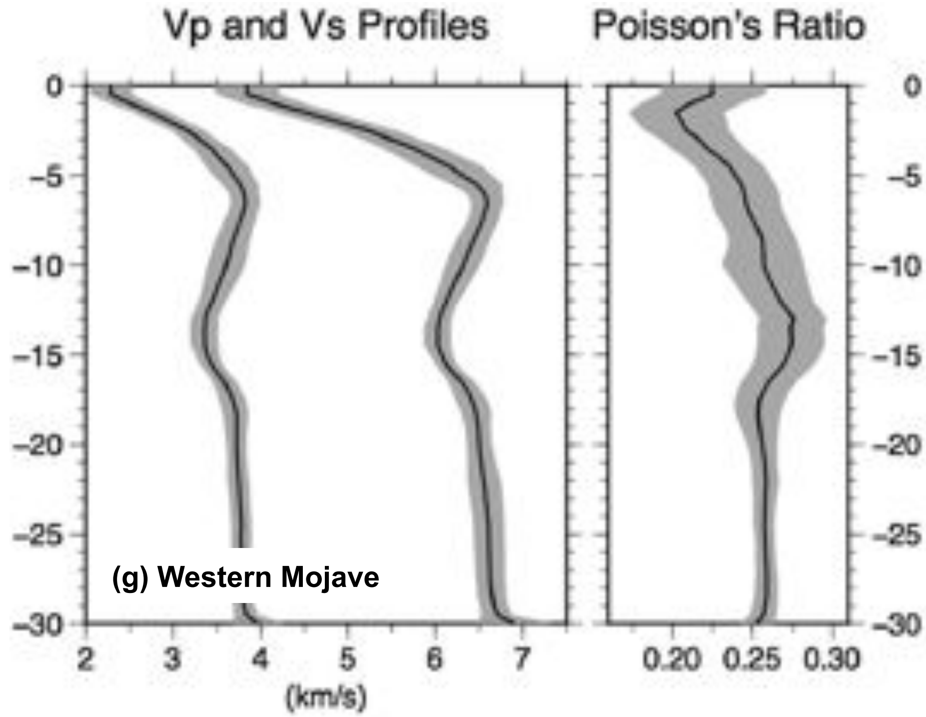

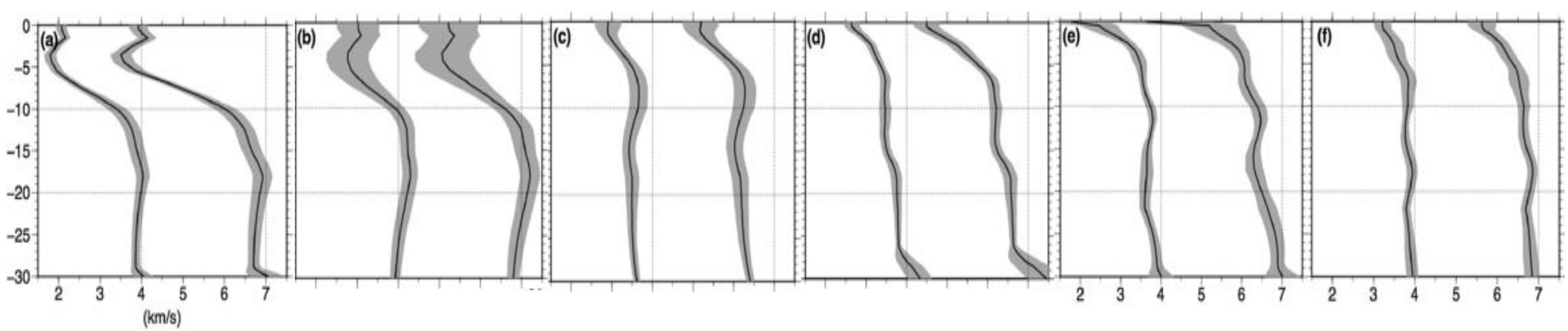

Examples of ANGF Waveform Fits

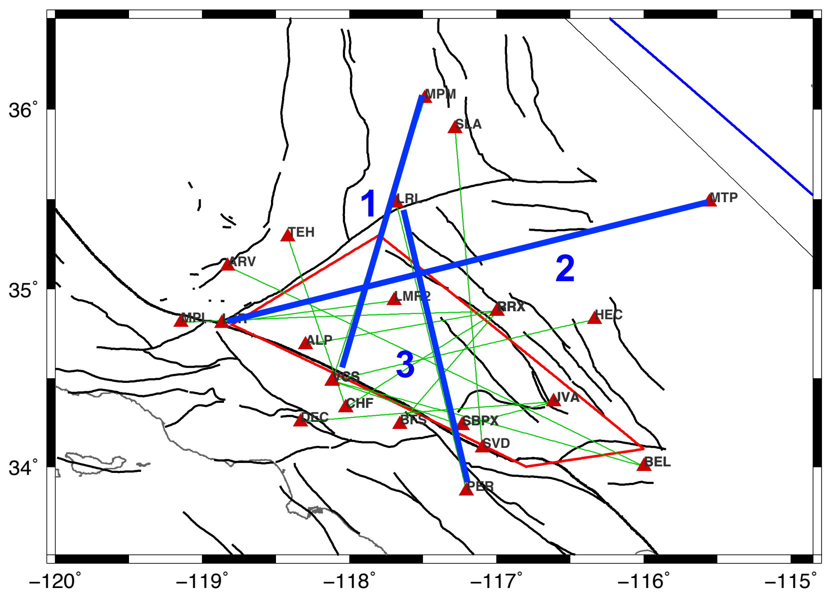

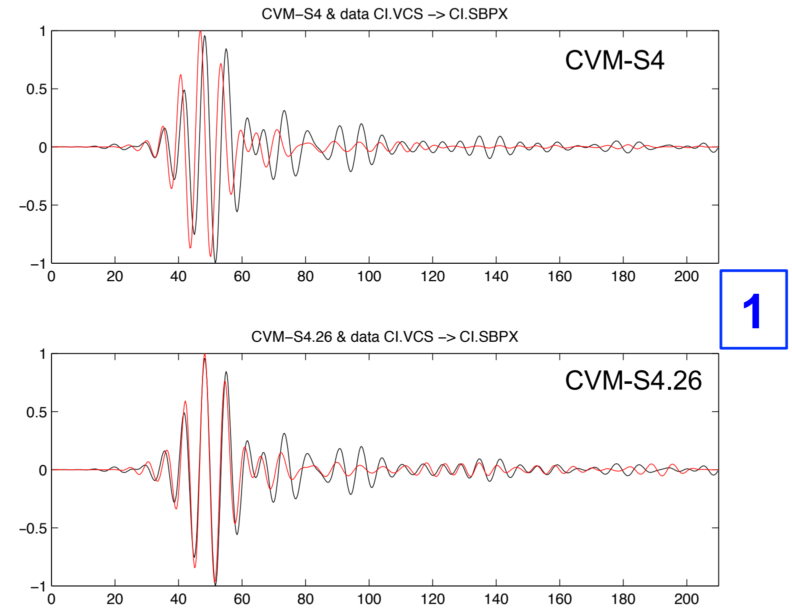

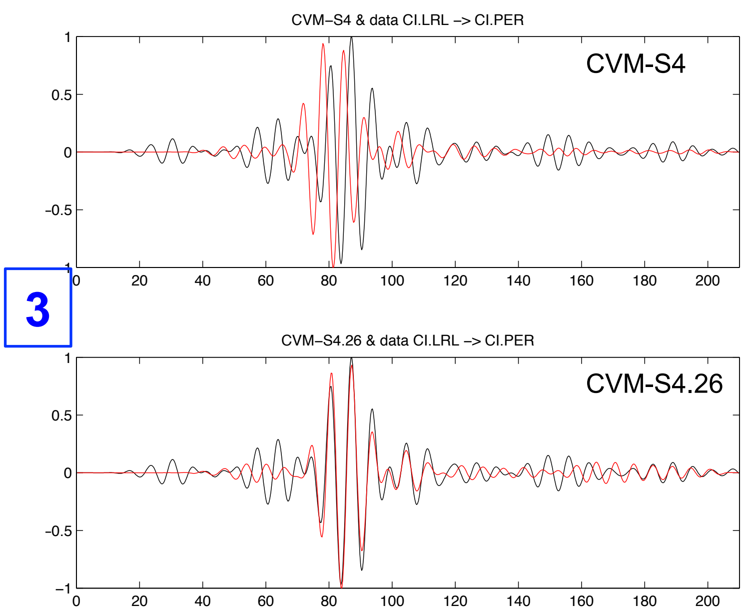

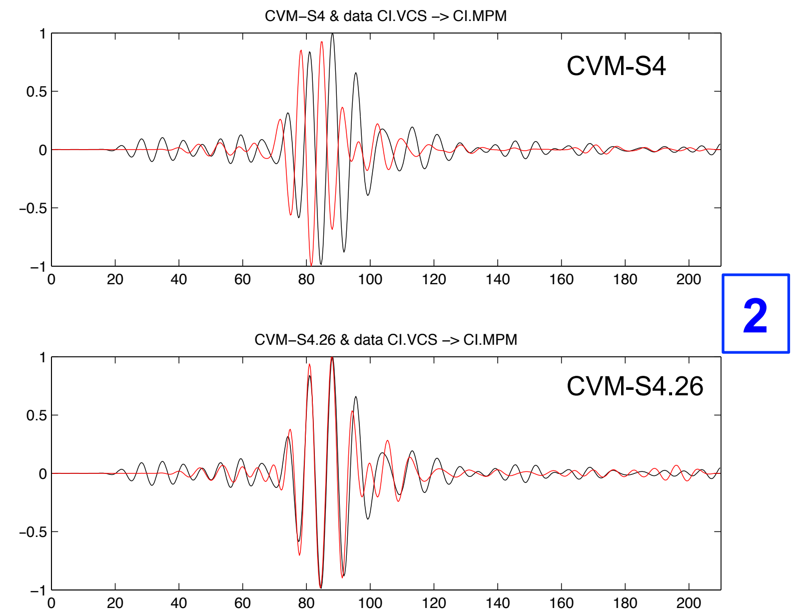

LARSE Profiles

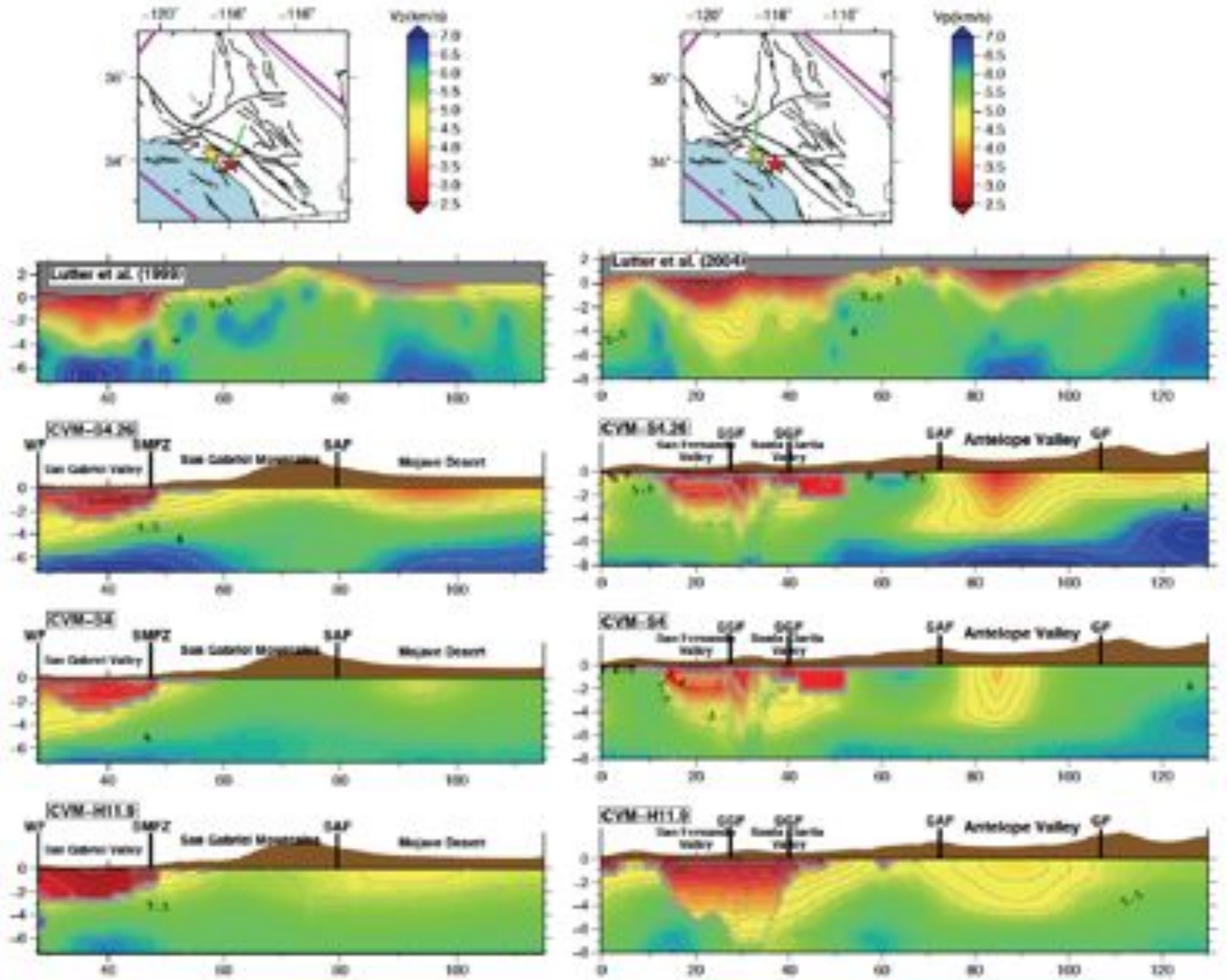

Basin Structures

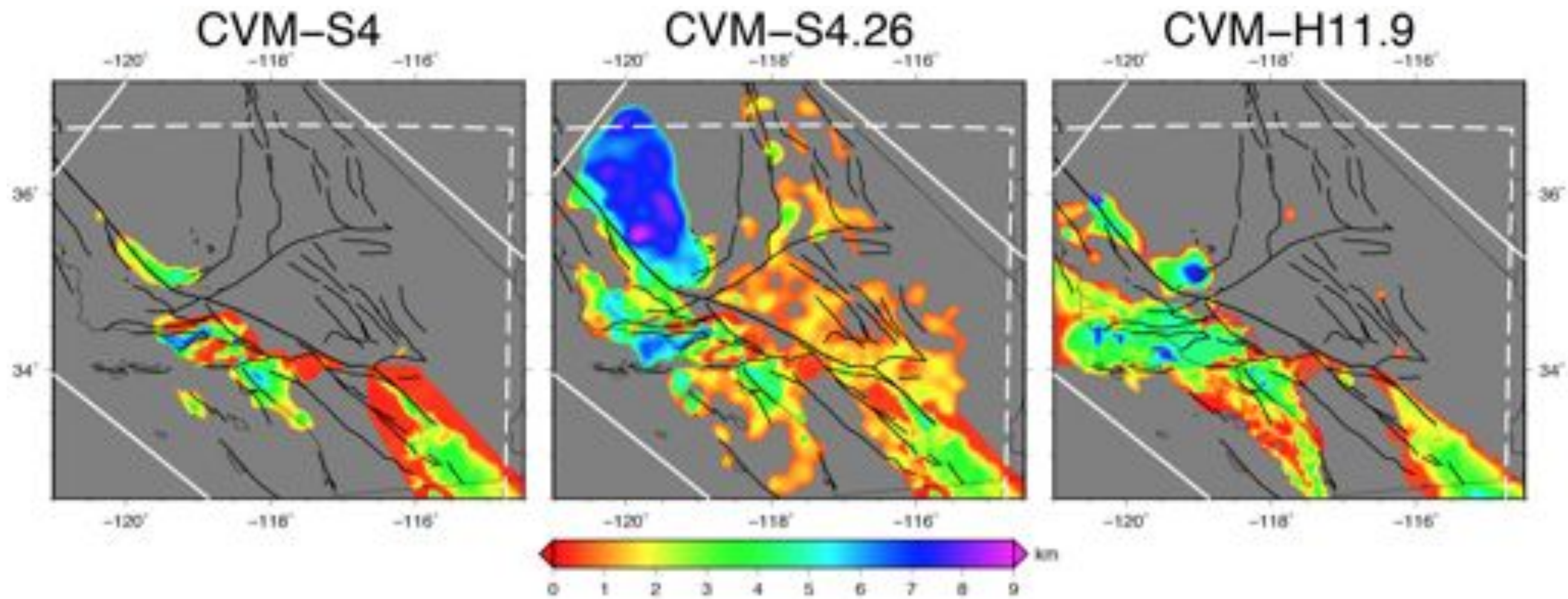

Z_{2500} : iso-velocity surfaces at $V_S = 2.5$ km/s

CVM-S4.26

Full-3D tomography model of Southern California crustal structure

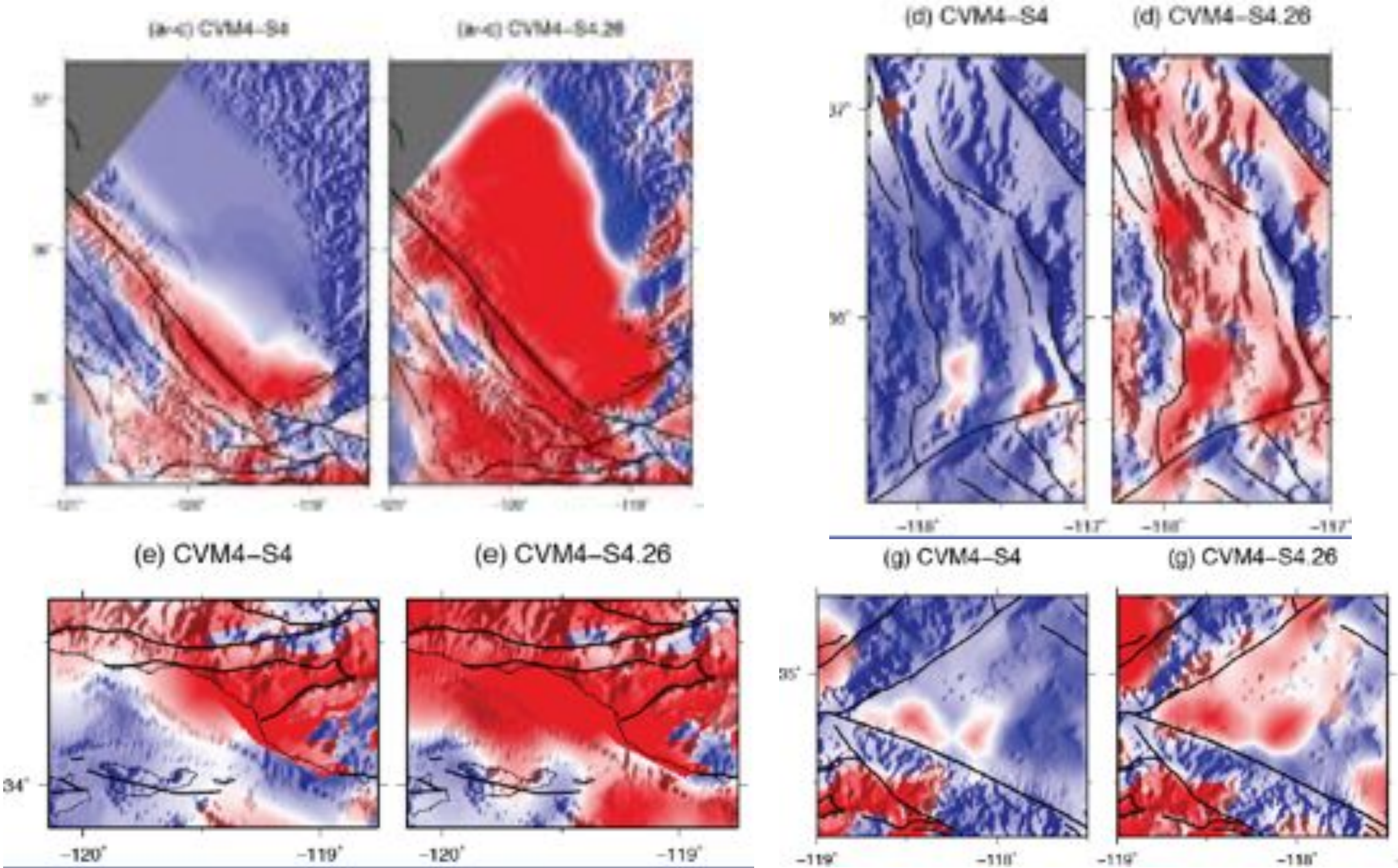

CVM-S4.26

Full-3D tomography model of Southern California crustal structure

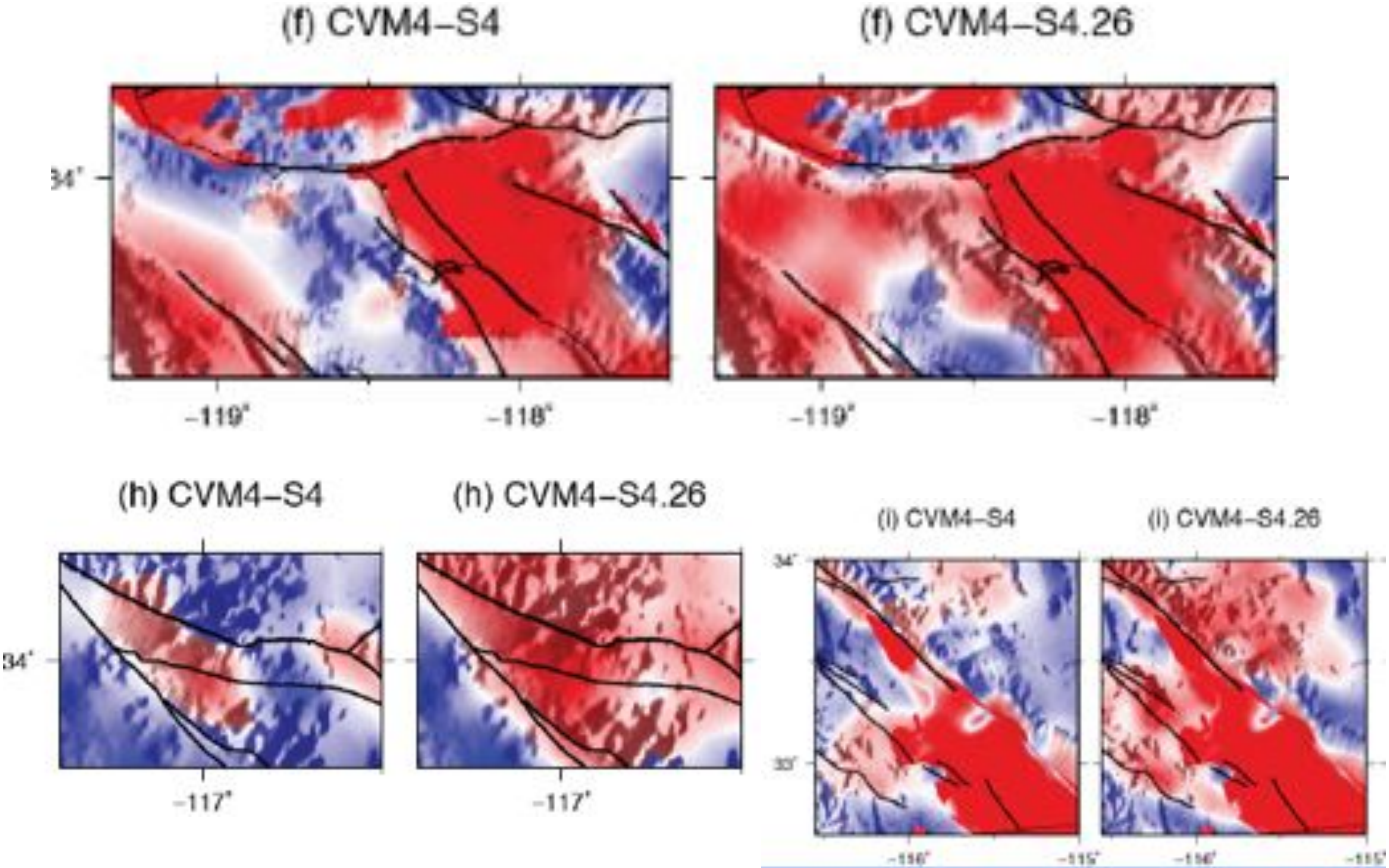

Checkerboard Resolution Tests

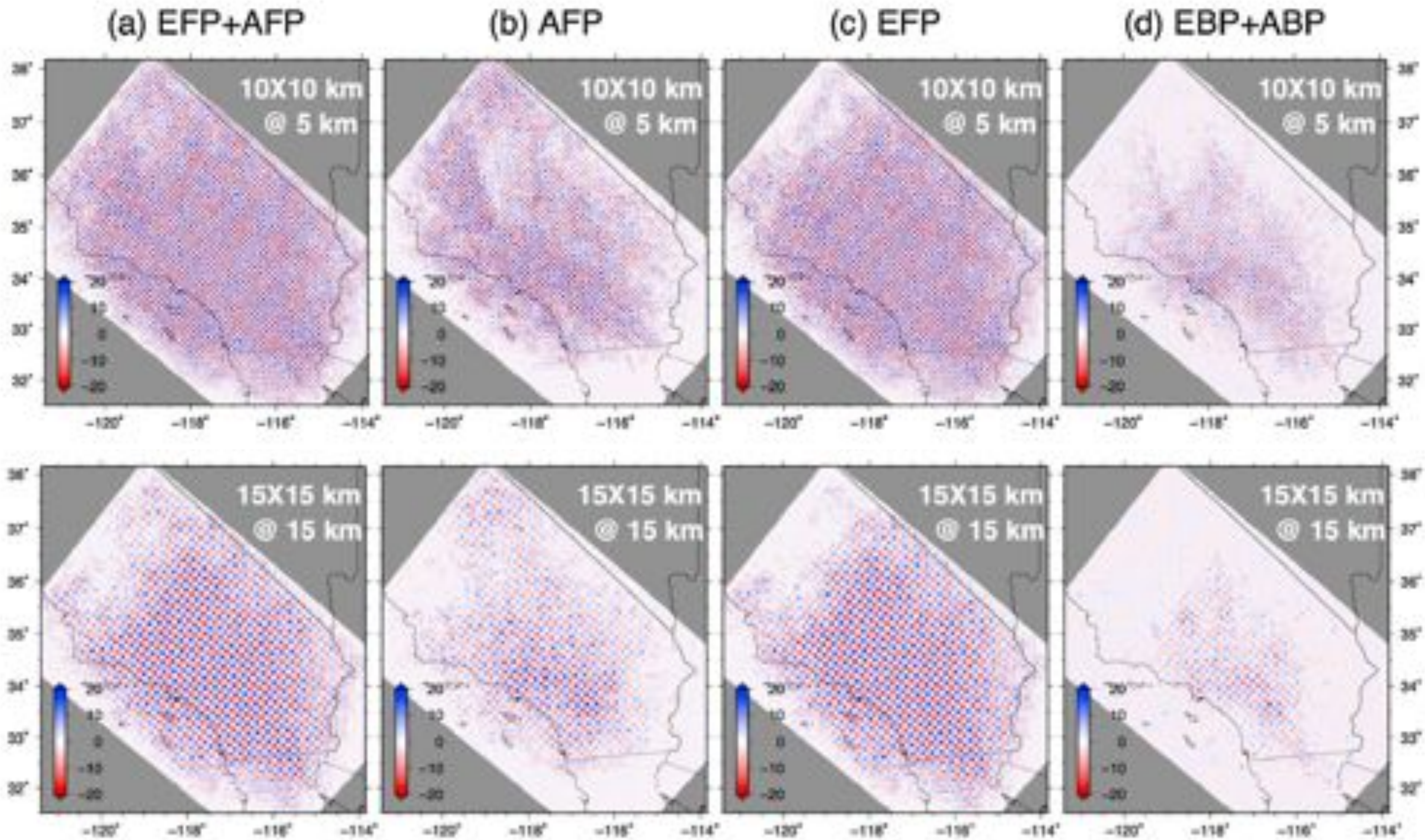

Checkerboard Resolution Tests

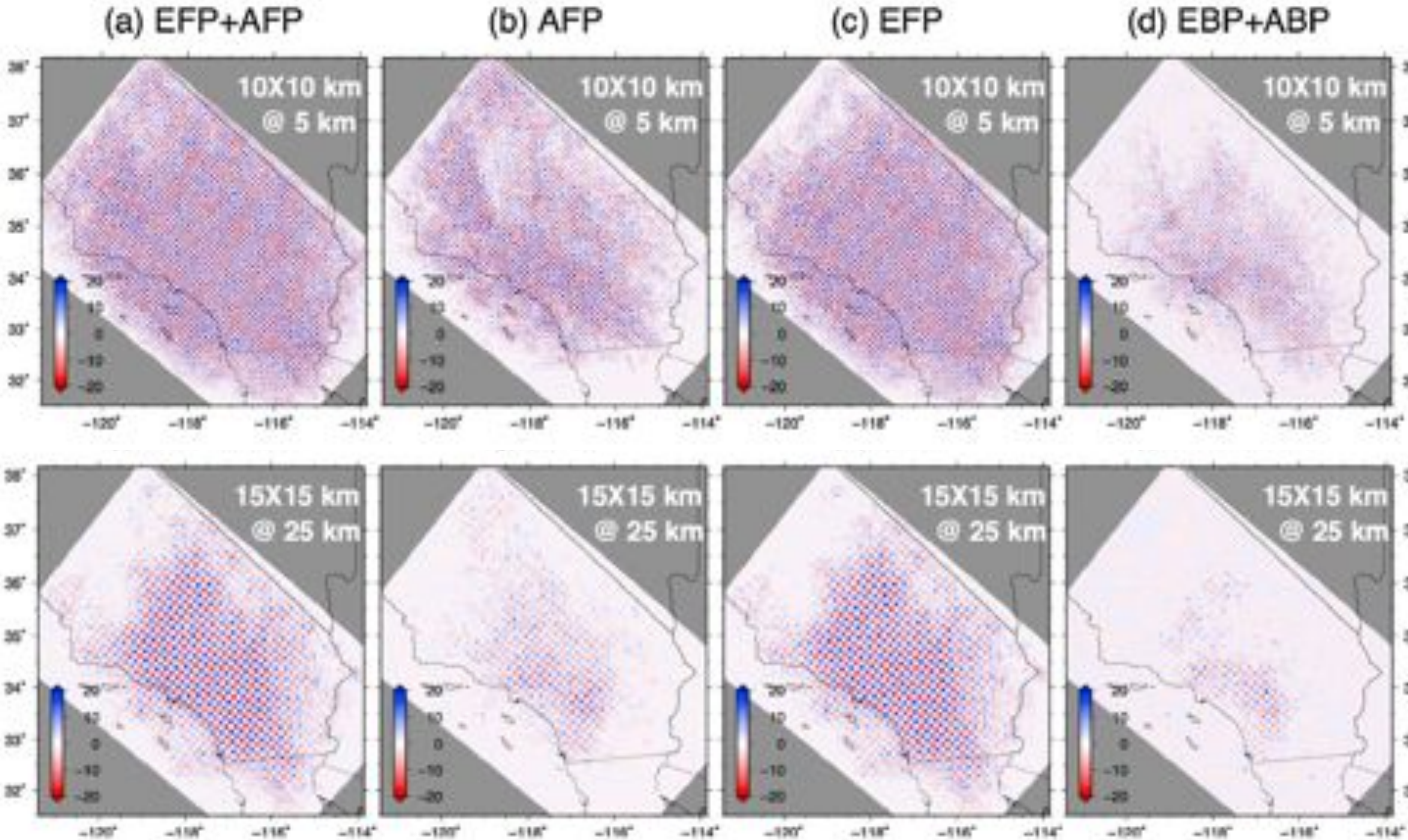

Inference Spiral of System Science

- Earthquake system science requires an iterative, computationally intense process of model formulation and verification, simulation-based predictions, validation against observations, and data assimilation to improve the model

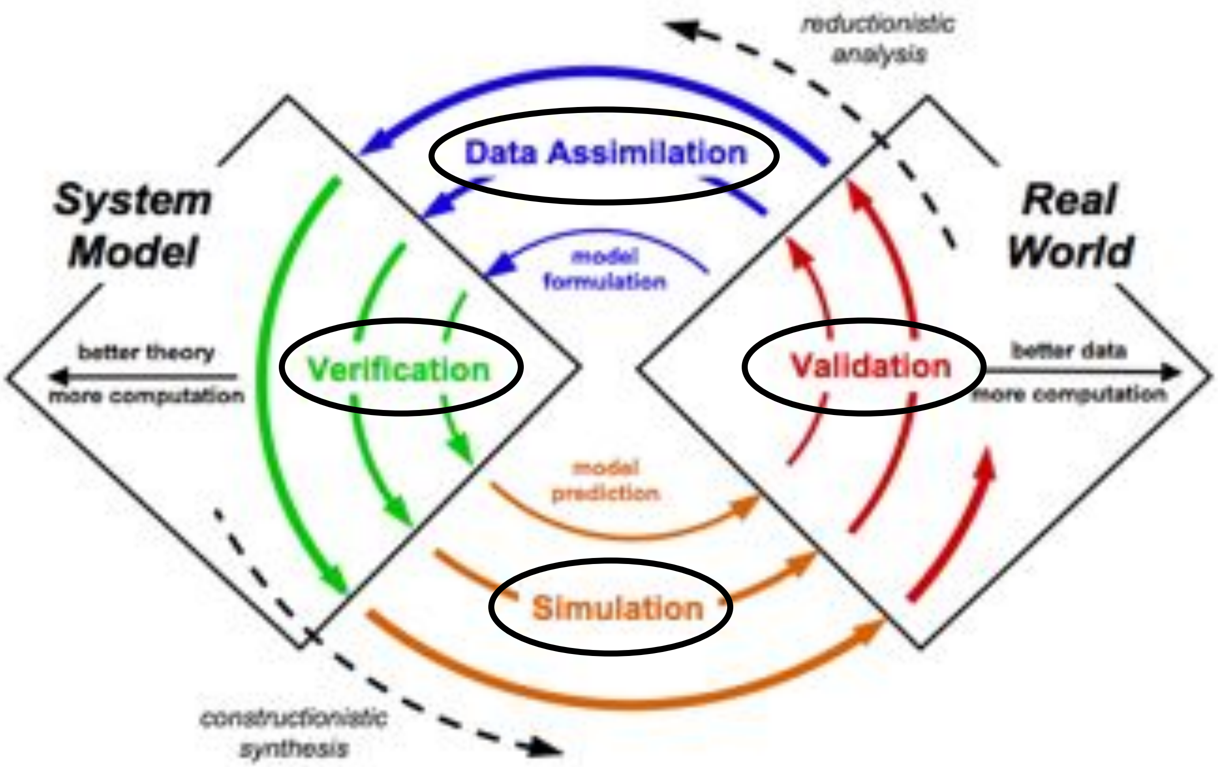

- As models become more complex and new data bring in more information, we require ever increasing computational resources

CVM comparisons

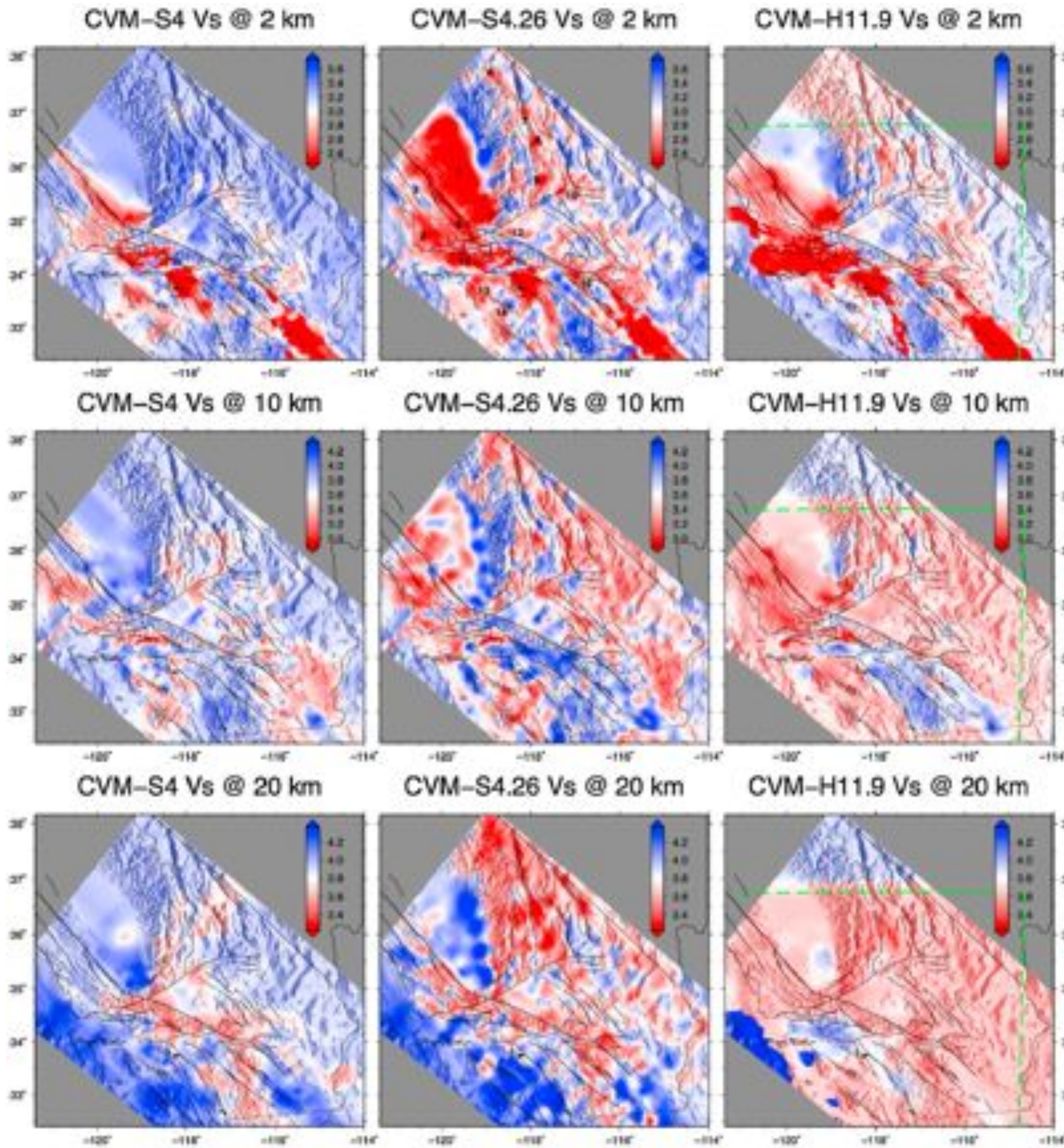

Relative Waveform Misfit

$$RWM_k = \frac{\int_{t_k}^{t'_k} [u_k(t) - \tilde{u}_k(t)]^2 dt}{\sqrt{\int_{t_k}^{t'_k} u_k(t)^2 dt \ \int_{t_k}^{t'_k} \tilde{u}_k(t)^2 dt}}$$

$$\omega_0 \, \Delta t_p = 1 \implies RWM = 0.92$$

$$\omega_0 \, \Delta t_q = 1 \implies RWM = 1.08$$

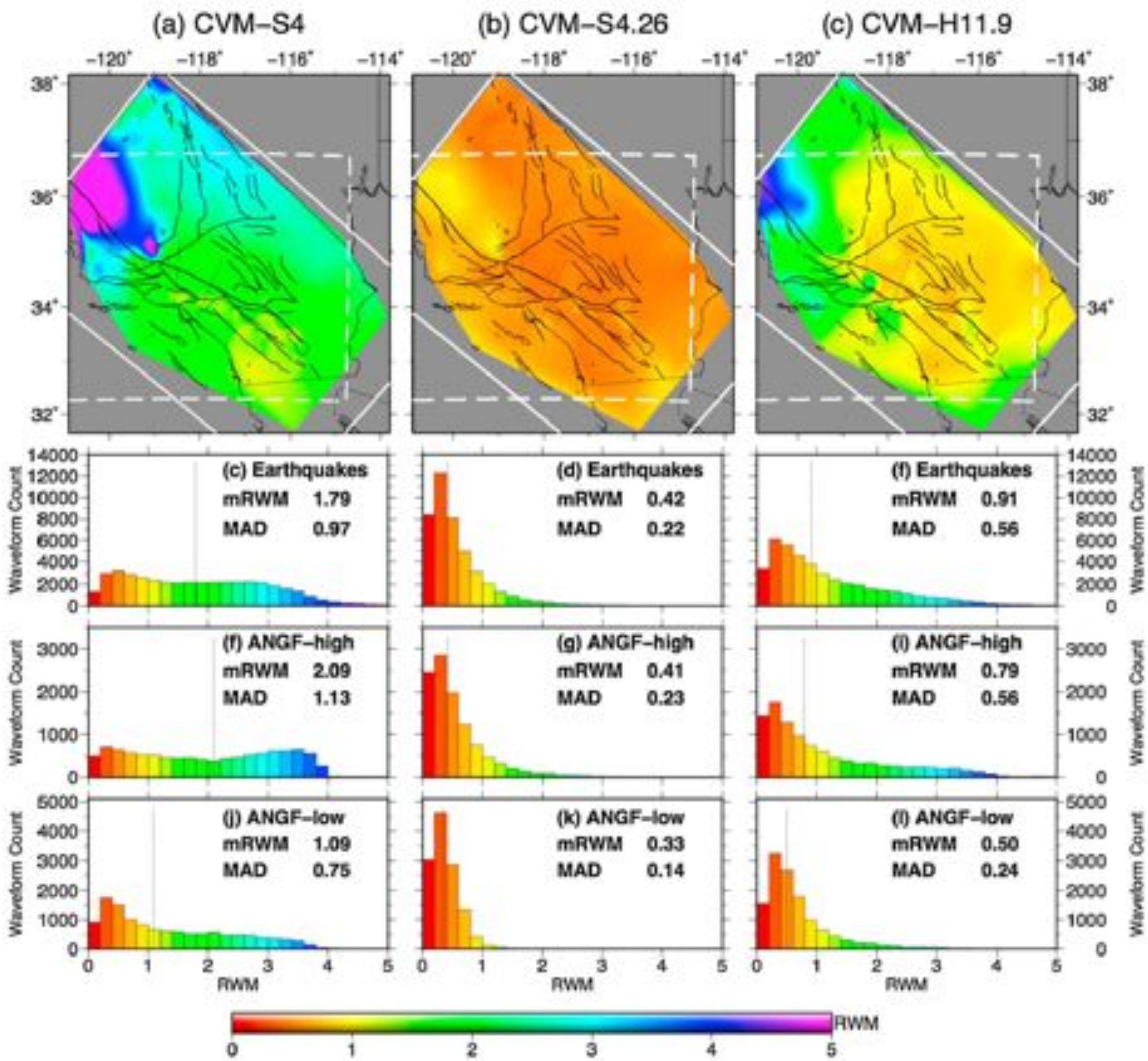

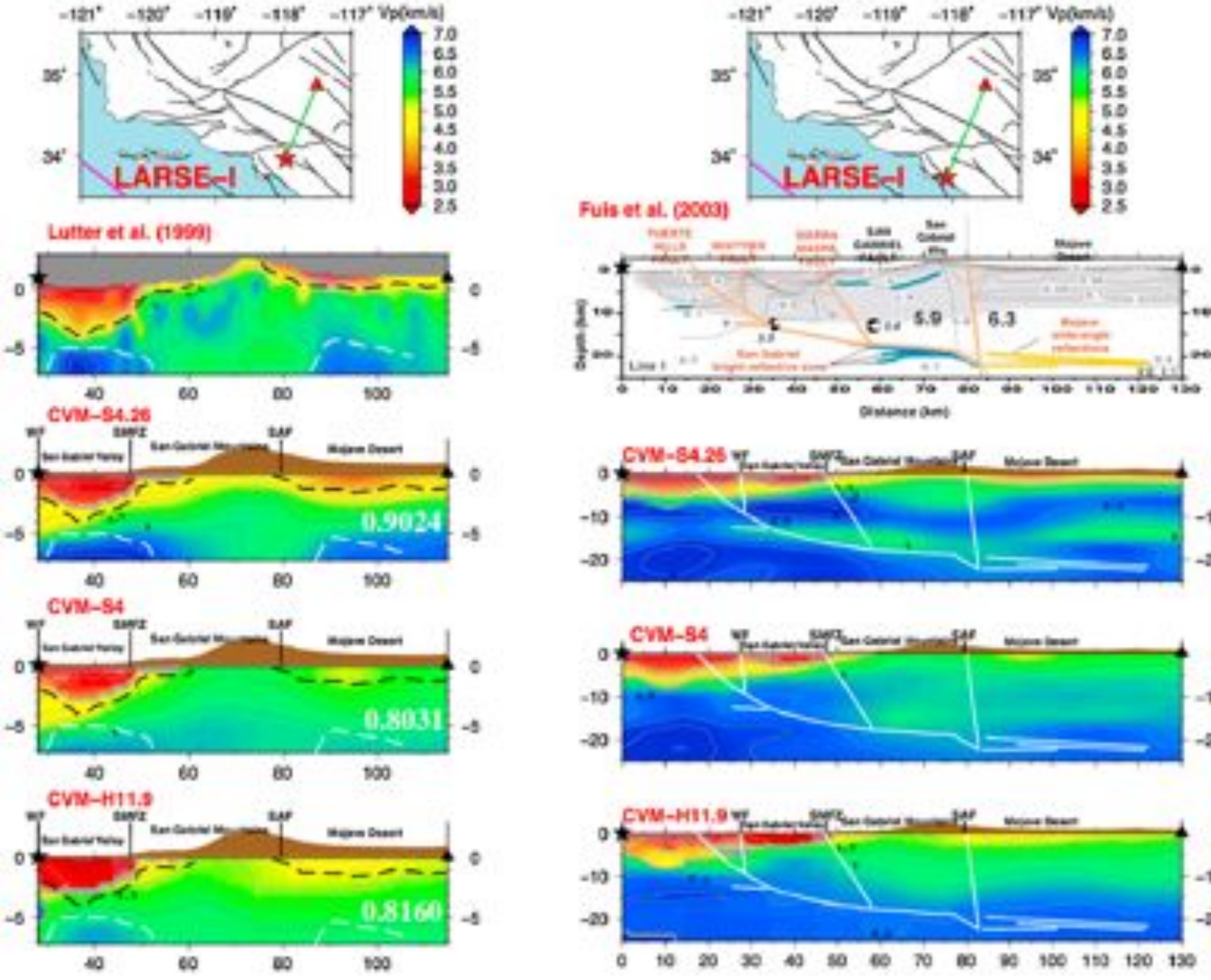

-121° -120° -119° -118° -117° Vp(km/s)
7.0 6.5 6.0 5.5 5.0 4.5 4.0 3.5 3.0 2.5
35°
34°
LARSE-I
Lutter et al. (1999)
Fuis et al. (2003)
5.9
6.3
Depth (km)
Distance (km)
Line 1
CVM-S4.26
CVM-S4
CVM-H11.9
WF
SMFZ
SAF
San Gabriel Valley
San Gabriel Mountains
Mojave Desert
0.9024
0.8031
0.8160

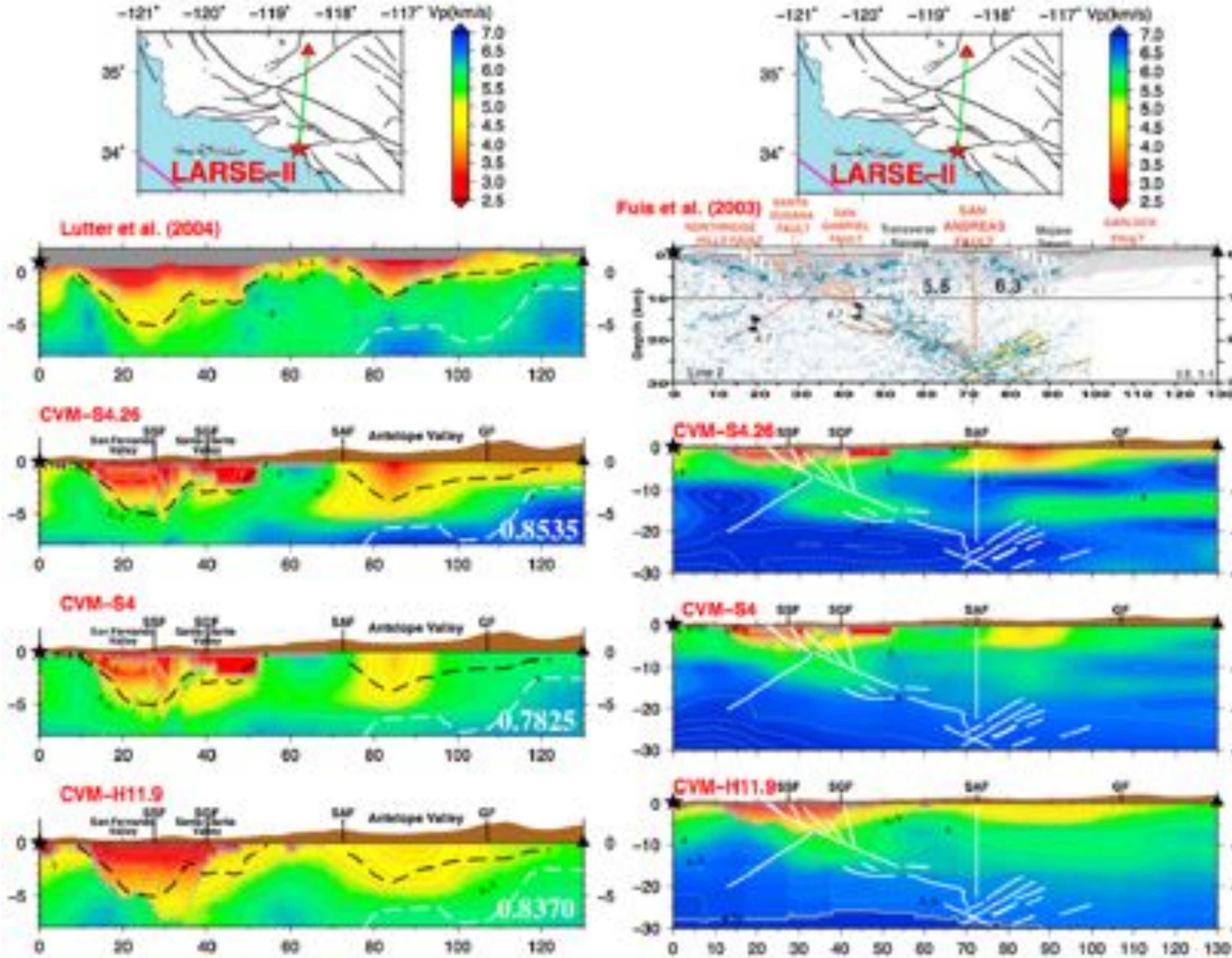
LARSE-II
LARSE-II
Vp(km/s)
Lutter et al. (2004)
Fuis et al. (2003)
CVM-S4.26
CVM-S4
CVM-H11.9
San Fernando Valley
Santa Clarita Valley
SSF
SGF
SAF
GF
Antelope Valley
0.8535
0.7825
0.8370
5.6
6.3

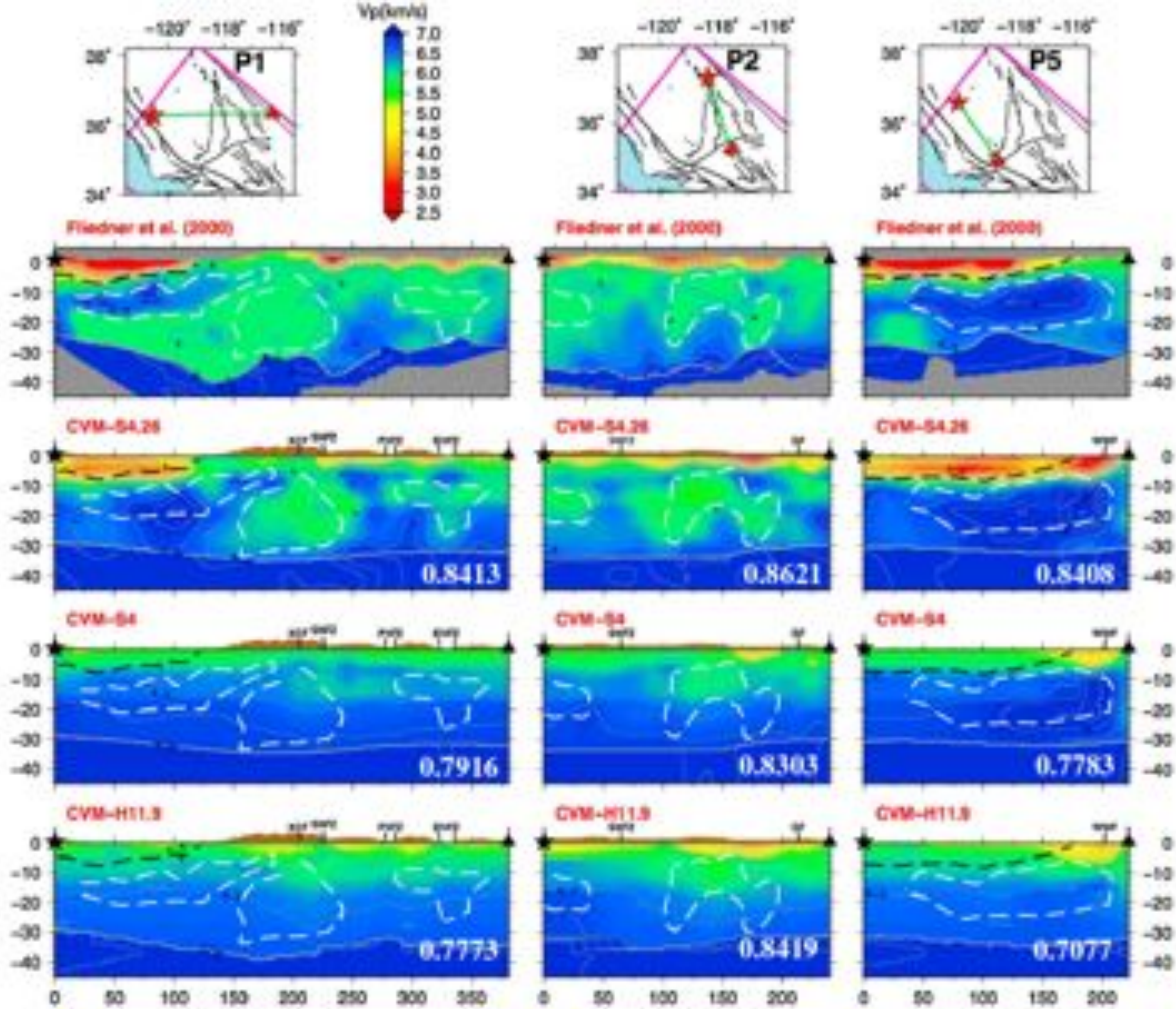

P1
P2
P5
Vp(km/s)
Fliedner et al. (2000)
CVM-S4.26
CVM-S4
CVM-H11.9
0.8413
0.8621
0.8408
0.7916
0.8303
0.7783
0.7773
0.8419
0.7077

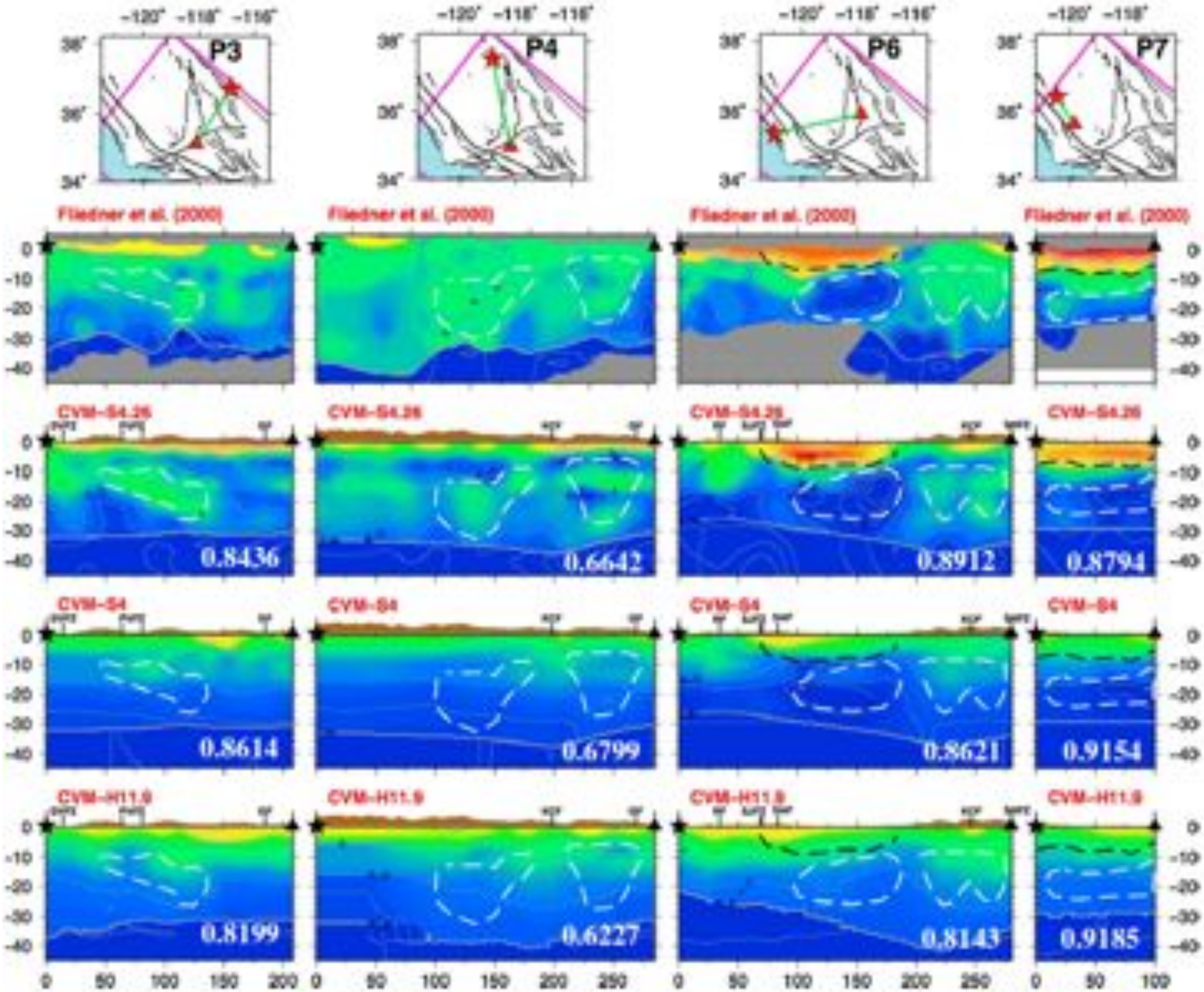
P3
P4
P6
P7
Fliedner et al. (2000)
CVM-S4.26
CVM-S4
CVM-H11.9
0.8436
0.6642
0.8912
0.8794
0.8614
0.6799
0.8621
0.9154
0.8199
0.6227
0.8143
0.9185

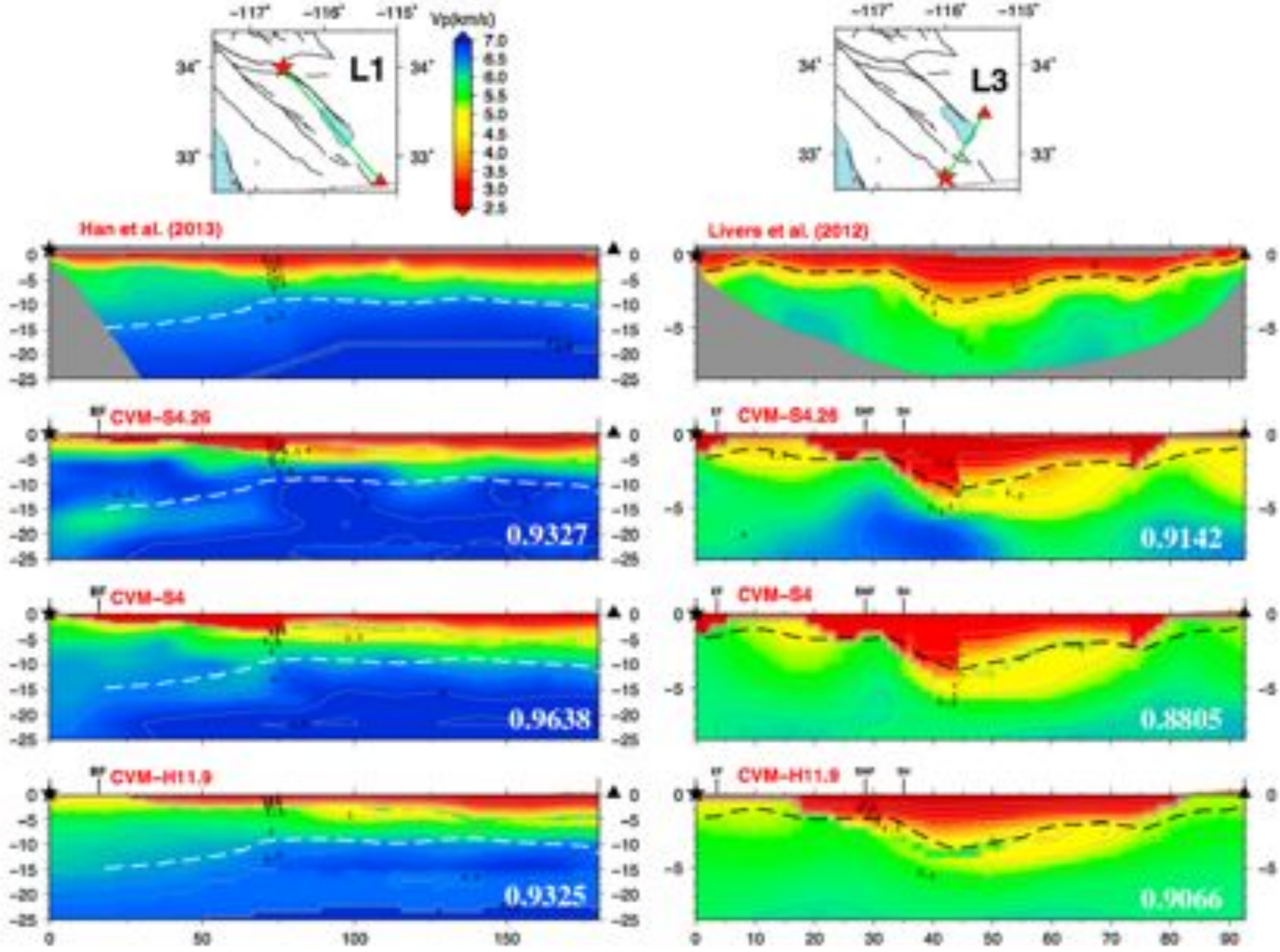

L1
L3
Vp(km/s)
Han et al. (2013)
Livers et al. (2012)
CVM-S4.26
CVM-S4
CVM-H11.9
0.9327
0.9638
0.9325
0.9142
0.8805
0.9066

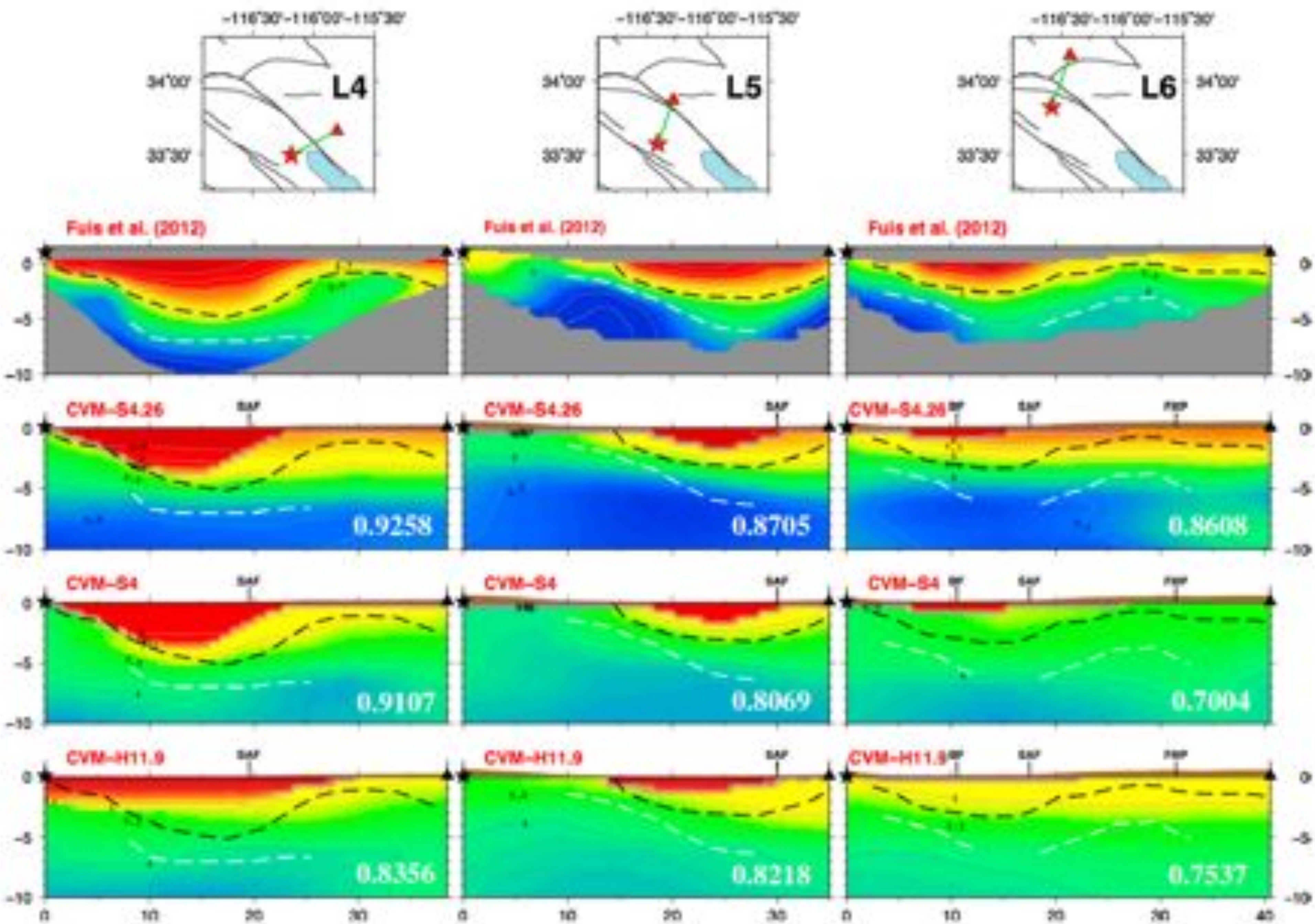

L4
L5
L6
Fuis et al. (2012)
CVM-S4.26
CVM-S4
CVM-H11.9
SAF
0.9258
0.8705
0.8608
0.9107
0.8069
0.7004
0.8356
0.8218
0.7537

03/28/14 La Habra Earthquake (M5.1)

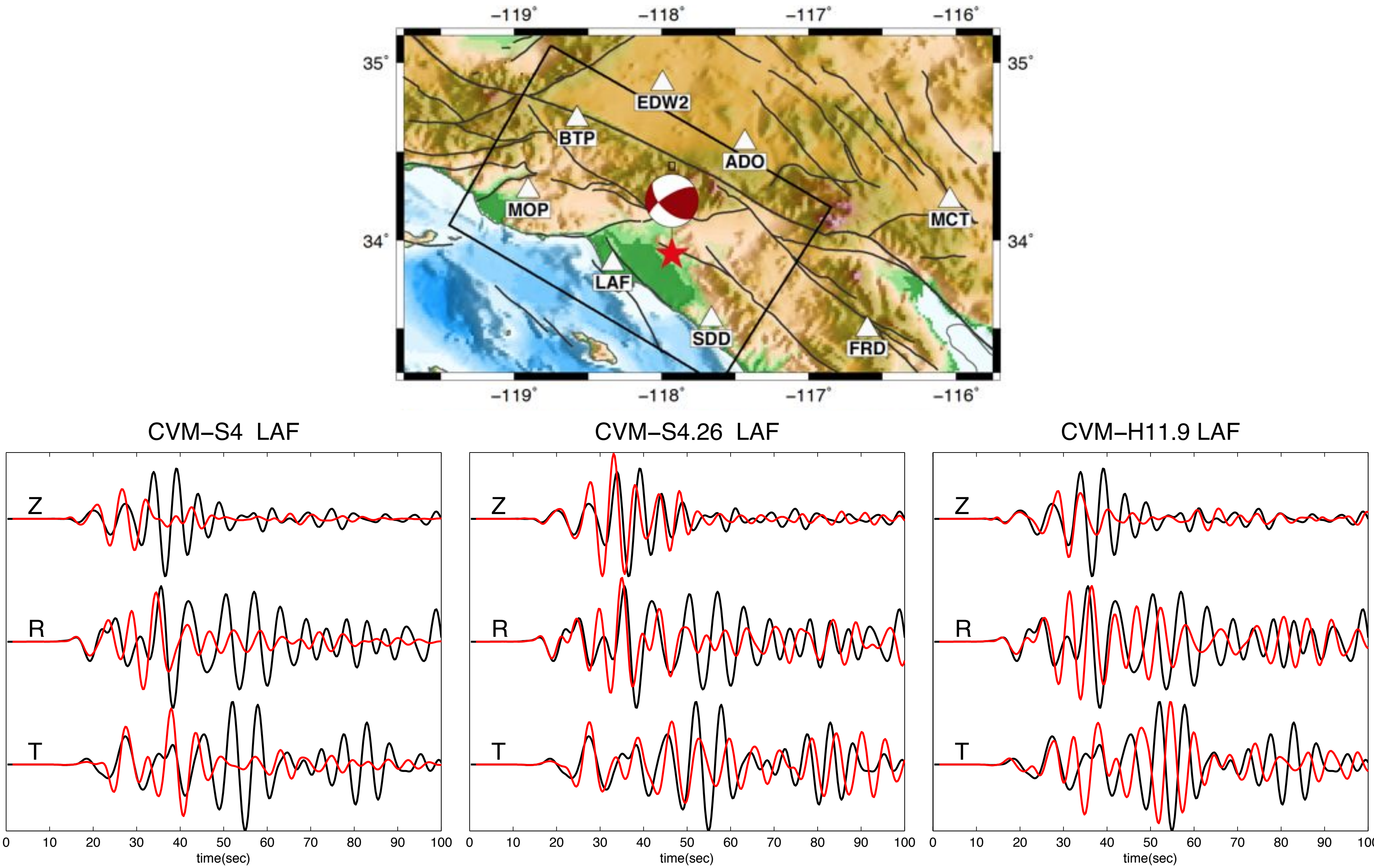

03/28/14 La Habra Earthquake (M5.1)

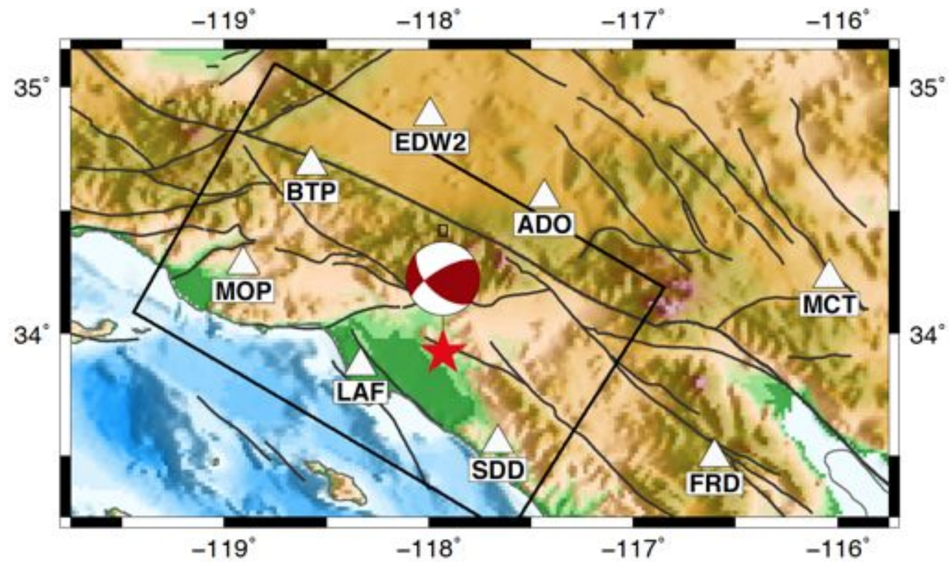

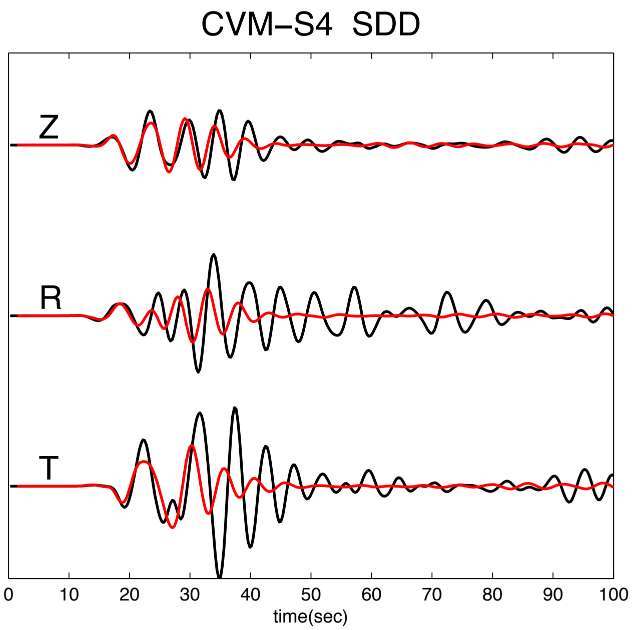

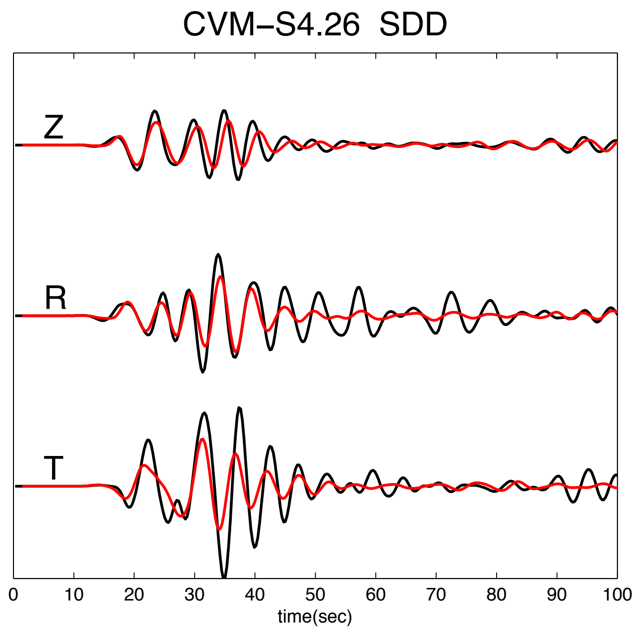

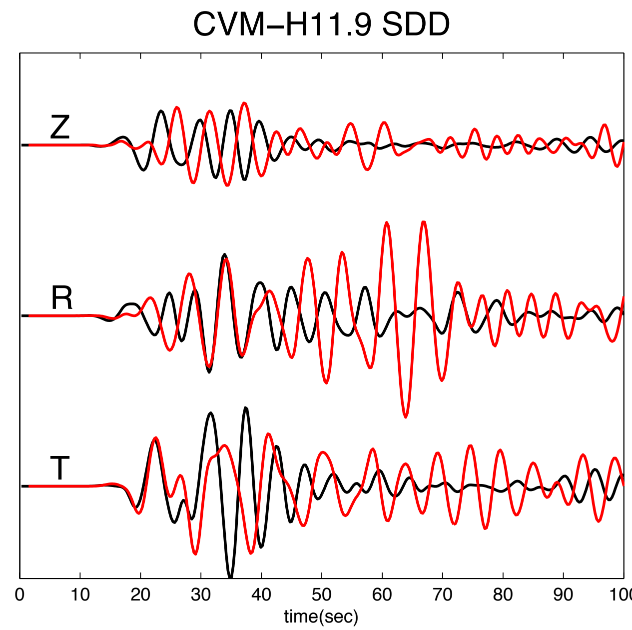

03/28/14 La Habra Earthquake (M5.1)

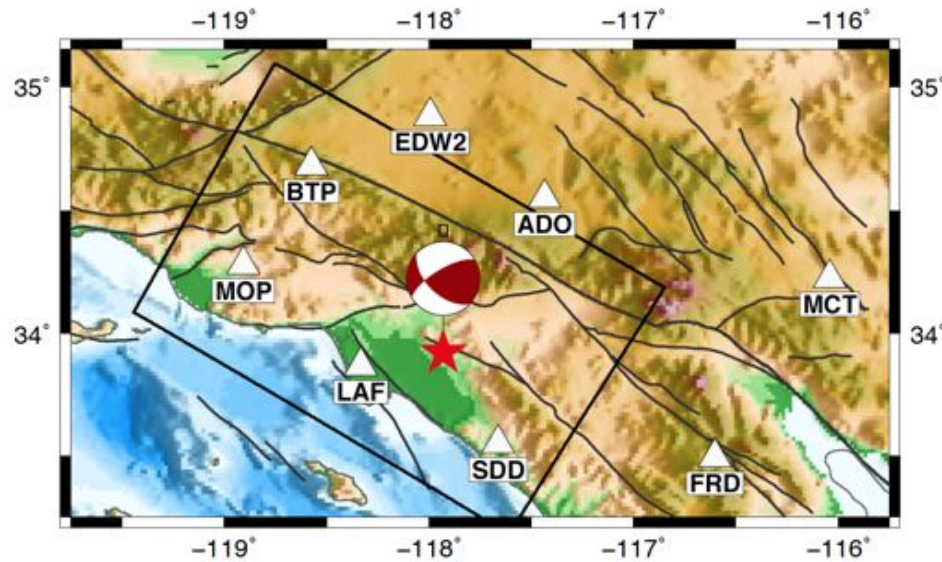

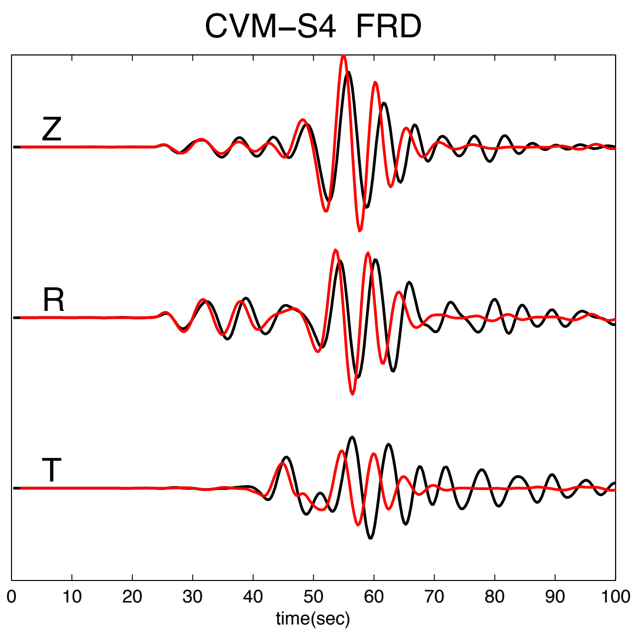

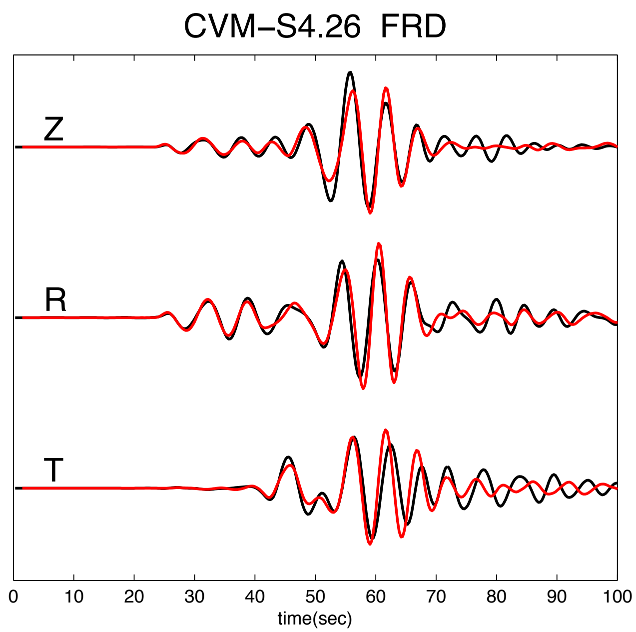

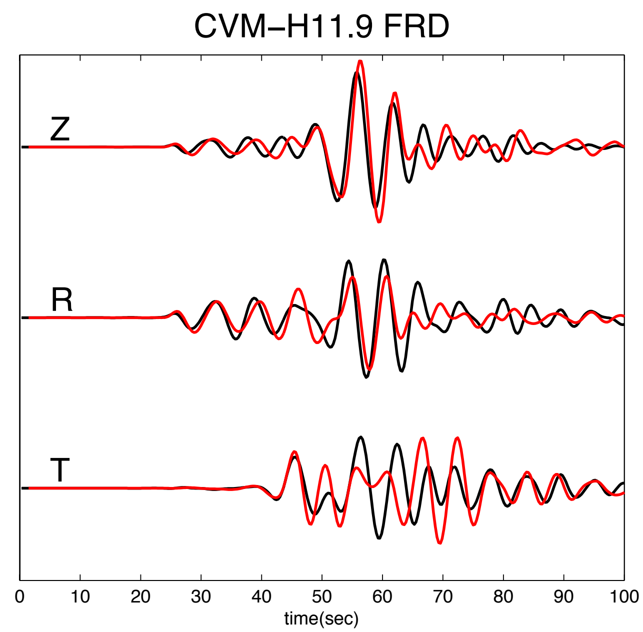

03/28/14 La Habra Earthquake (M5.1)

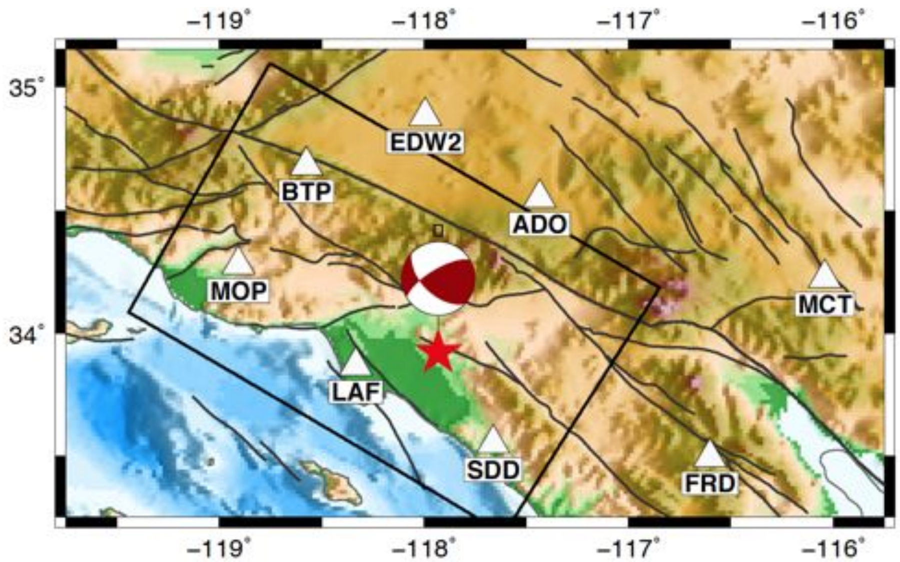

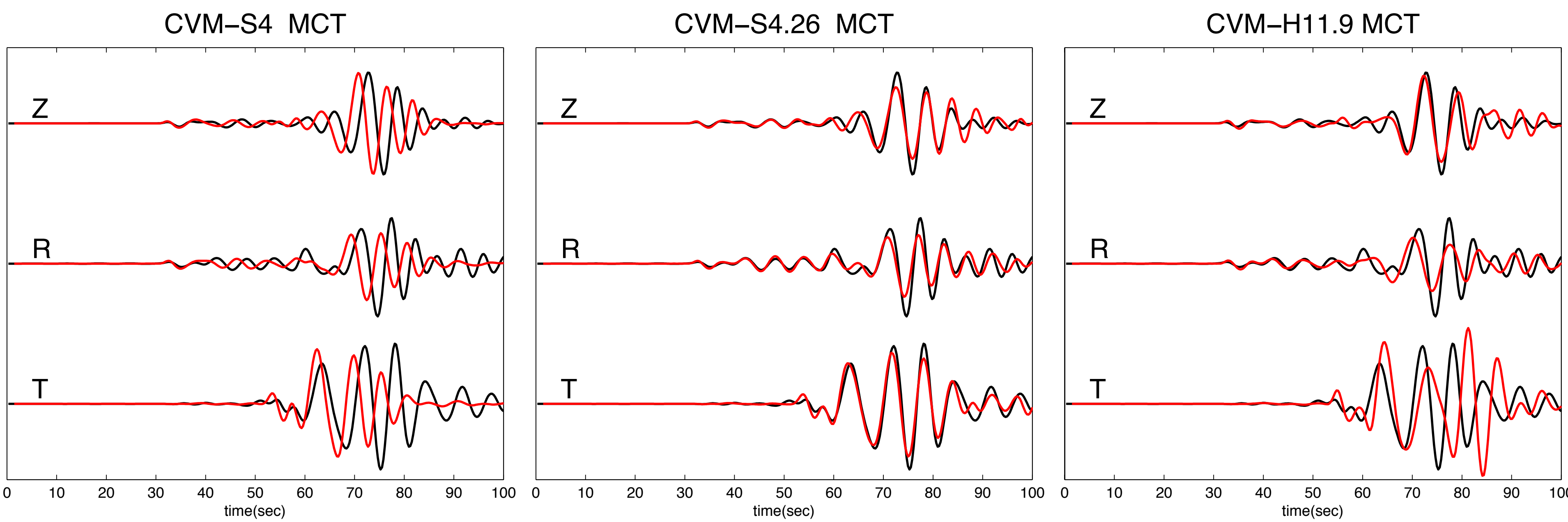

03/28/14 La Habra Earthquake (M5.1)

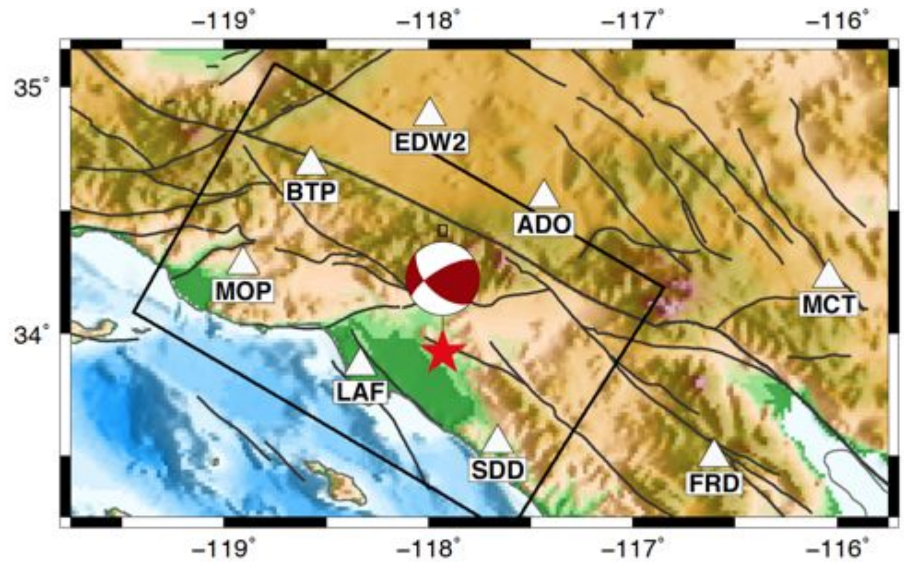

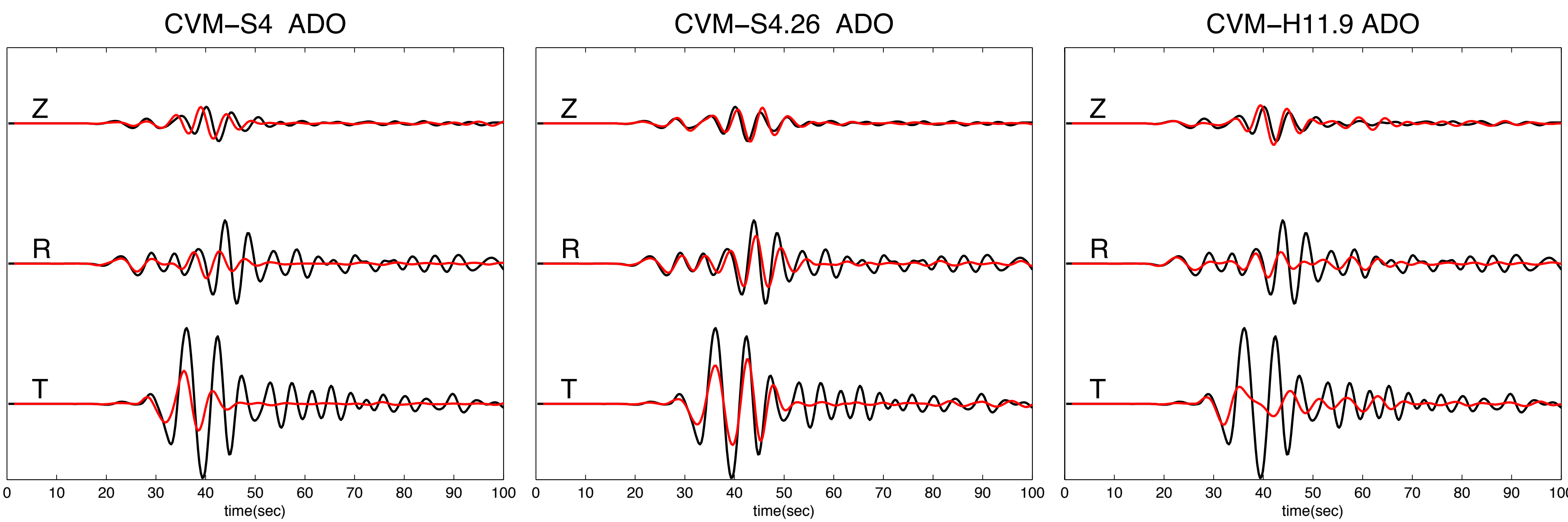

Southern California
Earthquake Center

03/28/14 La Habra Earthquake (M5.1)

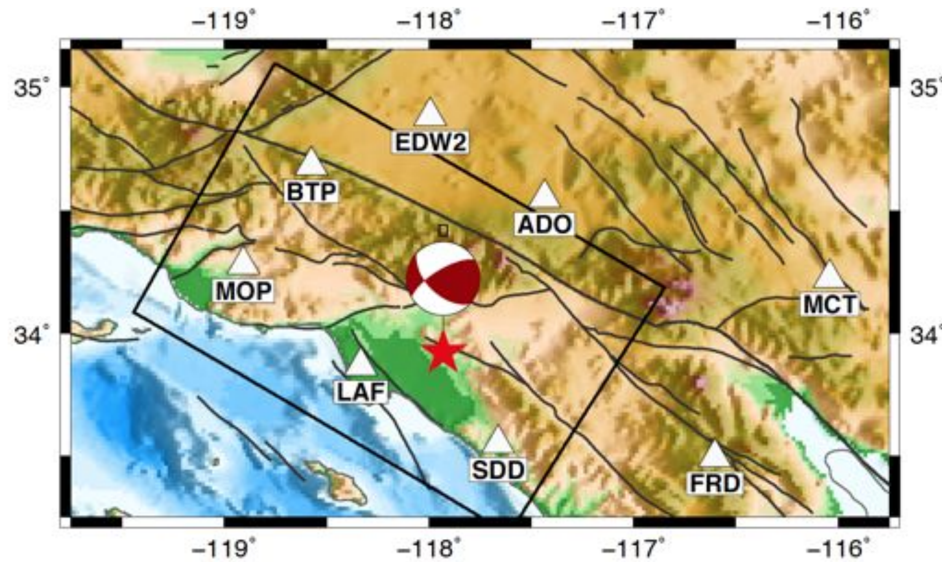

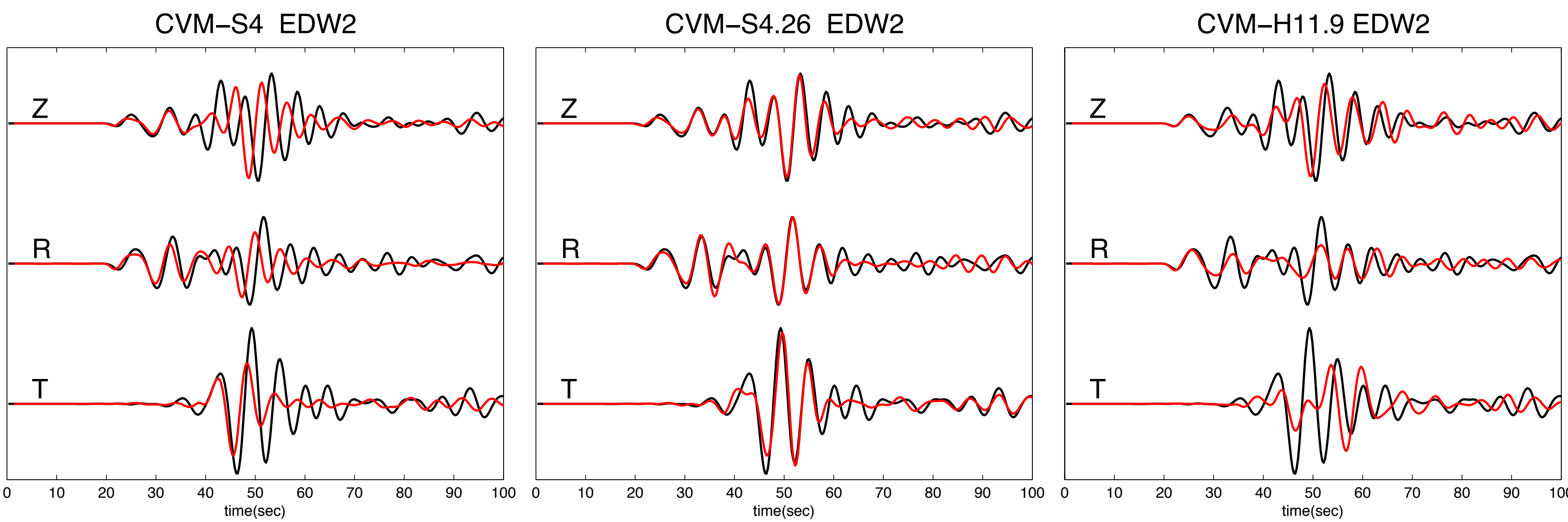

03/28/14 La Habra Earthquake (M5.1)

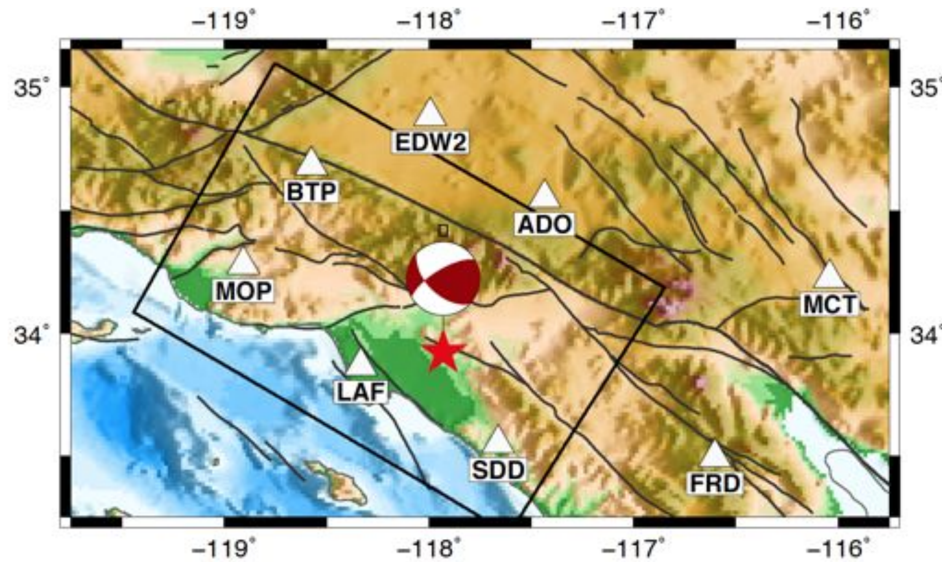

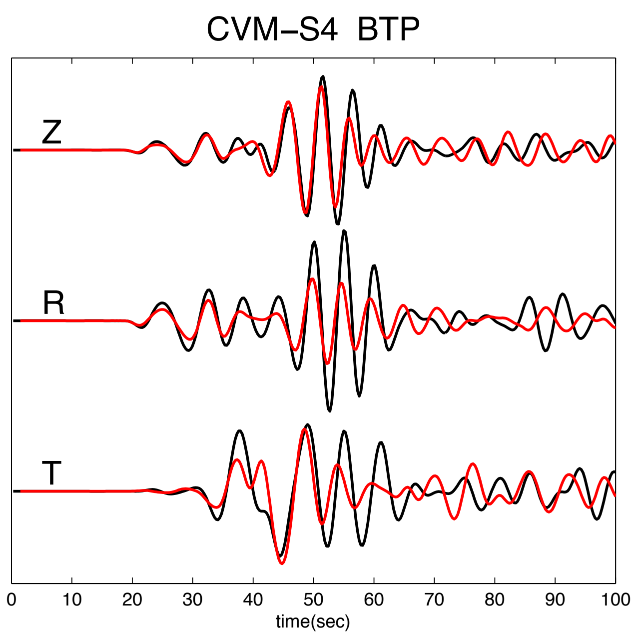

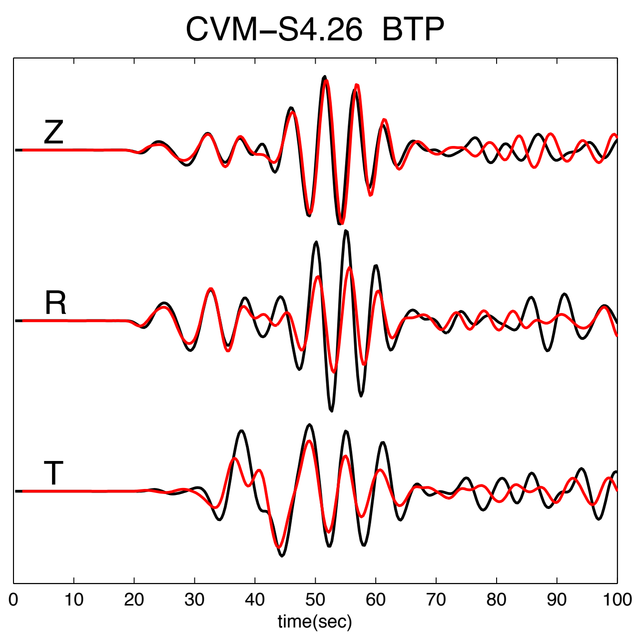

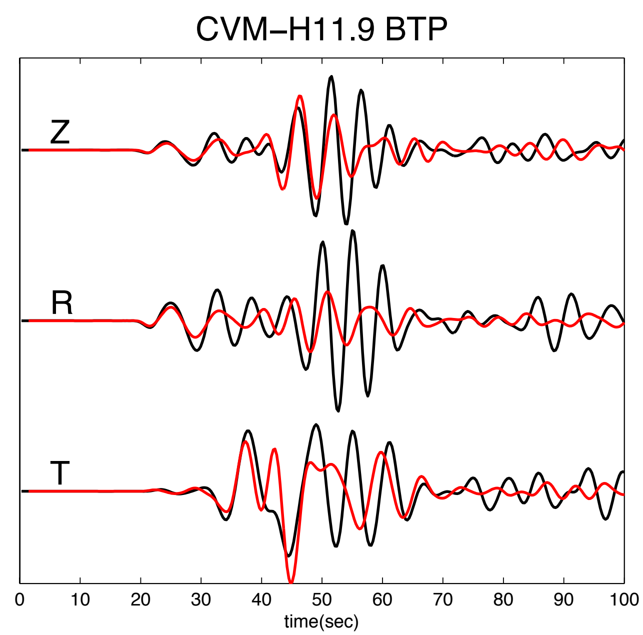

03/28/14 La Habra Earthquake (M5.1)

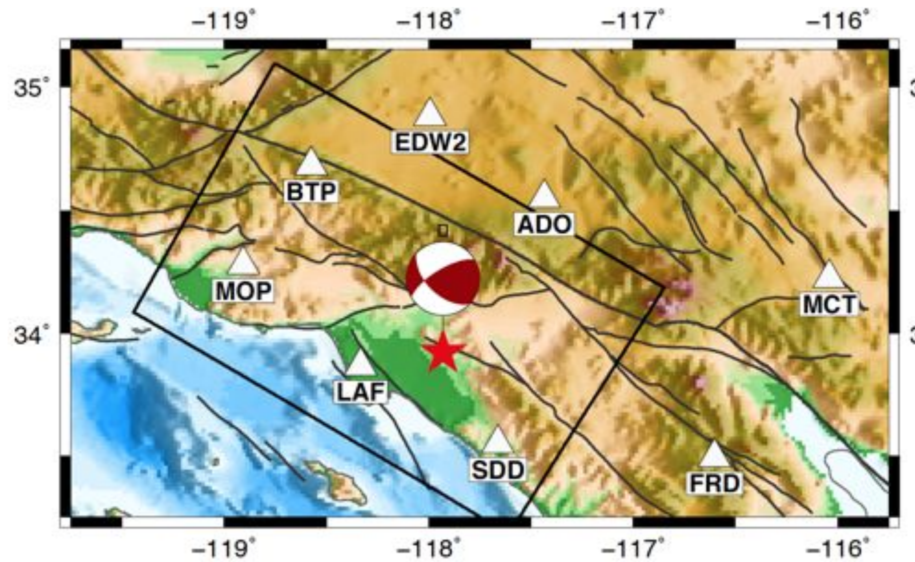

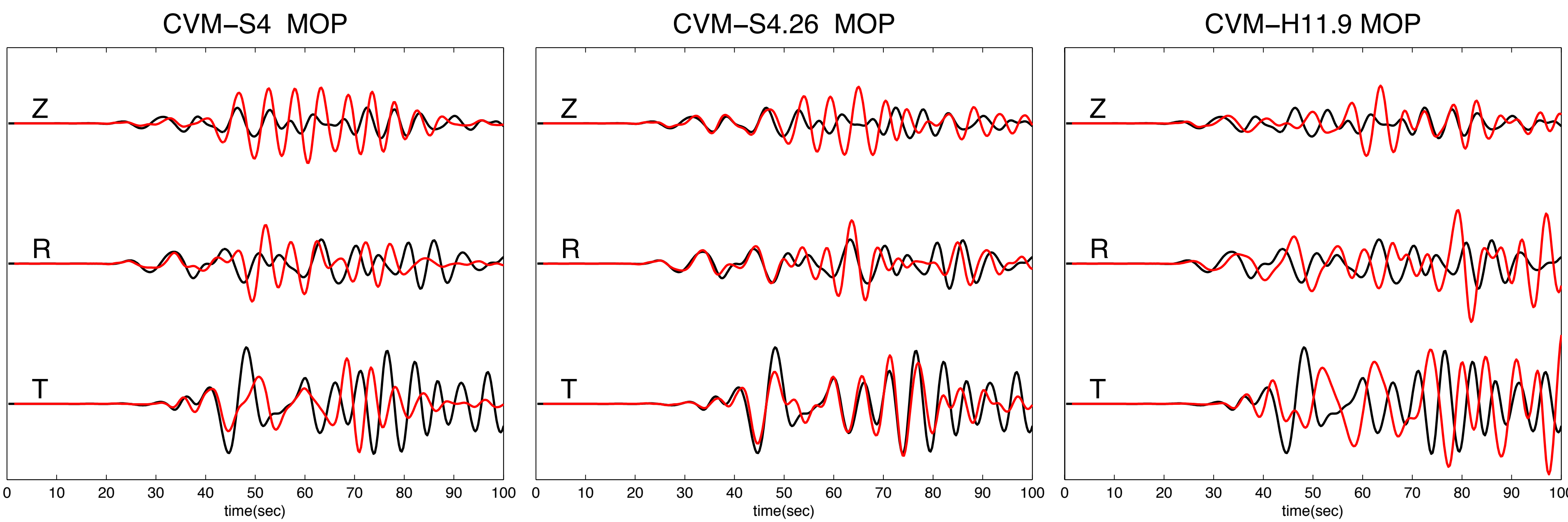

03/28/14 La Habra Earthquake (M5.1)

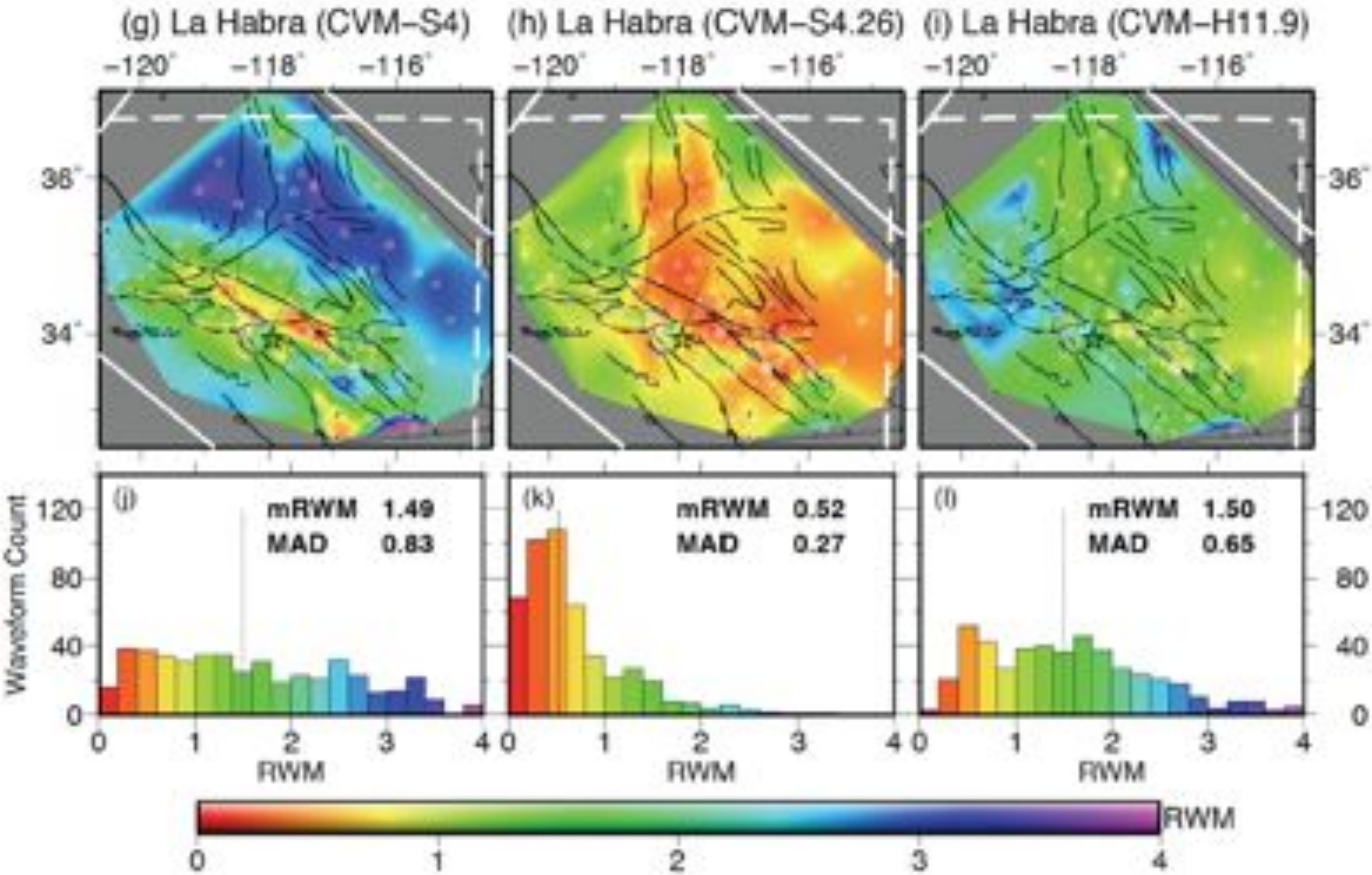

03/17/14 Encino Earthquake (M4.4)

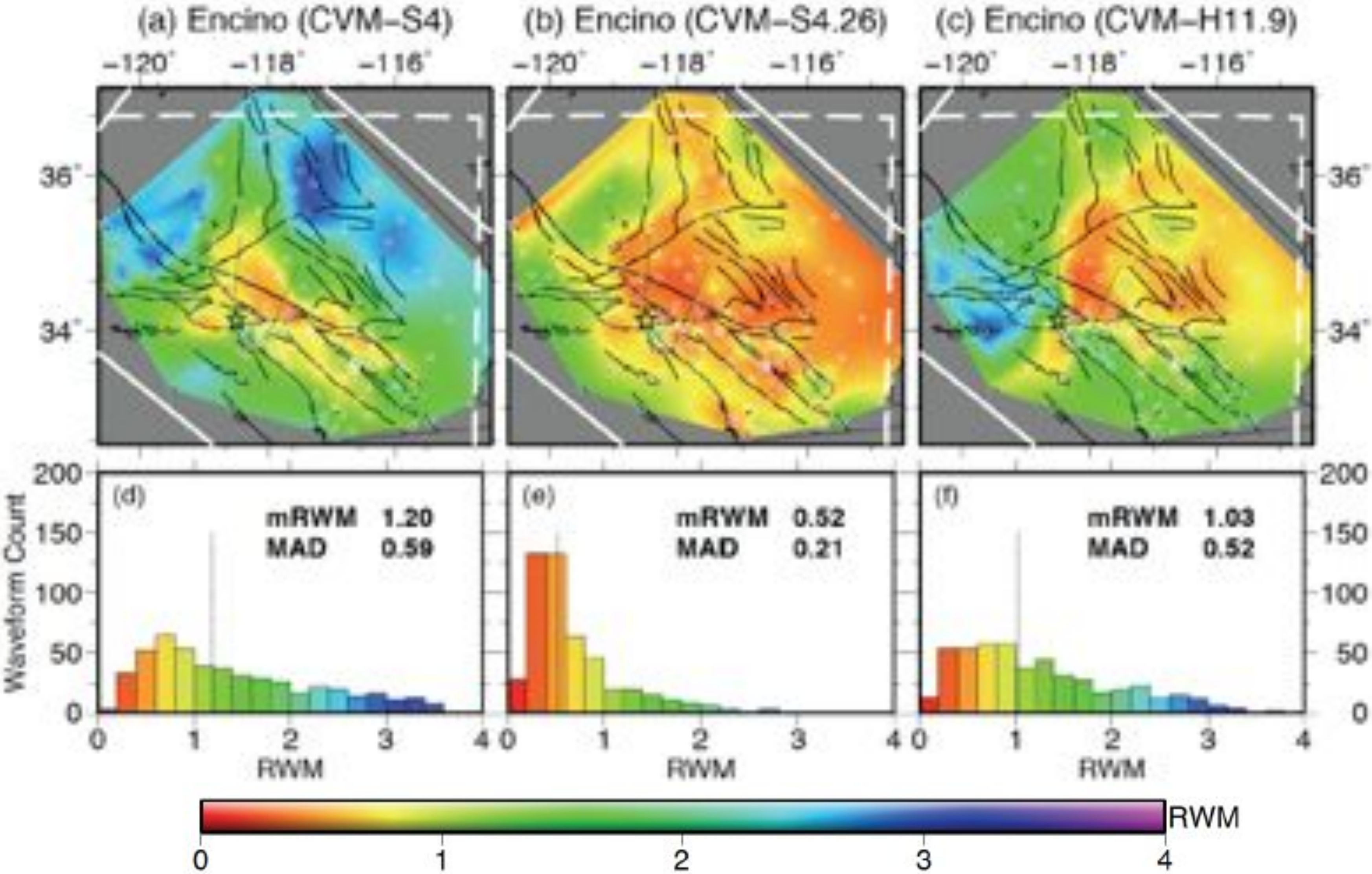

03/18/14 La Habra Earthquake (M5.1)

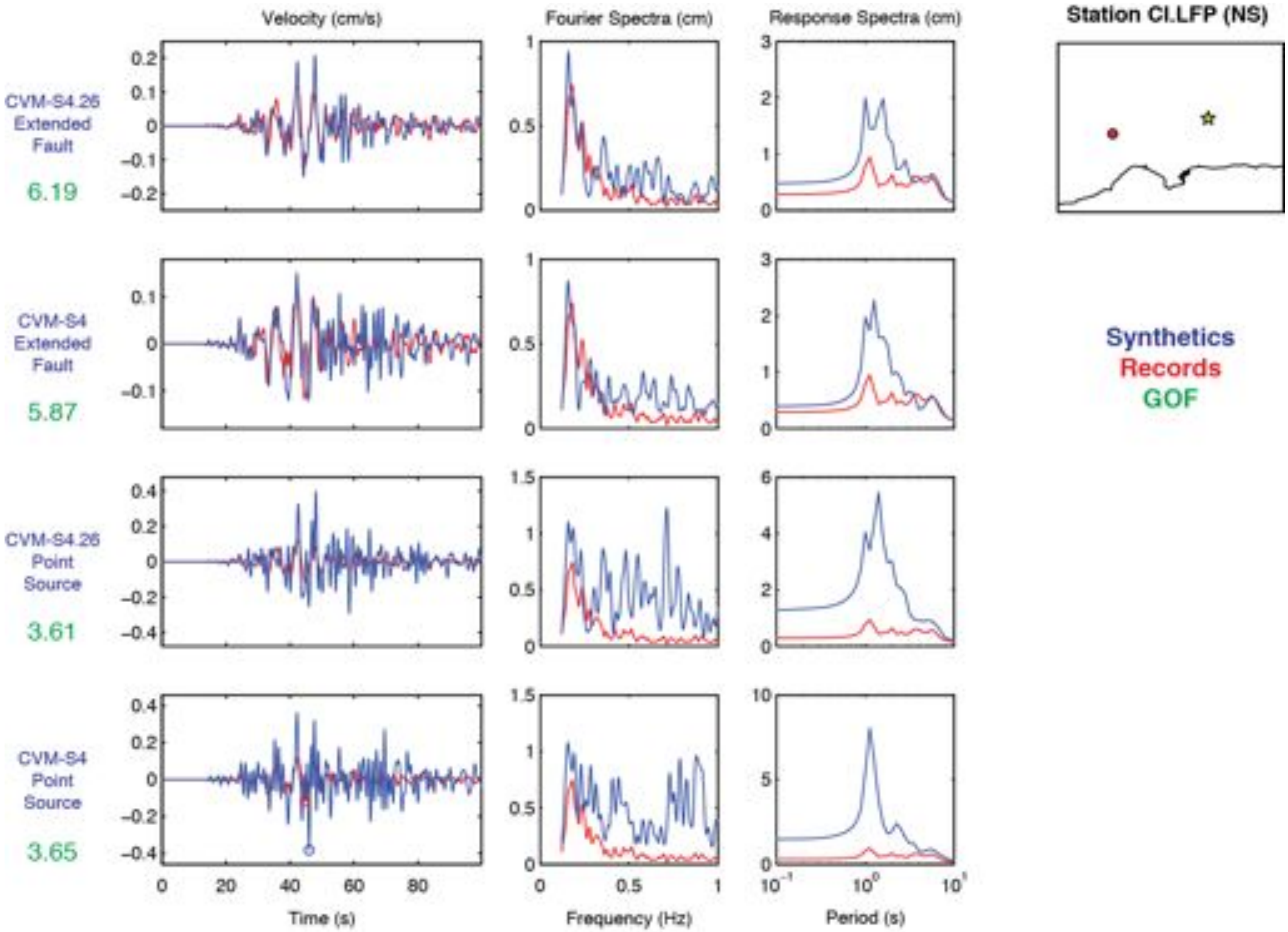

03/18/14 La Habra Earthquake (M5.1)

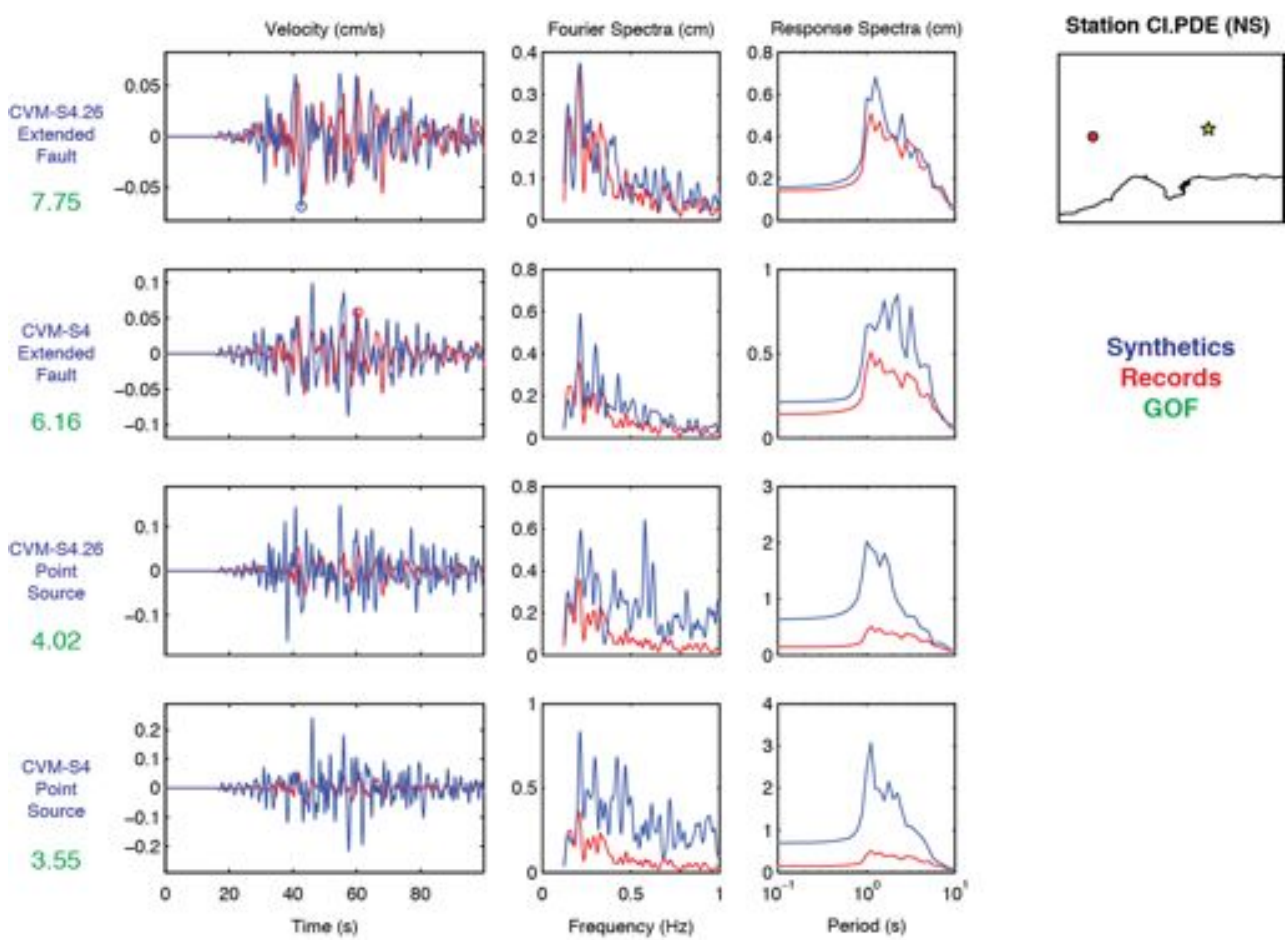

03/18/14 La Habra Earthquake (M5.1)

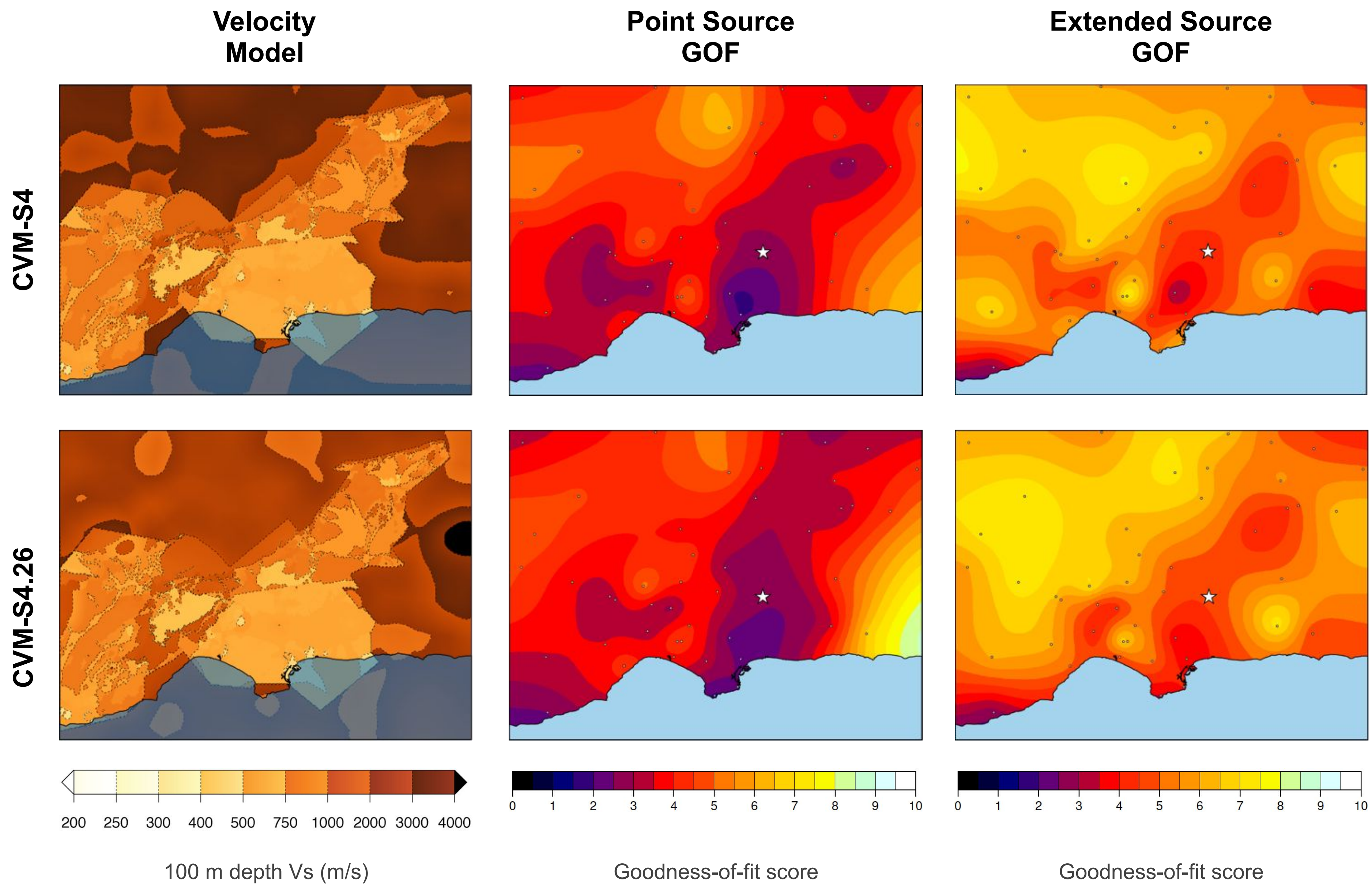

Outstanding Issues

- **USR interface problem**
  - **Representation of interfaces in structured and unstructured grids**
  - **F3DT perturbation of interfaces**
- **Importance of anisotopy**
  - **Bias in isotropic inversions**
  - **Anisotropic F3DT**
- **Push to higher frequencies**
  - **Representation of source complexity**
  - **Frequency-dependent attenuation**
  - **Small-scale near-surface heterogeneities**
  - **Stochastic F3DT**

Seismic Wavefield Representation

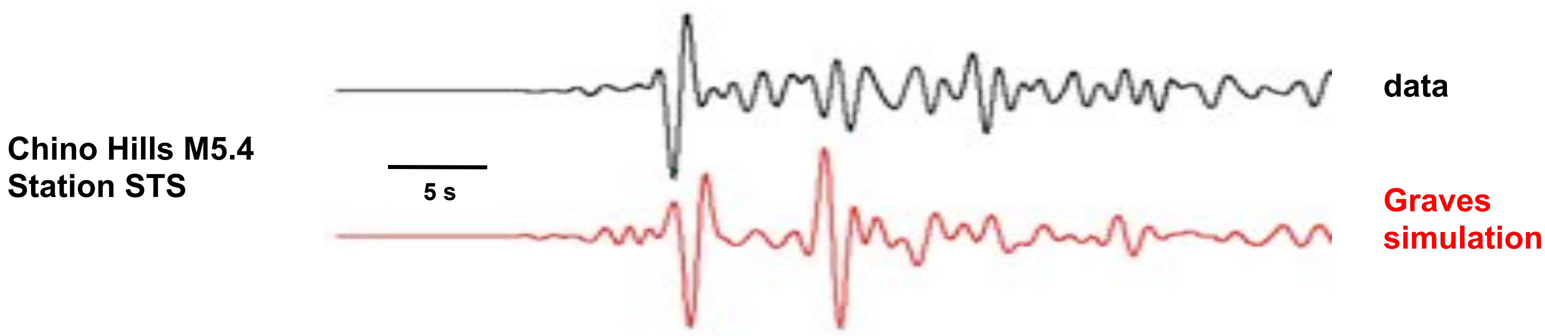

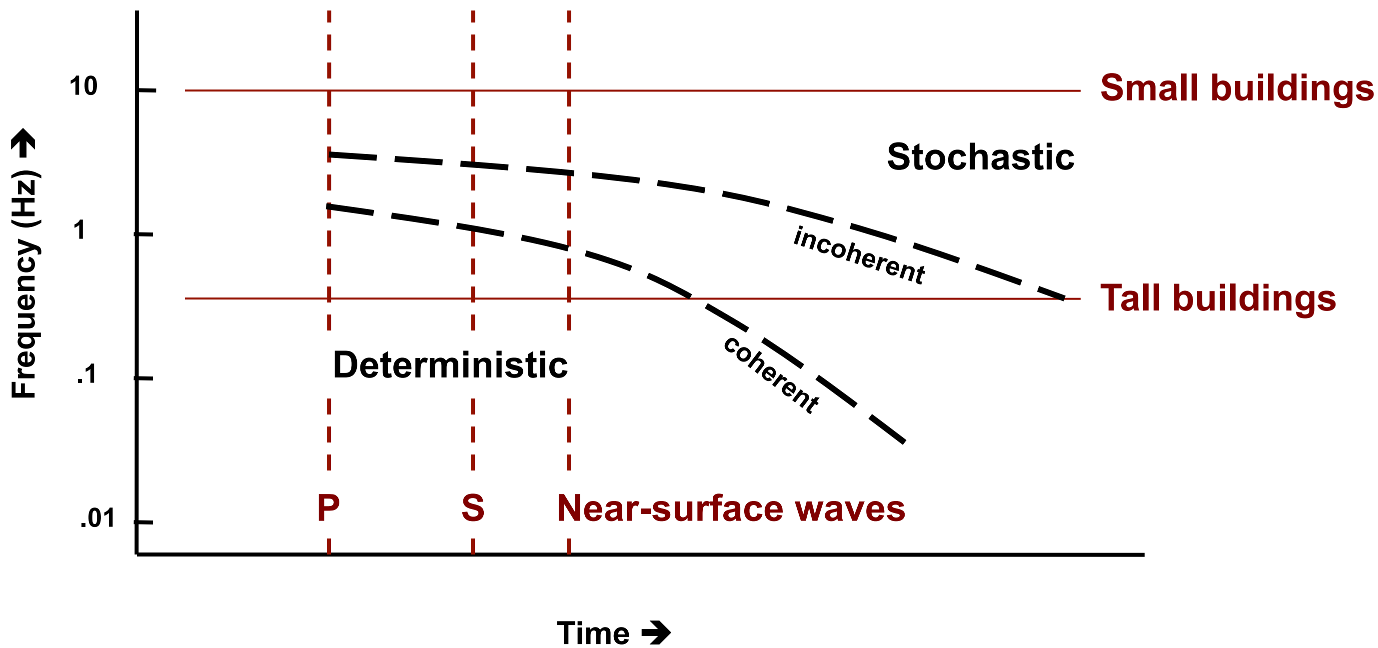

End

Generalized Seismolgical Data Functionals (GSDFs)

Effects of perturbing GSDF parameters by
T= 10 s, or
ωT = 1.39 rad

dt_q

dt_p

dt_a

dt_g

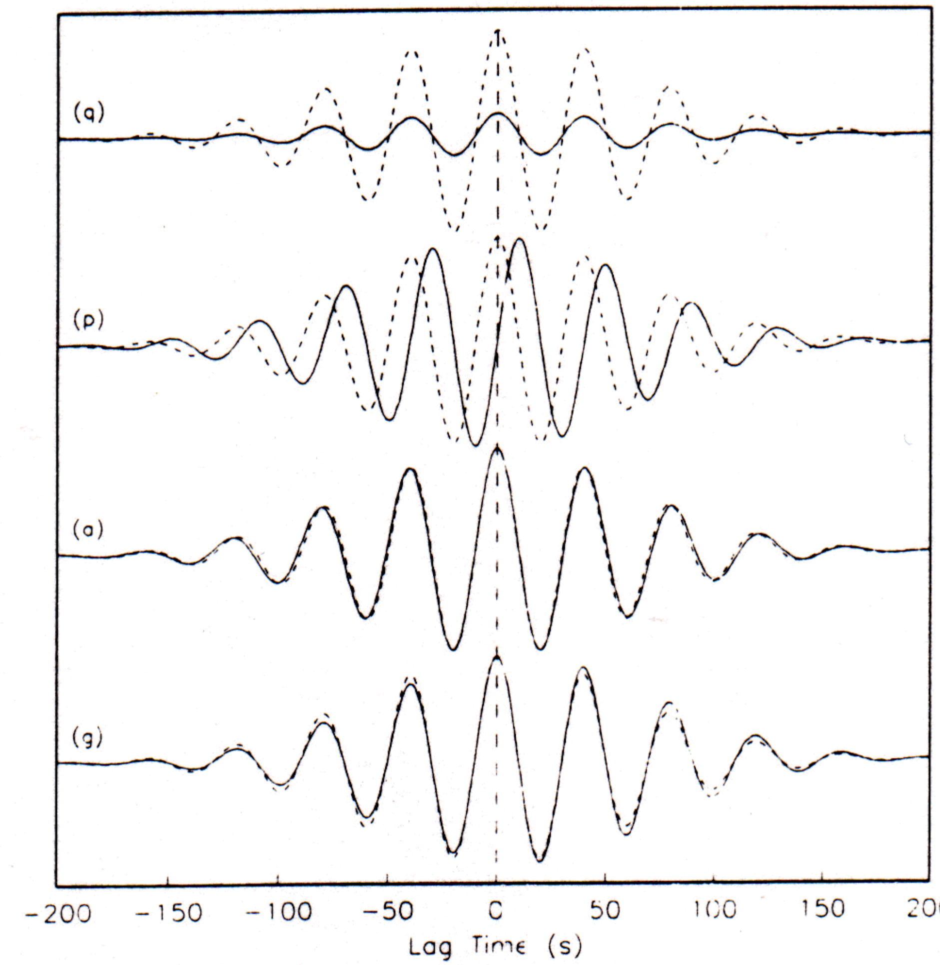

SCEC Community Fault Model (CFM)

Plesch, Shaw et al.

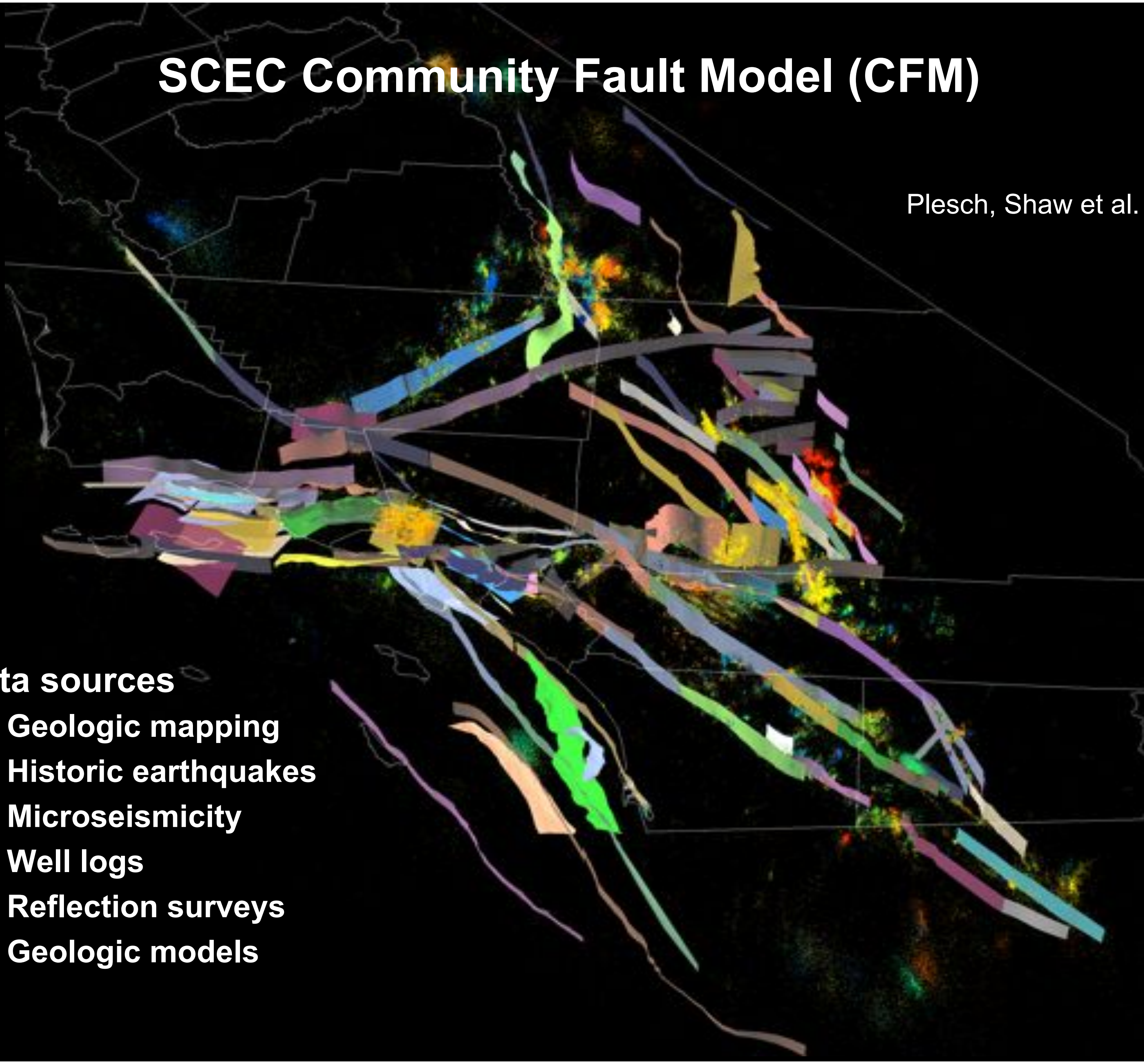

Data sources

- **Geologic mapping**
- **Historic earthquakes**
- **Microseismicity**
- **Well logs**
- **Reflection surveys**
- **Geologic models**